UNIVERSIDAD
DE GRANADA

DOCTORAL THESIS
Programa de Doctorado en Tecnologías de la Información y la Comunicación

Wireless Power for IoT

Presented by:

Fernando Moreno Cruz

Directed by:

Dr. Diego Pedro Morales Santos
Dr. Almudena Rivadeneyra Torres

University Department:

Electronics and Computer Technology

Developed at:

Infineon Technologies AG
BEX RDE RDF ISS
Munich, Germany

Granada, December 2020

Editor: Universidad de Granada. Tesis Doctorales
Autor: Fernando Moreno Cruz
ISBN: 978-84-1306-777-3
URI: http://hdl.handle.net/10481/66728

Wireless Power for IoT

Fernando Moreno Cruz

KEYWORDS:

Internet of Things (IoT), radio frequency energy harvesting (RFEH), ultra-low power, wireless sensor networks (WSN), wireless communication protocols (WCP), printed flexible technology, antennas.

ABSTRACT:

This doctoral thesis by compendium of publications addresses several fields of study around the main topic of wireless transference of energy for the Internet of Things devices, in particular, for nodes which are part of a wireless sensor network, and spotlighting the special case of radio frequency energy harvesting (RFEH), i. e., with no dedicated energy source.

During the doctoral period, and likewise condensed in the present document, we studied the current electromagnetic spectrum, we developed a tri-band antenna tailored to RFEH use-cases, we analyzed the state-of-the-art circuits and components for the autonomous rectification of high frequency low voltage signals, with the purpose of its energy extraction. We developed innovative circuits for the efficient power management previous to a dc/dc converter, that achieved a substantial improvement beyond the state-of-the-art. We studied the commercial dc/dc converters under ultra-low power conditions and novel components and methods for energy storage. We developed a novel wireless communication protocol intended for embedded and energy harvesting systems, that achieved up to 2 decades of lower power consumption than Bluetooth low energy, among other features. We examined application-related new components and materials with exceptional characteristics, such as, flexibility and lower power consumption and cost-effectiveness. And we investigated on new hardware and software concepts for increasing the security of the nodes, without increasing their power demands.

The success of the results was reflected in the published articles further on appended, which were accepted in journals of high academic impact within the first quartile in their classification and conferences of international relevance.

PALABRAS CLAVE:

Internet de las cosas, recolección de energía de ondas de radio frecuencia (RERF), ultra bajo consumo, redes de sensores inalámbricas, protocolos de comunicación inalámbricos, tecnología flexible e imprimible, antenas.

RESUMEN:

La presente tesis doctoral por compendio de publicaciones trata diversos campos de estudio alrededor del tema principal de transferencia de energía de forma inalámbrica para el Internet de las cosas, en particular, para nodos formando una red de sensores inalámbrica, y poniendo el foco sobre el caso especial de recolección de energía de ondas de radio frecuencia (RERF), es decir, sin una fuente dedicada de emisión.

Durante el período doctoral, y de la misma forma condensado a lo largo de esta tesis, se estudió el actual espectro electromagnético, se desarrolló una antena tri-banda personalizada a casos de uso de RERF, se analizaron circuitos y componentes del estado del arte para la rectificación autónoma de señales de alta frecuencia y bajo voltaje, con el objetivo de la extracción de su energía. Se desarrollaron circuitos innovadores para la gestión energética eficiente en la etapa previa a la conversión dc/dc, que lograron una mejora substancial al estado del arte. Se estudiaron los conversores dc/dc del mercado bajo condiciones de ultra baja potencia, además de componentes y métodos novedosos para el almacenamiento de energía. Se desarrolló un novedoso protocolo de comunicación inalámbrico para sistemas empotrados y con recolección de energía, que consiguió hasta 2 décadas de menor consumo de potencia que Bluetooth low energy, entre otras características. Se evaluaron nuevos componentes y materiales con propiedades excepcionales para la etapa de aplicación, como flexibilidad y más bajo coste y consumo. Y se investigó en nuevos conceptos hardware y software para aumentar la seguridad de los nodos, sin aumentar sus demandas de energía.

El éxito de los resultados se reflejó en los artículos publicados, adjuntos más adelante, aceptados en revistas de alto impacto científico y con rango del primer cuartal, así como en conferencias de relevancia internacional.

En memoria de
Jacinta Fernández López
y Juan A. Álvarez Lorente

Acknowledgments

One may walk faster alone, but will definitively arrive further together. In this stage of my life I have arrived quite far and therefore, I have a lot of people to be thankful to for sharing the path with me.

I want to thank Wolfgang Dettmann and Herbert Rödig for providing me with the resources for realizing this project and for believing in me from the first moment until the end, no matter how crazy my proposed ideas might have sounded. The creative and "go-out-of-the-box" environment where I have worked in is only their merit.

Diego P. Morales and Almudena Rivadeneyra, my thesis directors, are enormously responsible for the successful completion of this journey. They have not only given me extremely valuable academic counsel and feedback, but also pushed me forward in moments when the results did not reach yet the expected outcomes, not letting me give up for a second, neither leave aside ambitious objectives. Thank you.

This project would have never been completed either without the technical support of Víctor Toral and Marina Ramos. Both hard working engineers and undoubtedly people that you want to have in a near desk with a laptop. Thank you.

The cerebral impact of these three and a half years would have been way worse if it weren't for my colleagues from Campeon. Different origins, ages and genders that contributed to a great work atmosphere in which to thrive and find tech-tips. Antonio Escobar, Fran Cruz (when he still joined for the *merienda*), Juan Keimasoa, to mention some of the huge list: thank you.

My friends from Munich for sure should not be mentioned in these lines, since they have rowed in the opposite direction of anything similar to a PhD obtainment. In particular, Alberto Segura and Henry Hinz (when he was

single), among many others; but I will thank them anyway in the category of "necessary amusement". Thank you guys for being there every minute.

If talking about friends, I cannot forget my people from Aguadulce, even at 2000 km. Names that after 20 years sound more like family, as something that has been there forever. And indeed it will.

Neither my spread mates from Granada and Barcelona, with special mention to Ana Mellado, Germán Fernández and to La Carolina, in its own.

A continuación me permito la licencia de cambiar a mi lengua materna para referirme a mi familia. Podría excusarme en que así me podrán entender, pero es en realidad porque así lo siento más personal.

Las personas a las que más debo, que siempre están ahí, con confianza plena e incalculable afecto, son sin duda mis padres, Ángeles y Fernando y mi hermana Ángela. Gracias por ser como sois y demostrarlo cada día.

Pero también a mi abuela Gádor, mis tíos, tías y primos. Incluso en años difíciles que amenazan con alejarnos y en los que inevitablemente echamos de menos a seres queridos, nuestro mérito ha sido y es mantenernos unidos, como siempre hemos conseguido y como precisamente los que nos faltan desearían. Gracias por seguir empujando en la misma dirección.

I do not want, but certainly I do forget people. To them: thank you too.

Contents

List of Figures

Acronyms

IoT	Internet of Things
RFEH	radio frequency energy harvesting
WSN	wireless sensor network
RFID	radio frequency identification
EH	energy harvesting
GSM	global system for mobile communications
µC	microcontroller
ADS	Keysight Technologies' ADS 2020 software
WET	wireless energy transmission
OS	operating system
WCP	wireless communication protocol
BLE	Bluetooth Low Energy
QoS	quality of service
Q1	first quartile
SRD	short range devices
UHF	ultra-high frequency
IC	integrated circuit
HF	high frequency
CNT	carbon nanotube
IDE	interdigitated electrode

CMOS complementary metal-oxide-semiconductor

GO graphene oxide

"Test ideas by experiment and observation. Build on those ideas that pass the test. Reject the ones that fail. Follow the evidence wherever it leads and question everything. Take these rules to heart and the cosmos is yours."

– Neil deGrasse Tyson

Chapter 1

Introduction

Due to its massive deployment, the term Internet of Things (IoT) has nowadays become part of our society, not being reserved anymore for developer or academic circles. The fast growth of the number of devices is now a fact and is slowly changing our daily life with more and more applications in diverse areas, such as smart-home, transportation, smart-city, wearables and industry, among many others [1].

In this heterogeneous infrastructure where ordinary physical objects are constantly being merged with electronics, most of them belong to a wireless sensor network (WSN). This happens due to the expenses, inconvenience or even impracticability of wiring them, and induces to novel demands in terms of energy. The challenge appears with the need of feeding the nodes with no power cord for a minimum time frame of months or years and without compromising the quality of service (QoS).

A common option to address this is the use of batteries, especially non-rechargeable chemical ones (lithium). Their power densities get as far as $45\,\mu W/cm^3$ for around one year lifetime and $3.5\,\mu W/cm^3$ for ten [2]. However, they have great disadvantages related to the costs of their replacement (or recharge), their low expected lifetime and their harmful environmental impact, particularly in large-scale deployments [1], [2].

Within this framework appears energy harvesting (EH) as a technique for powering the nodes in a clean, temporally-unlimited and autonomous fashion. To this extent, an EH system gathers the energy present in the environment for converting it to electricity, being the most common sources solar, thermal, vibrational, RF electromagnetic waves, etc. Specifically, radio frequency energy harvesting (RFEH) captures the energy present in the far

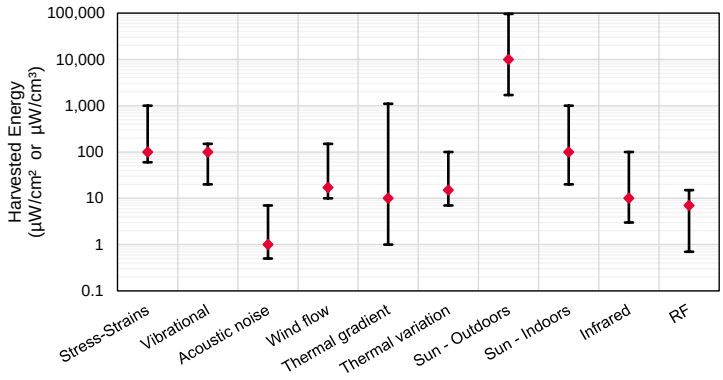

Figure 1.1: Comparison of the power able to be harvested by the most common EH sources [8]. Typical range and most frequent value.

field region of the signal carriers of the ambient radiation. The most profitable frequency range goes between some kilohertzs and hundreds of gigahertzs [3], where some studies assert that in bands of high utilization, such as the cellular network (global system for mobile communications [GSM] and its successors), TV broadcasting or wireless local networks; the energy levels in city open-spaces reach $-30\,\mathrm{dBm}$ and even $-20\,\mathrm{dBm}$ [4]–[6]. These levels are a direct consequence of the limitation on RF emissions given by the regions regulation (e. g., $500\,\mathrm{mW}$ effective radiated power in the short range devices [SRD] band of $868\,\mathrm{MHz}$ for Europe [7]).

RFEH offers clear advantages in regard to time stability and predictability, low-cost implementation and small form factor. Its largest drawback is the limited amount of power able to be harvested (barely tens of microwatts, as depicts Figure 1.1), being categorized as "ultra-low power" [3], [9]. Besides, in some cases (e. g., Wi-Fi router or mobile phone), the availability of the signal is not constant due to the duty cycle or random use of the service, or, in other cases (e. g., AM radio), the size of the antenna needed makes the system impracticable.

Seen from another perspective, RFEH can be identified as a wireless energy transmission (WET) technique. Nikola Tesla already demonstrated WET in the 1890's [10], although the current trend has left behind its hefty origins. WET differentiates from RFEH in the use of a dedicated energy source that actively radiates to the objective/s. This achieves higher energy levels, although not in an efficient manner due to the inverse square relation of the power with the distance to the radiation source, according to Friis

transmission equation [11]:

$$P_r = P_t G_t G_r (\frac{\lambda}{4\pi R})^2,$$

where P_r and P_t are the received and emitted power respectively, G_r and G_t the antenna gains, R the distance and λ the wavelength of the signal.

Another family of WET is the inductive coupling, which includes resonant inductive as well[1]. Both methods have been deeply investigated and are widely used with extraordinary RF-to-dc conversion efficiencies [12], e. g., radio frequency identification (RFID) tags and phone charging, respectively. In contrast, their transfer ranges are limited from a few millimeters to a few meters, since they operate at the near field region, which is attenuated with the cube of the distance [12]. That makes 60 dB of attenuation per decade, versus 20 dB for the far field region [3].

The power losses are then divided between the path (propagation) and presumable obstacles, and the efficiency of the energy management at the node. A typical IoT node intended for RFEH consists principally of a microcontroller (µC), at least one sensor or actuator, a radio transceiver with an antenna and the harvesting module. The last, in turn, starts with an antenna (or an array) for capturing the signal, followed by an impedance matching network. The next stage is typically a rectifier that converts the signal to dc. The power management stage goes next, which may implement different techniques for maximizing the efficiency [13]. It eventually includes a dc/dc converter that maintains a constant and appropriate voltage level for the application, generally in the form of a boost converter of charge pump. Once at the desired level, the energy is stored in a capacitor or battery, which is dimensioned according to the application needs. Figure 1.2 illustrates a basic example.

Regarding the applications, the RFEH scenarios encompass the ones with ultra-low power requirements, typically with a duty-cycled operation instead of a constant one, which are more energy demanding. Therefore, beyond the hardware, both the operating system (OS) and the wireless communication protocol (WCP) play an important role as well [14], since they determine the power consumption profile of each node. This refers to the periodicity of the measurements and communications, the complexity and duration of the processes performed in the µC, the WCP behavior and overhead, the security level implemented, among other features.

[1] Capacitive coupling has several disadvantages and is not spread.

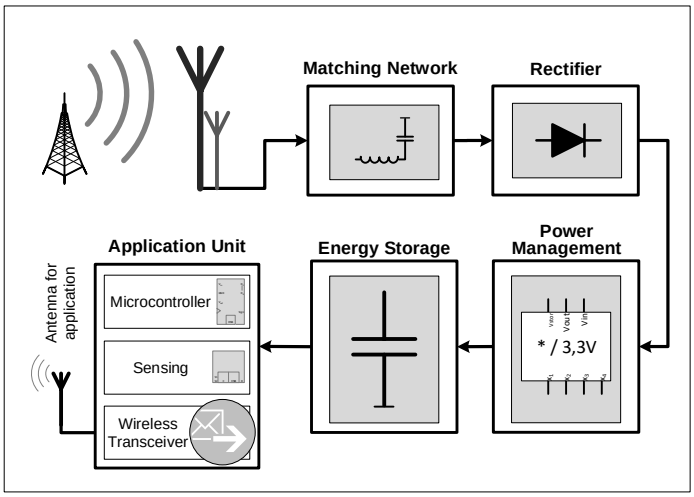

Figure 1.2: Block diagram of basic RFEH node.

In addition to the energy supply, security is as well one of the fundamental challenges of the IoT. The enormous amount of devices transferring sensitive data and their potential vulnerabilities given by the scarceness of resources, their simplicity or carelessness of the designs, embody critical security and privacy threats that need to be addressed. The focus here is distributed between the software, implementing different methods of encryption, anonymity or authentication, among others; and the hardware, for cases where the contact with the devices or their tampering is possible. On top of that, an extra handicap in every of these pursuits is to achieve secure systems while maintaining a low power consumption.

1.1 Motivation

Several factors have prevented heretofore that RFEH flourishes as a technology that solves the previously introduced challenges within the IoT. However, the conditions have favorably changed in the last years.

Coupled with the IoT growth, the deployment of 5G (fifth generation of mobile technology communications, GSM descendant) is occupying the city RF spectrums with micro-, pico- and femto-cells, which not only target high speed devices but also WSNs. This does not only mean a richer ambient radiation to harvest, dealing with the large propagation losses of high frequency

signals; but also an easier connectivity for the devices, resulting in lower power consumption.

With respect to the technology involved, the improvements on the circuits and components for high frequency signals rectification and low power dc/dc conversion and management have resulted in greater efficiencies that enable the exploitation of the RF environment, now possible for the ultra-high frequency (UHF) bands and above. In particular, the advances in high frequency complementary metal-oxide-semiconductor (CMOS) technology and Schottky diodes [12], the most important component of a rectifier; and the progresses in low power circuits have caught the researchers attention during the last decade.

Likewise, novel advanced techniques directly related to RFEH have emerged, such as multi-band schemes, antenna-arrays, higher antenna sensitivities, more efficient energy storage devices or dedicated energy management integrated circuits (ICs), among others [13]; as well as innovations on new materials, such as printed flexible electronics. The last brings not only improvements in the developing and manufacturing costs, but also new features that provide with new use-cases, as the flexibility for wearables or their physical resistance for goods monitoring [15].

Furthermore, the every-day reduction of the application power consumptions by the semiconductor manufacturers is an added value, since there has been a considerable decrease of the energy needs of µCs, sensors and radio transceivers, reaching the ultra-low power category. Similarly, the WCPs have adapted to this trend, with the wide spread of Bluetooth Low Energy (BLE), Zigbee, ANT, etc.

For all of this, the research on RFEH related technologies, including techniques that contribute to lower power consumptions within the IoT, appears as an attractive innovation topic that is on the crest of the wave of its development.

1.2 Objectives

The objectives of this doctoral work are the ones derived from the development at all stages of a complete IoT node powered autonomously by an RFEH module. The intended contributions to the state-of-the-art include hardware- and software-related targets and, following the order of the block diagram of Figure 1.2, are summarized as follows:

1. **RF investigation**

   (a) Study of the present electromagnetic ambient radiation, in order to select the most energy-profitable range of the spectrum to be harvested for every application or specific scenario considered.

   (b) Research on antennas, attending to their features, such as the polarization, directivity, efficiency and frequency band/s, in pursuance of novel syntheses that bring an added-value in RFEH scenarios.

2. **Power management investigation**

   (a) Study of rectification and impedance matching circuits in the conditions given by the previous objectives, towards the extraction of the highest amount of energy from the environment in form of dc power.

   (b) Research on power management techniques through innovative designs and methodologies, in furtherance of significant improvements in the performance that finally allow feeding a node in a battery-less fashion.

   (c) Study on dc/dc converter circuits and energy storage components, aiming to elements that satisfy the ultra-low power requirements of low voltage, low losses and leakage and high efficiency.

3. **IoT-application investigation**

   (a) Research on OSs and WCPs for embedded systems, exploiting the advantages over the power consumption of tailoring the workflow, processes and routines to EH devices.

   (b) Study on new ultra-low power µCs, sensors and radio transceivers, as well as the options of new materials and fabrication techniques, such as printed technology.

   (c) Research on security approaches that enhance the reliability of the IoT systems, while maintaining a fine balance with the power consumption.

1.3 Outline

The present document constitutes a thesis by compendium of publications. This means, formed by the most relevant published papers as result of the research carried out during the doctoral period. The work includes three indexed articles in scientific journals ranked in the first quartile (Q1)[2], two contributions to international conferences and two more articles at the moment in revision by scientific journals. We list them following:

- F. Moreno-Cruz, V. Toral-López, M. Ramos Cuevas, *et al.*, "Dual-Band Store-and-Use System for RF Energy Harvesting with Off-the-Shelf DC/DC Converters", *IEEE Internet of Things Journal*, pp. 1–1, 2020. DOI: 10.1109/JIOT.2020.3024017. IF: 9.936 (Q1)

- F. Moreno-Cruz, V. Toral-López, A. Escobar-Molero, *et al.*, "treNch: Ultra-Low Power Wireless Communication Protocol for IoT and Energy Harvesting", *Sensors*, vol. 20, no. 21, p. 6156, 2020, ISSN: 1424-8220. DOI: 10.3390/s20216156. [Online]. Available: http://dx.doi.org/10.3390/s20216156. IF: 3.275 (Q1)

- A. Rivadeneyra, A. Albrecht, F. Moreno-Cruz, *et al.*, "Screen Printed Security-Button for Radio Frequency Identification Tags", *IEEE Access*, vol. 8, pp. 49 224–49 228, 2020. DOI: 10.1109/ACCESS.2020.2979548. IF: 3.745 (Q1)

- F. Moreno-Cruz, A. Escobar-Molero, E. Castillo, *et al.*, "Why Use RF Energy Harvesting in Smart Grids", in *2018 IEEE 23rd International Workshop on Computer Aided Modeling and Design of Communication Links and Networks (CAMAD)*, IEEE, 2018, pp. 1–6. DOI: 10.1109/CAMAD.2018.8514966

- F. Moreno-Cruz, F. J. Romero Maldonado, N. Rodríguez Santiago, *et al.*, "Low-cost energy-autonomous sensor nodes through RF energy harvesting and printed technology", in *ALLSENSORS 2020: The Fifth International Conference on Advances in Sensors, Actuators, Metering and Sensing*, ser. 5, ISBN: 978-1-61208-766-5, Jaime Lloret Mauri et al., 2020

[2]Each subject group of journals is divided into four quartiles, occupying Q1 the top 25% of most prestigious ones in the list.

- F. Moreno-Cruz, M. Ramos-Cuevas, P. Padilla de la Torre, *et al.*, "Custom Tri-Band Antenna within RF Energy Harvesting", *UNDER REVIEW*, 2020

- F. C. Loghin, A. Falco, F. Moreno-Cruz, *et al.*, "Facile Manufacturing of Sub-mm Thick CNT-Based RC Filters", *UNDER REVIEW*, 2020

After presenting in Chapter 1 the Introduction to the matter with a brief review of the state-of-the-art and the Motivation and Objectives of the doctoral work, Chapter 2 appends the referred publications with an evaluation of their impact. To finalize, Chapter 3 assesses the Results and Conclusions of the work, as well as the Methodology followed.

Chapter 2

Publications

2.1 Publication 1

"Omne ignotum pro magnifico."
– Bram Stoker's Dracula

Dual-Band Store-and-Use System for RF Energy Harvesting with Off-the-Shelf DC/DC Converters

Fernando Moreno-Cruz[1,2], Víctor Toral-López[2], Marina Ramos Cuevas[3], José F. Salmerón[2], Almudena Rivadeneyra[2] and Diego P. Morales[2]

[1] Infineon Technologies AG, Munich (Germany)
[2] Department of Electronics and Computer Technology, University of Granada, Granada (Spain)
[3] Technical University of Munich, Munich (Germany)

IEEE Internet of Things Journal

- Received April 2020, Accepted September 2020
- DOI: 10.1109/JIOT.2020.3024017
- Impact Factor: 9.936
- JCR Rank: 3/156 in category *Computer Science, Information Systems* (Q1), 9/266 in *Engineering, Electrical & Electronic* (Q1) and 5/90 in *Telecommunications* (Q1)

Dual-Band Store-and-Use System for RF Energy Harvesting with Off-the-Shelf DC/DC Converters

Fernando Moreno-Cruz, Víctor Toral-López, Marina Ramos Cuevas, José F. Salmerón, Almudena Rivadeneyra and Diego P. Morales

***Abstract*—RF energy harvesting (RFEH) has recently become part of the alternatives for powering wireless sensor networks. Our focus in this paper was to introduce a design, *MSwitch*, able to use off-the-shelf dc/dc converters for running a real and self-powered Internet of Things (IoT) application. *MSwitch* is an RF dual-band energy harvesting stage employing the store-and-use principle, that mixes efficiently and in a dynamic manner both inputs. We proved an increase on the performance with respect to the single band case and to the most successful approaches found in the literature, achieving about 10% better efficiency and around 35% lower minimum power levels. Besides, we carried out an analysis on the commercial dc/dc converters, characterizing them for ultra-low power conditions. Likewise, we analyzed the state-of-the-art rectification circuits and commercial Schottky diodes, searching the best performance under our RFEH conditions. Finally, we manufactured our designs as a complete system and demonstrated its operation with an IoT concrete application.**

***Index Terms*—Radio frequency energy harvesting (RFEH), dc/dc converters, wireless energy transmission (WET), dual-band, rectification, wireless sensor networks (WSN), Internet of Things (IoT), Schottky diode.**

I. Introduction

THE MASSIVE deployment of Internet of Things (IoT) within our society is an irrefutable reality. Everyday ordinary objects, vehicles, buildings, etc., are being merged with electronics as part of a wireless sensor network (WSN), needing an energy source. They will provide new perspectives to a wide range of areas like industry, healthcare, transportation, telemetry, home and city automation, energy conservation and security, among others.

The power and longevity demands of IoT devices vary broadly depending on the application, in view of their heterogeneous nature. They become a challenge when powering the nodes for a minimum time frame of weeks or months, even years, without compromising the quality of service. A common choice for their power source are non-rechargeable chemical batteries (e. g., lithium, deeply contaminant) [1]. However, for several use-cases are impracticable: in a large-scale deployment or when the device is hard to access, frequent battery replacement or recharge are infeasible by cause of the cost; or simply due to the power consumption and expected run-time. Furthermore, the environmental influence of the massive use of batteries, rechargeable and not, might be enormous and undoubtedly harmful [2], [3].

In this context appears energy harvesting (EH), as the process of capturing small amounts of diverse ambient energy, converting it into electricity and storing it. More particularly, radio frequency energy harvesting (RFEH) devices capture the energy present at the signal carriers in the far field region of ambient radiation. The frequencies of operation are between some kilohertzs and hundreds of gigahertzs [4], which later on are converted to dc.

RFEH can be also used as a wireless energy transmission (WET) technique. The difference is the use of a dedicated energy source that actively radiates. The received power is higher and reaches the requirements of more applications, since the power levels handled in harvesting are typically three orders of magnitude lower [5].

As most of the EH sources within the IoT world and their applications, RFEH may be categorized as "ultra-low power" (barely tens of microwatts) [6]. Currently there is a lack of dc/dc converters in the market for such low levels of power, being them considered for "low-power" conditions (range of milliwatts). This makes the use of EH techniques harder, since the converter stage, needed for getting a proper and stable voltage level, must be custom designed. For that reason, we have developed a battery-less dual-band system capable of harvesting RF energy while using off-the-shelf low-power dc/dc converters. The setup is based on the the store-and-use principle [7], by means of an intermediate stage formed by an innovative autonomous and dynamic switched capacitor design.

A. Related Work

Since Nikola Tesla originally proposed and demonstrated WET in the 1890's [8], the field has grown and matured finding its way to commercial applications [9]. Particularly during the last decade, WET has caught research attention in its two variants (harvesting and active transfer) and far from its hefty origins, the trend has been moved to WSN, where the main objective is the increase of the rectification and conversion efficiencies for low power [5].

The efficiency rapidly drops when the load impedance or the input power decrease ($<1\,\mathrm{M\Omega}$ and $<-10\,\mathrm{dBm}$), and so does the dc output voltage if not controlled [7]. RF-dc conversion efficiencies around 80% has been reported for input powers greater than $10\,\mathrm{dBm}$, with an output load

Manuscript received April 20, 2020; accepted September 6, 2020.

F. Moreno-Cruz is with Infineon Technologies AG, Germany, e-mail: Fernando.MorenoCruz@infineon.com.

M. Ramos Cuevas is with the Technical University of Munich, Germany.

V. Toral, J.F. Salmerón, A. Rivadeneyra and D.P. Morales are with the Department of Electronics and Computer Technology, University of Granada, Spain, e-mail: (see http://electronica.ugr.es/index.php?sec=personal).

around $50\,\mathrm{k\Omega}$ at various microwave frequencies by Agrawal *et al.* [10]. With a 130 and $90\,\mathrm{nm}$ CMOS-based rectifiers, Oh and Wentzloff [11] and Stoopman *et al.* [12] respectively reached sensitivities of ~~32~~ and ~~27~~ dBm both at $1\,\mathrm{V}$ output, although with a capacitive load impedance. Table I summarizes the best efficiencies and minimum RF sensitivities achieved in the literature and the most recent studies to the best of our knowledge. Powercast [9] in turn, presents a commercial power receiver with a minimum sensitivity of ~~11~~$.5\,\mathrm{dBm}$ at $1.8\,\mathrm{V}$ dc output for $915\,\mathrm{MHz}$ using an internal ad hoc boost converter.

For the rectification there are two main technologies implementing diode-based circuits: CMOS, that allows a lower minimum RF input power, and silicon Schottky barrier diodes, with normally better peak efficiency. Additionally, voltage multiplier or a simple diode structure are the most employed circuits [5]. For instance, Chouhan *et al.* [8] and Park *et al.* [17] present cascading schemes for the voltage multiplier fabricated in $0.18\,\mu\mathrm{m}$ CMOS and Schottky barrier technology respectively. Asl and Zarifi [18] also reports a 13 stages rectifier in $0.18\,\mu\mathrm{m}$ CMOS.

Most of the studies aim at a specific frequency channel, although multi-band is employed as well [19]. These designs target arrays composed of multiple antennas or, less frequently, broadband circuitry, focused on the matching network, as Khansalee *et al.* [20]. Piñuela *et al.* [14] builds rectennas and compares different array architectures, demonstrating the operation in a real scenario with a commercial voltage converter (BQ25504) and an LED as application. Donno *et al.* [21] and Liu and Sánchez-Sinencio [22] propose custom dc/dc converters, both charge pump designs and [22] with hill-climbing maximum power point tracking (MPPT).

The store-and-use principle is introduced by Singh *et al.* [7] with a tuned rectifier, achieving promising results in efficiency for low powers. [7] employs two power gates for controlling the energy flow to the load. The first one which runs the store-and-use procedure is not described, the second one achieved by a commercial converter (LTC3108).

B. Contribution

In this work, we propose a complete autonomous system for enabling and simplifying the use of RFEH in IoT nodes through an innovative design based on the store-and-use principle and using commercial dc/dc converters. Figure 1 shows the block diagram including the final application.

Two independent antennas capture the incident RF power at two different frequencies (dual-band), whose impedances are adapted to the rectifier stage by both matching networks. The dc power is now stored in two capacitors. The output of these capacitors to the converter stage is regulated by the logic of *MSwitch* depending on their voltage levels, being able even to completely isolate them. This mechanism enables their charging process in adverse power conditions, since the voltage level never collapses. The harvested energy enters the dc/dc converter, which finally maintains constant the output voltage for the application through a third storage capacitor.

The modularity of the system and versatility of *MSwitch* allow to change easily the frequency band or even to take advantage of its benefits for other EH techniques by only changing the energy input, being compatible with a broad range of power levels.

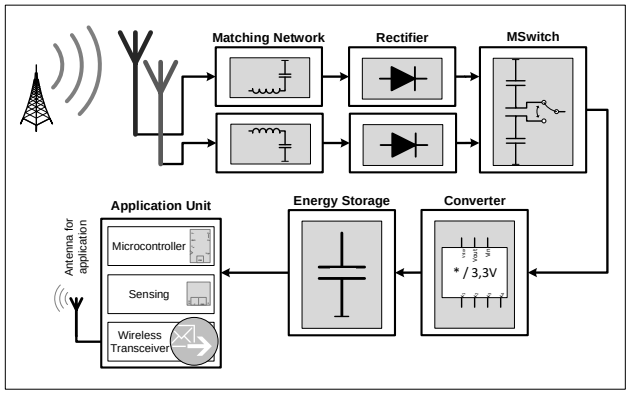

Fig. 1. Overview of whole system.

The main contributions of this paper are outlined as follows.

1) We present an innovative dual-band store-and-use auto-regulated and autonomous design for RFEH (or any other energy source), demonstrating an improvement to the state-of-the-art for its use with commercial dc/dc converters.
2) We analyze the best options of rectifier circuits and diodes, first with simulations and later in the laboratory under the expected power conditions.
3) In parallel, we perform a search among all commercially available dc/dc converters to date and analyze the most efficient ones with ultra-low power levels, taking them often out of the data-sheet characterization. The idea behind was to identify under which circumstances of low power and low voltage they can operate correctly and with which efficiency.
4) We characterize and develop the rest of the system needed stages, targeting an IoT application and manufacturing the best combination.
5) We demonstrate its operation with a model IoT application at the $949\,\mathrm{MHz}$ global system for mobile communications (GSM) band, formed by a $2.4\,\mathrm{GHz}$ transceiver and a temperature sensor.

For the detailed understanding, the model of the initial conditions is presented in Section II; in Section III, we describe the whole system and its operation. In Section IV, we analyze the performance achieved in every stage, focusing Section V on the whole system results and finally, Section VI, draws the main conclusions of this work.

II. System Model

In this section, we present the initial conditions found when diving into RFEH for WSN.

A. Electromagnetic Spectrum

The electromagnetic spectrum is regulated by allocating the different communication bands and, for safety and interference

TABLE I
PERFORMANCE COMPARISON OF STATE-OF-THE-ART CIRCUITS AND SYSTEMS FOUND IN THE LITERATURE

Related Work	Technology	Frequency	Minimum RF P_{in} @ Output Voltage	Conversion Efficiency @ RF P_{in}
Powercast 2110B [9]	-	915 MHz	−11.5 dBm @ 1.8 V	N. A.
Agrawal *et al.* [10]	HSMS-2852	900 MHz	−10 dBm @ 1.3 V	80% @ −10 dBm (60 kΩ)
Franciscatto *et al.* [13]	HSMS-2852	2.45 GHz	0 dBm @ 1.2 V	70.4% @ 0 dBm
Oh and Wentzloff [11]	130 nm CMOS	915 MHz	−32 dBm @ 1 V (cap. load)	N. A.
Stoopman *et al.* [12]	90 nm CMOS	886–915 MHz	−27 dBm @ 1 V (cap. load)	40% @ −17 dBm (1 MΩ)
Piñuela *et al.* [14]	SMS-7630	886–915 MHz	−25 dBm (converter)	40% (end-to-end, real GSM)
	+dual band		−29 dBm (converter)	15% (end-to-end, real GSM)
Nguyen *et al.* [15]	65 nm CMOS	950 MHz	−20 dBm @ 0.9 V	57% @ −10 dBm (10 kΩ)
Xu *et al.* [16]	65 nm CMOS	2.45 GHz	−17.1 dBm @ 0.4 V	48.3% @ −3 dBm (conv.)

reasons, limiting the emitting power. Several studies [23]–[25] assert that the present energy levels in city open-spaces reach $-30\,\mathrm{dBm}$ and even $-20\,\mathrm{dBm}$ at bands of high utilization, as the cellular network (GSM and its successors), TV broadcasting or wireless local networks; although the duty-cycle also varies.

For instance, a typical GSM base station in the $900\,\mathrm{MHz}$ band with a rating of $30\,\mathrm{W}$ and a $17\,\mathrm{dBi}$ antenna gain produces a theoretical power density of $600\,\mu\mathrm{m/m^2}$ at $500\,\mathrm{m}$, according to the Friis transmission equation [5]. Although the signals pathloss follows this equation, it is only valid in free space propagation and assuming direct line-of-sight, being normally received a lower level. Hence, the maximum received power with a standard monopole antenna of $2\,\mathrm{dBi}$ will be up to $8\,\mu\mathrm{W}$ ($-20\,\mathrm{dBm}$).

B. Energy Harvesting

Once the antenna captures the signal, a matching network is needed (maximum power transfer theorem) in order to maximize the power transmission to the rectifier and minimize the reflection coefficient.

Assuming a $50\,\Omega$ commercial antenna, the open-circuit voltage seen at the antenna of the example given above will be $20.5\,\mathrm{mV\,RMS}$. Accordingly, even with the voltage boosting of an ideal matching network at its resonant frequency, these levels do not suffice for reaching the turn-on threshold of present electronics at the rectifier. In addition, due to the high frequency of the bands we are dealing with, fast switching circuits are needed. For these reasons, Schottky diodes with a fast metal-semiconductor junction emerge as one of the only valid technologies.

For a proper application operation, the rectified voltage must be stable and at a specific level. A dc/dc converter runs this action, although with commercially available ones, we find several restrictions derived from the calculations made before: 1) too low voltage input, even though some converters can boost voltages as low as $20\,\mathrm{mV}$; 2) too low energy input, normally they can start their operation at around $50\,\mu\mathrm{W}$; and 3) too low input impedance, which drives the whole system to even lower voltage levels. Trying to solve these constrains with a custom design brings 4) higher price and effort. Therefore, an intermediate stage as the one presented in this paper appears as a promising solution.

Furthermore, the losses while storing the energy can be significantly adverse. Low leakage capacitors must be used (up to $0.5\,\mu\mathrm{A}$ at $3\,\mathrm{V}$) and in case of needing bigger capacitance (super-capacitors, up to $5\,\mu\mathrm{A}$ at $5.5\,\mathrm{V}$), special attention must be given to the storage voltage level in pursuance of the lowest leakage current, as well as to the time of storage.

C. Application Unit Requirements

An IoT application unit consists mainly of a microcontroller (μC), at least one sensor or actuator and a transceiver with an antenna. The target applications are those which do not require constant operation but a duty-cycled one, and which use ultra-low power radio-transceivers and sensors.

In this way, for a simple node measuring ambient temperature, humidity and air pressure and sending it to a gateway, the energy demand is around $1\,\mathrm{mJ}$ during the active mode (where the measurements and communication are done). In deep-sleep mode (where the batteries or capacitors are charged again) the consumption is close to null (less than $300\,\mathrm{nW}$ in some μCs) [4]. To sum up, the average power consumption for periods of, for example, $1\,\mathrm{h}$ would be around $600\,\mathrm{nW}$.

III. RFEH CIRCUIT DESIGN AND IMPLEMENTATION

During the design and implementation of the proposed system, we evaluated each stage independently with the evident dependencies at the interfaces (see Figure 1) and later on, we assembled them together, pursuing the best efficiency and lowest RF input power to start running the harvester. Before fabricating the final prototype, we carried out diverse simulations to prove our assumptions and improve the chosen circuits and components.

A. RF Bands, Antennas and Matching Network

We first examined the legal distribution of the spectrum in Europe from the electronic communications committee (ECC) [26] and followed the studies referred in Section II-A about its utilization. We concluded that the most convenient technologies to harvest from are the cellular network for outdoor use-cases (from GSM until 4G) and the Wi-Fi network for indoor. In any case, the modular design facilitates its exchange in a broad frequency range.

Due to the existence of several frequency bands within the cellular network, whose presence depends on the service providers and the base stations nearby, we performed a spectrum

measurement on our test environment to identify the most favorable bands. The scenario consists of an office area on the outskirts of Munich (Germany) of around $0.22\,\mathrm{km}^2$ from which $0.1\,\mathrm{km}^2$ is free space and the rest three-floors buildings. The measurements were made with a Keysight FieldFox Handheld N9917A spectrum analyzer. The most energetic frequencies found were $949\,\mathrm{MHz}$, corresponding with the 935–$960\,\mathrm{MHz}$ GSM band; $2159\,\mathrm{MHz}$, from the 2110–$2170\,\mathrm{MHz}$ international mobile telecommunications (IMT) band (i. e., 2G and 3G) and the $2.4\,\mathrm{GHz}$ Wi-Fi band for indoor. The energy levels confirmed the model described in Section II-A.

The chosen antennas were commercial antennas with $50\,\Omega$ impedance, an SMA connector and gains between 2 and $4\,\mathrm{dBi}$ for the target frequencies.

The matching networks were designed with Keysight Technologies' ADS 2020 software [27] (ADS), evaluating different topologies and adapting to a simulated impedance determined out of the available models of the next stages. The final topology adopted was a L-matching network due to its broader bandwidth. The final components values were obtained directly measuring with the vector network analyzer (VNA) E5063A from Keysight.

It is worth pointing out that the rectifier impedance depends on the input power due to the nonlinear characteristic of the diodes [19]. Consequently, the theoretical impedance was calculated assuming the target power levels (between -30 and $-15\,\mathrm{dBm}$) and for the two different paths after the rectification, described in the following Section III-C. In particular, the matching networks were designed without load for input 1 (i. e., as an open circuit after the rectification, favoring the charging process) and for input 2 with the equivalent impedance until the application block (favoring the cold-start, i. e., with no energy at all in the whole node).

B. Rectifier

Two analysis were made for the rectifier, relating to which diode and which rectification circuit to use.

1) Diode Selection: Besides the required low turn-on voltage and high switching speed mentioned in Section II-B that make Schottky diodes essential, in applications with high frequency and power restrictions, the junction capacitance and equivalent series resistance are critical for a good performance [28]. Hence, the importance of a good diode selection.

We tested several manufacturers with their Spice models and among them, we selected for further analysis Avago HSPS and HSMS series, Skyworks SMS7630, MACOM MA4E2502, Infineon BAT series, NXP BAT754, ST BAR42-43 and Panasonic DB27308. From which, the outstanding results were given by Infineon BAT63 and BAT15, Skyworks SMS7630 and Avago HSMS2850.

When working with high frequency the package parasitic elements become decisive. Thus, the chosen diode was Infineon BAT15 [29] as the one with by far the best performance including the package model for a series configuration, even when SMS7630 appeared beforehand as better. In this case, the simulation steps were made with ADS (see Figure 2) with a Greinacher circuit [17] and a matching network designed

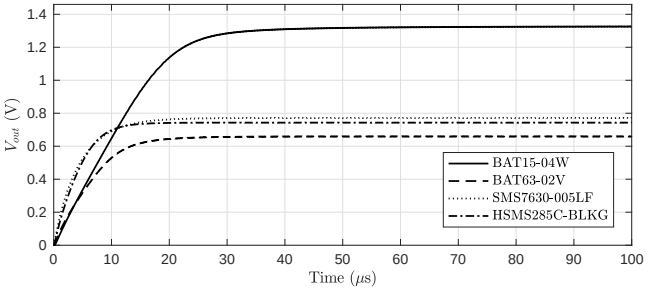

Fig. 2. Simulation of diodes performance in Greinacher configuration with package parasitic elements and impedance matching (ADS), showing V_{out} in time for $-20\,\mathrm{dBm}$ of input power with $100\,\mathrm{pF}$ capacitive load.

with large-signal s-parameter (LSSP) simulation in every case, optimizing between -30 and $-20\,\mathrm{dBm}$ of power input.

2) Circuit Selection: The rectifier purpose is not only the rectification of the input signal, but also a voltage boost. Each diode stage brings a higher voltage level, but on the other hand, it increases the losses by its power dissipation. Furthermore, the converter needs a minimum voltage to start operating and has as well a range with greater efficiency. Therefore, the circuit and its number of stages must be precisely designed for the expected conditions.

We analyzed the rectifying circuits of Greinacher, Cockcroft–Walton (both with 1, 2, 3 and 4 stages), Delon, diode bridge, peak detector, Greinacher quadrupler (full wave) and Dickson for RF (1 and 2 stages). From a first simulation with Spice (LTspice XVII [30]), the circuits of Cockcroft–Walton, Greinacher and Delon stood out. The next simulations were made with ADS, considering already the package parasitic elements of the diode BAT15-04W. A matching network was again designed for every case for the same conditions. A $100\,\mathrm{pF}$ capacitor was used as load instead of a bigger capacitor for faster simulation, since, due to the presence of the series capacitance of the diodes, its size has negligible effect. No resistive load was used as we supposed the next stage (*MSwitch*) in charging phase, i. e., with the switch open and isolated from the converter.

The simulation results (see Figure 3) threw that, for low input powers (e. g., at $-20\,\mathrm{dBm}$), Greinacher (1 stage) has the greatest efficiency (20%), while Delon the lowest (13%) and 2-stages Greinacher and Cockcroft–Walton similar ones halfway (16%). On the contrary, the last two circuits exhibit higher boost, as expected. The rest of versions with N-stages follow the trend, until the fourth stage in both circuits, where the voltage does not increase further for the target power. Although with the simplest Greinacher the voltage is already at valid levels, even for $-30\,\mathrm{dBm}$ as seen in Figure 3-b; we expected losses not reflected in the simulations dropping the output voltage. Consequently, we selected the Greinacher and Cockcroft–Walton circuits until the third stage for further study in the laboratory.

C. Store-and-Use Stage: "MSwitch"

The *MSwitch* stage is an innovative and autonomous dual-input circuit based on the store-and-use principle and on a

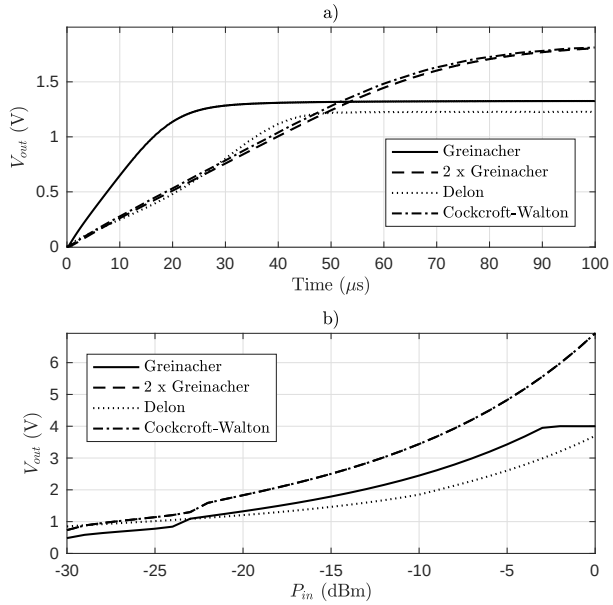

Fig. 3. Simulation of rectification circuits (ADS): (a) V_{out} in time at $20\,\mathrm{dBm}$ (transient) and (b) V_{out} vs. the power input (HB). (2xGreinacher and Cockcroft-Walton overlap).

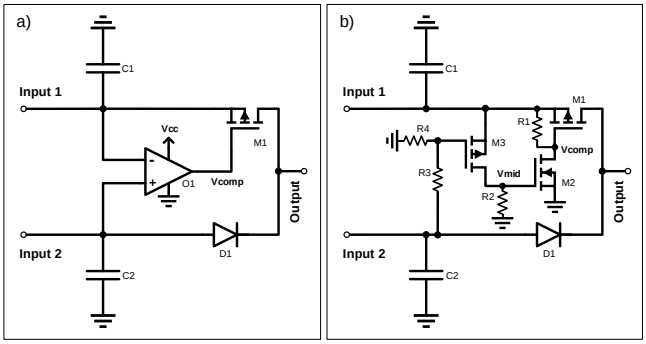

Fig. 4. Schematics of both versions of the store-and-use stage *MSwitch*: (a) with comparator (*Version 1*) and (b) with MOSFETs (*Version 2*).

switched capacitor design, capable of reducing the minimum average input power needed per RF band for an IoT application to operate.

MSwitch, in our two developed variants (see Figure 4), performs three functions: 1), it stores energy in time until the level is enough for running the electronics of the next stage (e. g., dc/dc converter) and for delivering it efficiently; 2), it mixes and regulates both input lines of the system in a dynamic manner, prioritizing the cold-start; and 3), it isolates the energy source from the load in order to not let the voltage drop, again being able to run the following electronics.

1) Working Principle: MSwitch adjusts the current delivery on both lines, being dragged largely from a line while the voltage remains higher than the other one, and even cutting it if the voltage drops, until the level rises again.

During the regular operation, power on both inputs is assumed and of around the same magnitude. *MSwitch Version 1* will perform a cycle where both inputs take turns to deliver energy (see Figure 5). The comparator (O1 in Figure 4) will

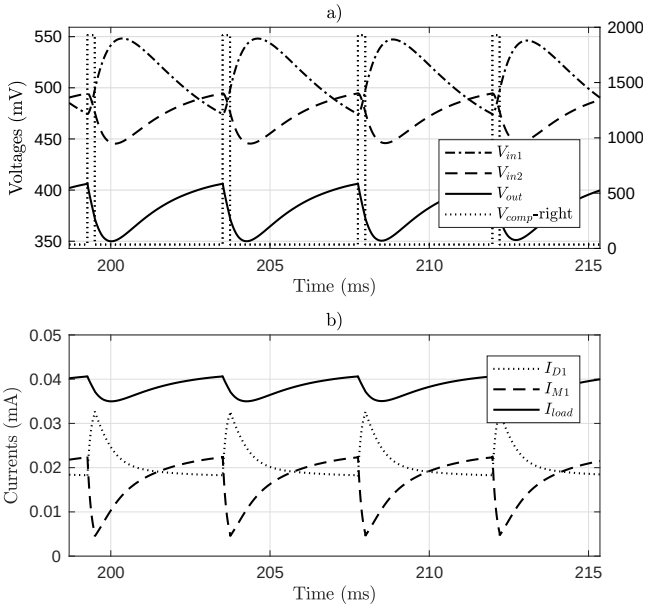

Fig. 5. *MSwitch Version 1*: Simulation of regular operation with Spice models. Cycles of input and output voltages (a) and currents (b). Dc input at every line of $45\,\mu\mathrm{W}$ at $700\,\mathrm{mV}$ open circuit. Load of $10\,\mathrm{k}\Omega$ and capacitors of $100\,\mathrm{nF}$.

switch on the transistor (M1) when the level of input 1 (V_{in1}) is above input 2 (plus some hysteresis) and, therefore, line 2 will be cut. As capacitor C1 discharges, C2 charges again and will eventually reach a higher level. Then, the comparator will switch off the transistor and the cycle will start again with the charge of C1. This process will not get corrupted over time decreasing the voltage level because of the comparator delay time, hysteresis and the proper election of the capacitors size.

For operating from cold-start, V_{cc} will be $0\,\mathrm{V}$ (it comes back from the converter stage, which is not charged yet), so V_{comp} will remain low as well by default. In this way, both lines conduct, self-adapting their currents through the diode until the dc/dc converter reaches a level where the comparator is able to operate (around $0.9\,\mathrm{V}$). Once this condition is satisfied, the store-and-use cycle starts, reaching lower power levels as described above.

In *Version 2*, the behavior of the comparator is replaced by two MOSFETs. We save its power consumption and dependence on the next stage, in exchange of giving up the hysteresis and using a voltage divider for adjusting V_{in2} in the comparison.

In this circuit, both lines auto-regulate their contribution at their best combination, maintaining an efficient voltage level and current flow. It achieves smoother changes, making easier the stabilization of the circuit without marked cycles and favoring the non-appearance of undesired voltage peaks. With Version 2, although the characteristic cycling of Version 1 appears only under special conditions of input power, the store-and-use principle still persists, since a line will only conduct when the voltage reaches a certain value. This means that under adverse energetic circumstances, a line would be cut as well, storing energy meanwhile.

Looking at both circuits from another perspective, *MSwitch*

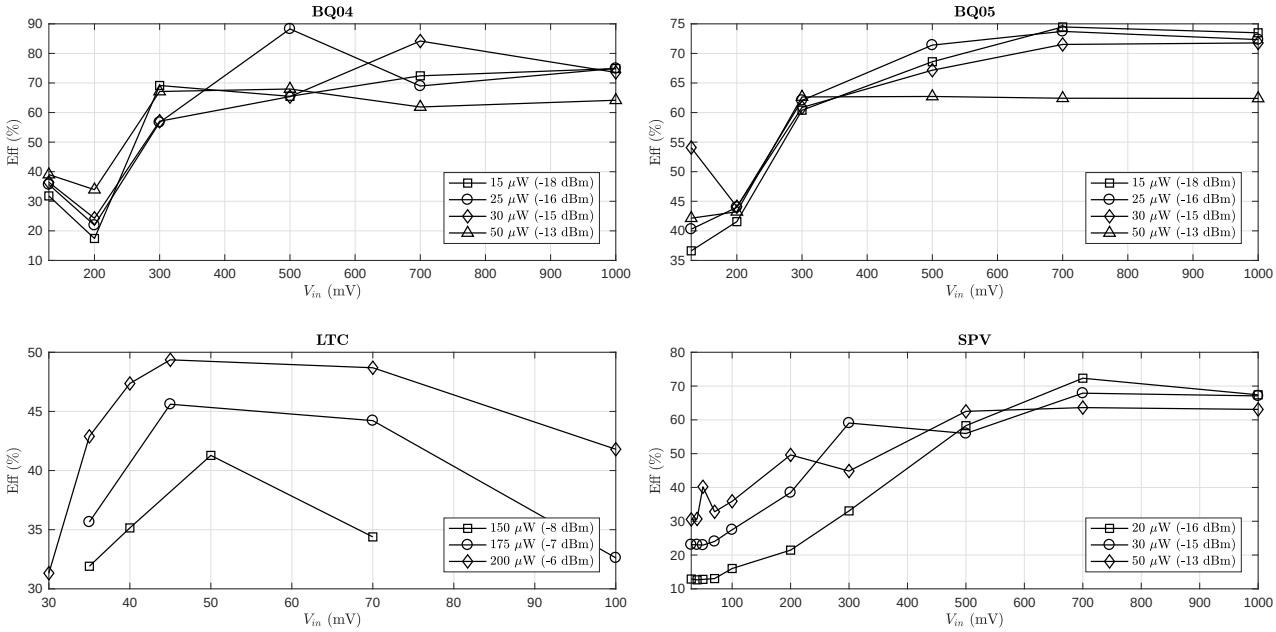

Fig. 6. Simulation of dc/dc converters efficiencies for different voltage and power inputs.

takes a variable voltage reference (input 2) for performing: in Version 1, a cyclic more-energetic burst operation; and in Version 2, an automatic adaption of the simultaneous delivered current. However, in our designs the voltage reference also delivers power. In addition, the fact that this reference is variable plays an important role for EH, since the voltage level depends on the ambient conditions and a fixed value would not be efficient.

Before the actual designs, we employed a P-channel MOSFET in depletion mode instead of the diode. This circuit was symmetrical and had a smoother cycle, as well as lower voltage barrier. These transistors are however not available on the market, so we opted for a Schottky diode without affecting significantly the operation.

D. DC/DC Converters Analysis

A study of the market options for ultra-low power made us focus on BQ25504, BQ25505, SPV1050 and LTC3108, after discarding BQ25570, MB39C831 and MCP1623 through a preliminary study of the features. We based our analysis first on the data-sheet information, carrying out afterward simulations with the available Spice models and the circuit designs recommended by the manufacturers. We went out of the specifications as needed while the model allowed it, and finally manufactured independent boards for their experimental characterization (see Section IV-C).

Figure 6 reports the results of simulations for a range of input voltages at different input powers, starting always from the lowest feasible in cold-start. The efficiency was calculated for an application period, from the triggering of the active mode to the recovery of the voltage using the converters flag. In the transient Spice simulations, we used a triggered load with two states, simulating sleep and active modes according to Section II-C. The configuration for the voltage output was always the closest to $3.3\,\mathrm{V}$ and MPPT was used when available.

The graphics in Figure 6 present BQ25504 [31] standing out with best efficiencies in general for a broad range of input powers, followed closely by BQ25505. LTC3108 and SPV1050 on the other side, cannot operate at low power inputs, although have a lower voltage level from where they can start running. In particular, LTC3108 reaches $30\,\mathrm{mV}$ at $-6\,\mathrm{dBm}$, although at that configuration it cannot work at voltages greater than the shown in the figure.

Due to the expected energy bursts as input of *MSwitch* Version 1, we also simulated this capability on the selected converters. The requirements are reduced to the ability of continuing their activity between pulses for the lower energy levels, avoiding to enter in the cold-start phase for each cycle (what would imply much lower efficiency). The simulations were successful for every converter at the target input powers for capacitances up to $140\,\mathrm{mF}$ (super-capacitor). This limit appeared as trade-off between, on one side, the losses of commercial super-capacitors and time of charging and, on the other side, the energy stored and delivered.

1) Load Energy Storage: The last energy storage element must be dimensioned according to the needs of the application. The energy of an application cycle must be encompassed in the capacitor within the voltage levels where the μC can operate, setting this the minimum capacitance. A too large one would be inefficient as well, since the charging time would substantially increase. Finally, we selected low leakage capacitors with the minimum value recommended by the converters data-sheets, since they sufficed for our application. For instance, in the case of the BQ25504, it meant 4.7 and $100\,\mu\mathrm{F}$ at the main and reserve outputs respectively.

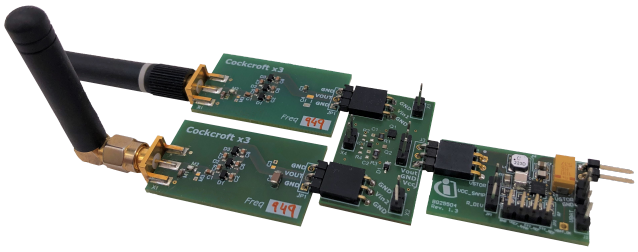

Fig. 7. Picture of the whole harvesting system (no application unit).

E. Application Stage

The chosen application unit for the IoT demonstrator was the Nordic nRF52 development kit [32]. This single board consists on an ARM Cortex M4 system on chip and a 2.4 GHz transceiver including the antenna. Most importantly, the theoretical power consumption according to the data-sheet is within the required range described in Section II-C.

The operation work-flow was developed to be duty-cycled as explained in Section II-C and the internal die temperature sensor was selected for the transmissions. A star topology was set, where the transmitted packets were received by another kit acting as gateway.

IV. Performance Analysis

With the best designs of every stage, we fabricated a prototype in standard FR4 technology for further analysis in the laboratory and demonstration purposes. Figure 7 depicts its modular fashion and dimensions with the circuits selected (see schematic in Figure S1). Following comes a performance analysis based on the measurements.

A. Impedance Matching and Rectification

Figure 8 presents the results of the manufactured rectifiers for 949 MHz. We used only one frequency for simplicity of our designs. The open circuit voltage measurement was made with a signal generator N9310A from Keysight and an Agilent 34461A multimeter in high Z mode. The S_{11} parameter measurement was carried out with the output connected to V_{in2} and to BQ25504 in cold-start. We included the envelop detector circuit as reference, although it was not considered as a solution.

As expected, losses appear in contrast with the simulations, being the measured output voltage around 50% lower than the ideal scenario (see Figure 3-b). Although other factors also affect the result (including the measurement itself), the achieved S_{11} parameter influences highly the efficiency of the boards. Additionally and differing also from it, the circuits of 2xGreinacher and 2xCockcroft-Walton do not exactly overlap, having the last one a greater voltage.

This causes that, at least, a third stage must be used, since BQ25504 requires, according to the data-sheet, a minimum input of 600 mV for cold starting. Finally, we selected the circuit of 3xCockcroft-Walton, as its output voltage reaches the objectives (see Figure 8-a).

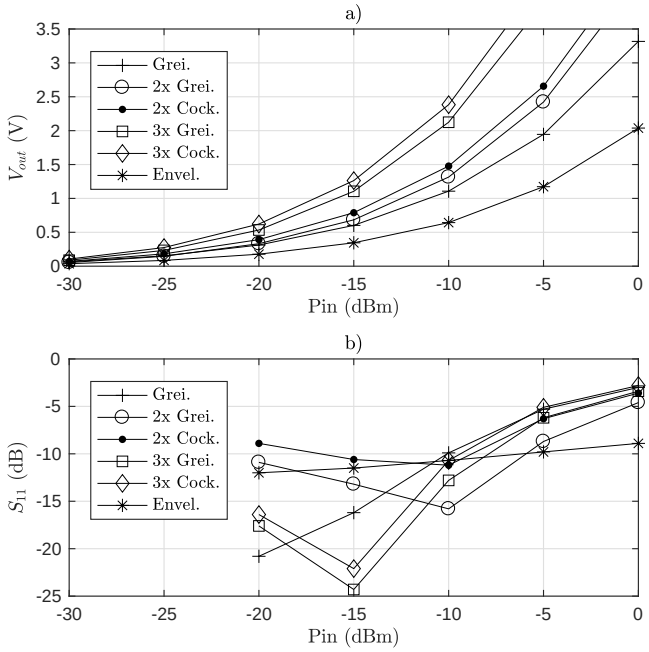

Fig. 8. Measurement of voltage output in open circuit (a) and S_{11} parameter with output connected to V_{in2} and to BQ25504 in cold-start (b) for the developed rectifiers at different power inputs and at a frequency of 949 MHz.

B. MSwitch

We manufactured both versions of the circuit (Figure 4) and both worked as expected, presenting different features that make them interesting for different use-cases.

1) Version 1: It follows the behavior from the simulations (see Figure 5), with its marked cycles clearly seeing in Figure 9. It offers excellent performance for long-term store-and-use cycles in extremely low power scenarios, potentially charging a big capacitor and providing a powerful burst. Nevertheless, the need of a voltage source to run the comparator makes that the following stage must be able to stay powered on during these cycles or with only energy from input 2. Likewise, in more energy-favorable situations, the cycles can be shorter (meaning also smaller capacitors).

Notice that a big difference between the bands energy levels may cause that the voltage-drop in one line while conducting does not go below the other line, remaining this one always cut. In this case, although it is part of the casuistic, it may imply that the energy level on the conducting line is already enough for running the following electronics.

2) Version 2: It tends, on the other side, to the dual and simultaneous conduction over the pronounced cycles, as also expected from the simulations. Once a first dynamic voltage threshold is surpassed (with a powerful burst that helps the cold-start of the converter), the current on each line is self-adapted to the best conditions on the junction by the MOSFETs logic. Additionally, since there is no need of an external power source, the current delivery control initiates from the cold-start as well, increasing the efficiency and therefore the minimum harvested power.

It should be noticed in this version too, that due to the continuous dual conduction, a line would be very rarely

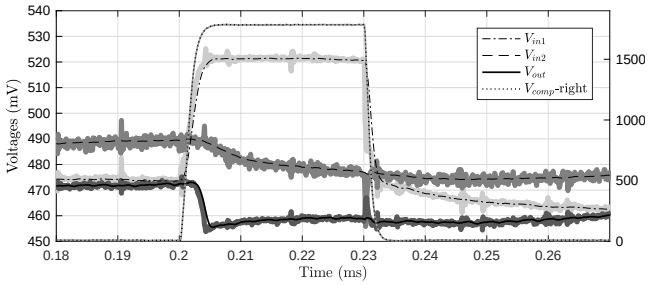

Fig. 9. Measurement of *MSwitch Version 1* cycle in time for an average of $110\,\mu\mathrm{W}$ and $10\,\mathrm{k}\Omega$ input power (dc) and impedance at both lines, with capacitors of $100\,\mathrm{nF}$. BQ25504 in cold-start used as load and V_{cc}. *Filtered data over shaded real measurements, for clearer view.*

completely cut. Only in case of sudden changes in the input or the load the MOSFETs logic would cut a line, avoiding a voltage-collapse and making it rise again, tending fast to the stabilization. This maintains high efficiency also in case of great difference in energy between the inputs or of a too power demanding load.

C. DC/DC Conversion

Our custom boards improved the performance of the converters evaluation kits. However, the measurements, as seen in Figure 10, reveal differences with the simulations of the Spice models (see Figure 6), where the minimum power for starting the operation from cold-start was higher in most of the cases.

The evaluation consisted of a first step where the converter was cold-started and brought to normal operation, measuring also the time needed (Table II). Next, with a variable load mimicking the application (as described in Section III-E), we measured the efficiency during an application cycle. For inputs too low for cold-starting, we brought the converter into operation and later decreased the input levels.

BQ25504 from Texas Instruments demonstrated as expected better response for ultra-low power conditions, counting with the best efficiencies and the lowest power inputs for cold-starting ($15\,\mu\mathrm{W}$ according to the data-sheet, although we measured $30\,\mu\mathrm{W}$). It needs, however, a minimum of $600\,\mathrm{mV}$ (as corrected in the data-sheet [31]) and it behaves at the input as a voltage source of $350\,\mathrm{mV}$, fixing the voltage until the MPPT is able to operate during normal charging process.

As also simulated in Section III-D, we characterized the timings of the converters with a $1\,\mathrm{mF}$ capacitor in every case (for equal conditions). Table II outlines, in the first column, the range of cold-start charging times for the power and voltage inputs measured in Figure 10 and with the application in sleep mode as load. The second and third columns detail the time that every converter is able to maintain adequate voltage levels for the µC with the application in active and sleep modes respectively, and no power input. Finally, the last column depicts the time able to remain out of the cold-start mode with the application in sleep mode and no power input. The results are consistent with the simulations, being every converter capable of operating in burst-mode with the tested conditions.

TABLE II
MEASUREMENT OF TIME CHARACTERIZATION OF DC/DC CONVERTERS

Converter	Charging Time (s)	Active Time (ms)	Sleep Time (s)	Alive Time (s)
BQ04	4160–42	54	237	242
BQ05	1551–69	114	202	706
LTC	16–2	33	355	871
SPV	843–66	118	431	636

D. IoT Application

The power measurements confirmed the awaited results. The energy consumption measured during the active mode was around $85\,\mu\mathrm{J}$; from which the transmission, set to the minimum, represented around $25\,\mu\mathrm{J}$. The deep-sleep power consumption was as well below the expected limit, around $300\,\mathrm{nA}$, although we decided to use a MOSFET as load-switch with the gate connected to the converters flag, in order to avoid boot problems at the cold-start.

V. WHOLE SYSTEM RESULTS

Once every stage was optimized, we tested the whole system with the innovative *MSwitch*. We also analyzed three more different approaches, alternatives to it for proper comparison: direct connection between rectifier and converter (single band), junction through two diodes with storing capacitors behind (exactly like input 2 of *MSwitch*) and in-series connection (as the design from Piñuela *et al.* [14]).

We carried out two experiments: 1), cold-start test, for finding the minimum input power with which can start operating and its efficiency throughout the whole input power range; and 2), hot operation test, for determining the minimum input power with which can maintain its operation, and its efficiency at a reference power level ($-15\,\mathrm{dBm}$). The efficiency was calculated, in the case of hot operation test, with the averaged application-cycle time (in a range between some seconds and a couple of minutes) and the known power consumption of the application active mode. In the the cold-start test, it was calculated with the time until the first packet was received and the energy needed to charge the capacitors of the dc/dc converter. For the setup, we used the previously mentioned signal generator and VNA, and for the in-series circuit, where two different grounds are required, we connected one of them to the grid through a transformer. In every case, the input power was equal at the two lines.

The results are summarized in Table III and Figure S2 and reveal how *MSwitch Version 2* responds better in every aspect analyzed. *MSwitch Version 1*, with similar performance as the in-series design, improves as well the single band and diode + capacitor cases. Comparing the absolute results of Table III with the literature results of Table I, we find a shift in both minimum input power and efficiencies. Since we tested as well under the same conditions the single-band and the in-series circuit [14] (that gives the best performance within the state-of-the-art) and in every case the operation was improved by *MSwitch*, we can therefore assure that this shift comes from a better implementation of the previous stages, in particular, the matching network and rectification. Besides, our system is

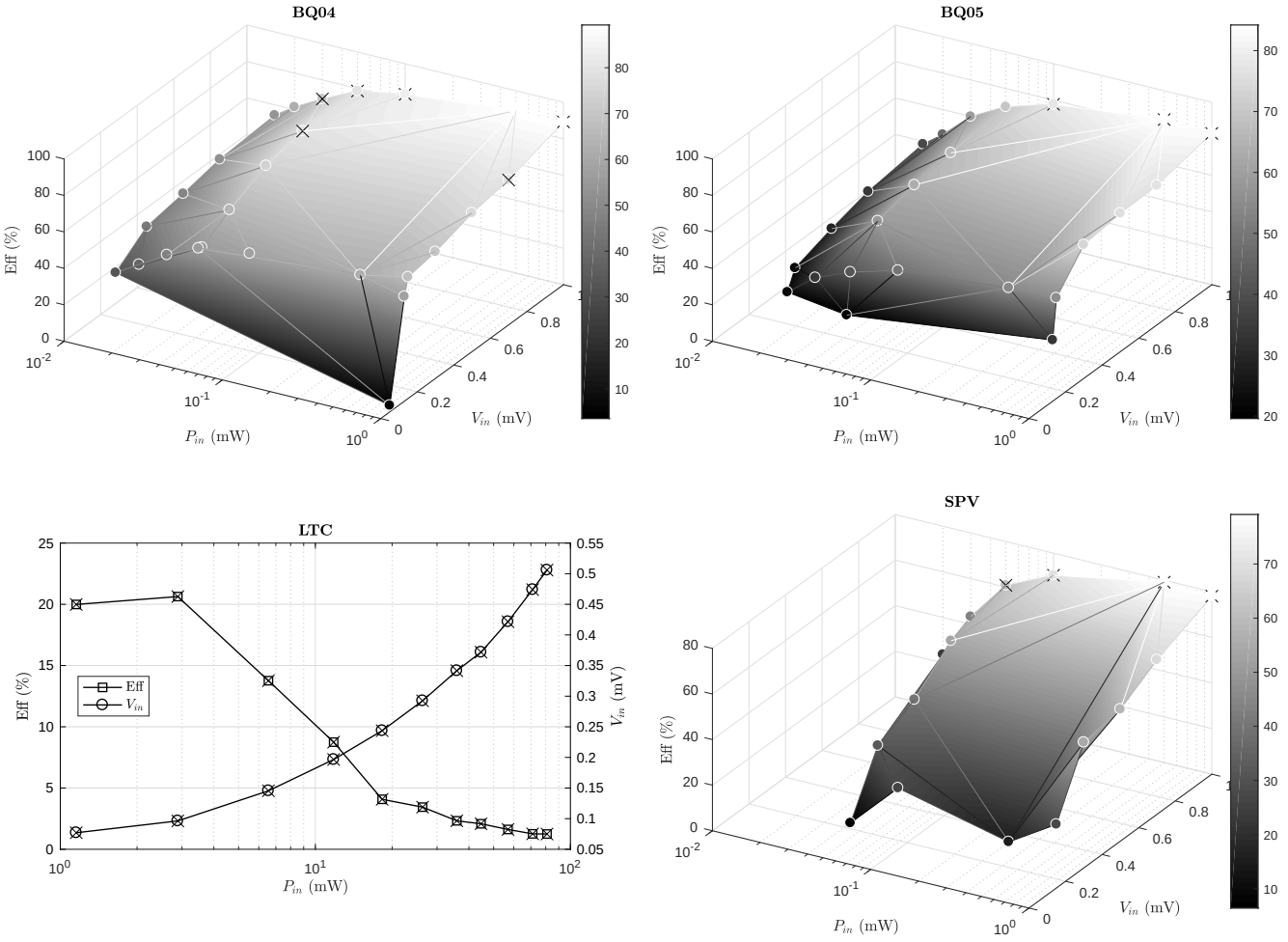

Fig. 10. Measurement of dc/dc converters efficiencies for different voltage and power inputs. Marked points (X) correspond to power-voltage input combinations able to cold-start.

the only one using a real IoT application, while most of the cases of Table III employ a resistor, or even a capacitive load, seeking for the best match to the output.

MSwitch Version 2 emerges with better performance in both cold-start and hot operations. It brings lower minimum input power for starting and maintaining its activity, and better efficiency. This turns into lower first-charge and cycle times for its IoT application. The lack of a component that needs a minimum voltage level for functioning (the comparator in Version 1) and its independent adaption of the currents per line (in contrast with the in-series circuit), make it perform at its best from the beginning and adapt quickly the contribution per line.

Besides, both *MSwitch* designs present an advantage over the in-series design, since its efficiency decreases extremely when one of the inputs is more powerful than the other. For instance, we applied an input of $\cancel{1}2.5$ and $\cancel{1}9.5\,\mathrm{dBm}$ at each line ($\cancel{1}5\,\mathrm{dBm}$ in average). The efficiency was improved by a 4.9 and 4.7% for Version 2 and 1 respectively, while it decreased by a 3% for the in-series circuit. It remained the same for the diode + capacitor design. In this situation, the current forced by the more powerful line makes collapse the voltage on the other input. This does not happen with the *MSwitch* auto-regulation, since it takes advantage of the powerful source without collapsing the second one.

VI. Conclusion

In this work, we have introduced an innovative RFEH dual-band design for energy-autonomous IoT nodes, that improves the current state-of-the-art in numerous perspectives. The circuits, in two different versions, were tested and demonstrated within a complete developed system including rectification, dc/dc conversion and a final IoT application.

We analyzed likewise with several simulations and measurements the whole spectrum of dc/dc converters in the market, characterizing their responses for ultra-low power conditions, often out of the data-sheet descriptions. BQ25504 from Texas Instruments appeared as the best candidate, reaching the lowest input power levels and implementing MPPT, although fixing its input at $350\,\mathrm{mV}$ during its cold-start.

Furthermore, we carried out a deep analysis of the commercially available diodes and state-of-the-art rectification schemes, selecting Infineon BAT15, due to the package parasitic elements; and Greinacher and Cockcroft-Walton circuits

TABLE III
PERFORMANCE OF MSWITCH SYSTEMS IN COMPARISON WITH OTHER SOLUTIONS AND SINGLE BAND

Technology	**Frequency**	**Minimum RF P_{in} @ Output Voltage ***			**Conversion Efficiency @ RF P_{in} ***	
MSwitch v1 BAT15 Schottky	949 MHz	Cold-start	~~1~~5 .0 dBm (IoT app)	+11%	13.1% @ ~~1~~5 dBm (end-to-end, lab., hot oper.)	+9.2%
		Hot Oper.	~~1~~6 .6 dBm (IoT app)	+29%		
MSwitch v2 BAT15 Schottky	949 MHz	Cold-start	~~1~~6 .3 dBm (IoT app)	+34%	13.3% @ ~~1~~5 dBm (end-to-end, lab., hot oper.)	+9.5%
		Hot Oper.	~~1~~6 .8 dBm (IoT app)	+31%		
Single band BAT15 Schottky	949 MHz	Cold-start	~~1~~4 .5 dBm (IoT app)	-	3.7% @ ~~1~~5 dBm (end-to-end, lab., hot oper.)	-
		Hot Oper.	~~1~~5 .1 dBm (IoT app)	-		
Diode + cap. / line BAT15 Schottky	949 MHz	Cold-start	~~1~~5 .6 dBm (IoT app)	+22%	5.9% @ ~~1~~5 dBm (end-to-end, lab., hot oper.)	+2.1%
		Hot Oper.	~~1~~5 .8 dBm (IoT app)	+15%		
In-series [14] BAT15 Schottky	949 MHz	Cold-start	~~1~~5 .1 dBm (IoT app)	+13%	10.2% @ ~~1~~5 dBm (end-to-end, lab., hot oper.)	+6.4%
		Hot Oper.	~~1~~6 .6 dBm (IoT app)	+29%		

**Last sub-column compares the result over the single band option.*

(up to a third level), in spite of the quality of the matching network influencing severely their performances.

The whole system presented finally an improvement over the single band case of a 34 and 31% in the minimum RF power input for the cold-start and hot operation respectively, and of a 9.5% in the efficiency at ~~1~~5 dBm (value taken as reference). Moreover, while *MSwitch Version 1* exhibits similar results as the in-series design (the best performing circuit up to the date to the eyes of the authors [14]); *Version 2* improves by a 21 and 2% its minimum RF power input for the cold-start and hot operation respectively, and by a 3.1% its efficiency (see Table III). Besides, when the inputs have different power levels, both versions of *MSwitch* even increase their efficiencies, while the operation of the rest of the circuits get compromised. We encountered nonetheless an offset of the absolute values in our experiments in relation to the literature. We attribute it to a better implementation of the impedance matching and rectification stages and to the use of a real IoT application, since, under the same conditions, both in-series circuit and single-band exhibited lower performance than *MSwitch*, as described above.

In conclusion, we demonstrated how *MSwitch* is able to operate with off-the-shelf dc/dc converters under ultra-low power conditions and in real dynamic environments, where the band levels do not have to be equal or constant; with RFEH or any other harvesting method, mixing in an efficient manner two power lines.

ACKNOWLEDGMENT

This work was partially supported by the ECSEL Joint Undertaking through the Electronic Component Systems for European Leadership Joint Undertaking under grant agreement No 737434. This Joint Undertaking receives support from the German Federal Ministry of Education and Research and the European Union's Horizon 2020 research and innovation program and Slovakia, Netherlands, Spain, Italy.

REFERENCES

[1] G. Zhou, L. Huang, W. Li, and Z. Zhu, "Harvesting ambient environmental energy for wireless sensor networks: a survey," *Journal of Sensors*, vol. 2014, pp. 1–20, 2014.

[2] P. Kamalinejad, C. Mahapatra, Z. Sheng, S. Mirabbasi, V. C. Leung, and Y. L. Guan, "Wireless energy harvesting for the internet of things," *IEEE Communications Magazine*, vol. 53, no. 6, pp. 102–108, 2015.

[3] H. Jayakumar, K. Lee, W. S. Lee, A. Raha, Y. Kim, and V. Raghunathan, "Powering the internet of things," in *Proceedings of the 2014 international symposium on Low power electronics and design*. ACM, 2014, pp. 375–380.

[4] F. Moreno-Cruz, A. Escobar-Molero, E. Castillo, M. Becherer, A. Rivadeneyra, and D. P. Morales, "Why use rf energy harvesting in smart grids," in *2018 IEEE 23rd International Workshop on Computer Aided Modeling and Design of Communication Links and Networks (CAMAD)*. IEEE, 2018, pp. 1–6.

[5] X. Lu, P. Wang, D. Niyato, D. I. Kim, and Z. Han, "Wireless networks with rf energy harvesting: A contemporary survey," *IEEE Communications Surveys & Tutorials*, vol. 17, no. 2, pp. 757–789, 2015.

[6] F. Moreno-Cruz, V. Toral López, F. J. Romero, C. Hambeck, D. P. Morales, and A. Rivadeneyra, "Use of low-cost printed sensors with rf energy harvesting for iot," in *2019 Smart Systems Integration (SSI)*, 2019.

[7] G. Singh, R. Ponnaganti, T. Prabhakar, and K. Vinoy, "A tuned rectifier for rf energy harvesting from ambient radiations," *AEU-International Journal of Electronics and Communications*, vol. 67, no. 7, pp. 564–569, 2013.

[8] S. S. Chouhan, M. Nurmi, and K. Halonen, "Efficiency enhanced voltage multiplier circuit for rf energy harvesting," *Microelectronics Journal*, vol. 48, pp. 95–102, 2016.

[9] Powercast Co., "Power harvester development kit," http://www.powercastco.com/products/development-kits/#P2110-EVB, accessed: 26-04-2019.

[10] S. Agrawal, S. K. Pandey, J. Singh, and M. S. Parihar, "Realization of efficient rf energy harvesting circuits employing different matching technique," in *Fifteenth International Symposium on Quality Electronic Design*. IEEE, 2014, pp. 754–761.

[11] S. Oh and D. D. Wentzloff, "A- 32dbm sensitivity rf power harvester in 130nm cmos," in *2012 IEEE radio frequency integrated circuits symposium*. IEEE, 2012, pp. 483–486.

[12] M. Stoopman, S. Keyrouz, H. J. Visser, K. Philips, and W. A. Serdijn, "Co-design of a cmos rectifier and small loop antenna for highly sensitive rf energy harvesters," *IEEE Journal of Solid-State Circuits*, vol. 49, no. 3, pp. 622–634, 2014.

[13] B. R. Franciscatto, V. Freitas, J.-M. Duchamp, C. Defay, and T. P. Vuong, "High-efficiency rectifier circuit at 2.45 ghz for low-input-power rf energy harvesting," in *2013 European Microwave Conference*. IEEE, 2013, pp. 507–510.

[14] M. Piñuela, P. D. Mitcheson, and S. Lucyszyn, "Ambient rf energy harvesting in urban and semi-urban environments," *IEEE Transactions on microwave theory and techniques*, vol. 61, no. 7, pp. 2715–2726, 2013.

[15] T.-L. Nguyen, Y. Sato, and K. Ishibashi, "A 2.77 μw ambient rf energy harvesting using dtmos cross-coupled rectifier on 65 nm sotb and wide bandwidth system design," *Electronics*, vol. 8, no. 10, p. 1173, 2019.

[16] P. Xu, D. Flandre, and D. Bol, "Analysis, modeling, and design of a 2.45-ghz rf energy harvester for swipt iot smart sensors," *IEEE Journal of Solid-State Circuits*, vol. 54, no. 10, pp. 2717–2729, 2019.

[17] J. Park, Y. Kim, Y. J. Yoon, J. So, and J. Shin, "Rectifier design using distributed greinacher voltage multiplier for high frequency wireless power transmission," *Journal of electromagnetic engineering and science*, vol. 14, no. 1, pp. 25–30, 2014.

[18] M. B. Asl and M. H. Zarifi, "RF to DC micro-converter in standard CMOS process for on-chip power harvesting applications," *AEU - International Journal of Electronics and Communications*, vol. 68, no. 12, pp. 1180–1184, dec 2014.

[19] U. Muncuk, K. Alemdar, J. D. Sarode, and K. R. Chowdhury, "Multi-band ambient rf energy harvesting circuit design for enabling batteryless sensors and iot," *IEEE Internet of Things Journal*, vol. 5, no. 4, pp. 2700–2714, 2018.

[20] E. Khansalee, K. Nuanyai, and Y. Zhao, "A dual-band rectifier for RF energy harvesting," *Engineering Journal*, vol. 19, no. 5, pp. 189–197, oct 2015.

[21] D. D. Donno, L. Catarinucci, and L. Tarricone, "An UHF RFID energy-harvesting system enhanced by a DC-DC charge pump in silicon-on-insulator technology," *IEEE Microwave and Wireless Components Letters*, vol. 23, no. 6, pp. 315–317, jun 2013.

[22] X. Liu and E. Sánchez-Sinencio, "A highly efficient ultralow photovoltaic power harvesting system with mppt for internet of things smart nodes," *IEEE transactions on very large scale integration (vlsi) systems*, vol. 23, no. 12, pp. 3065–3075, 2015.

[23] M. Russo, P. Šolić, and M. Stella, "Probabilistic modeling of harvested gsm energy and its application in extending uhf rfid tags reading range," *Journal of Electromagnetic Waves and Applications*, vol. 27, no. 4, pp. 473–484, 2013.

[24] A. Palaios, V. Miteva, J. Riihijärvi, and P. Mähönen, "When the whispers become noise: A contemporary look at radio noise levels," in *Wireless Communications and Networking Conference (WCNC), 2016 IEEE*. IEEE, 2016, pp. 1–7.

[25] M. Yılmaz, D. G. Kuntalp, and A. Fidan, "Determination of spectrum utilization profiles for 30 mhz–3 ghz frequency band," in *Communications (COMM), 2016 International Conference on*. IEEE, 2016, pp. 499–502.

[26] Electronic Communications Committee (ECC) within the European Conference of Postal and T. A. (CEPT), "The european table of frequency allocations and applications in the frequency range 8.3 khz to 3000 ghz (eca table)," 2016.

[27] Keysight Technologies, "Advanced design system (ADS) 2020," Sep. 2019.

[28] D. Pavone, A. Buonanno, M. D'Urso, and F. Della Corte, "Design considerations for radio frequency energy harvesting devices," *Progress In Electromagnetics Research B*, vol. 45, pp. 19–35, 2012.

[29] Infineon Technologies, *Series silicon RF Schottky diode pair. BAT15-04W datasheet*, Jun. 2018.

[30] Linear Technologies, "Ltspice XVII," Apr. 2020.

[31] Texas Instruments, *Ultra Low-Power Boost Converter With Battery Management For Energy Harvester Applications. BQ25504 datasheet*, Oct. 2011, revised Nov. 2019.

[32] Nordic Semiconductor, *nRF52 DK for Bluetooth LE, Bluetooth mesh, ANT and 2.4 GHz applications. nRF52 product brief*, Apr. 2019.

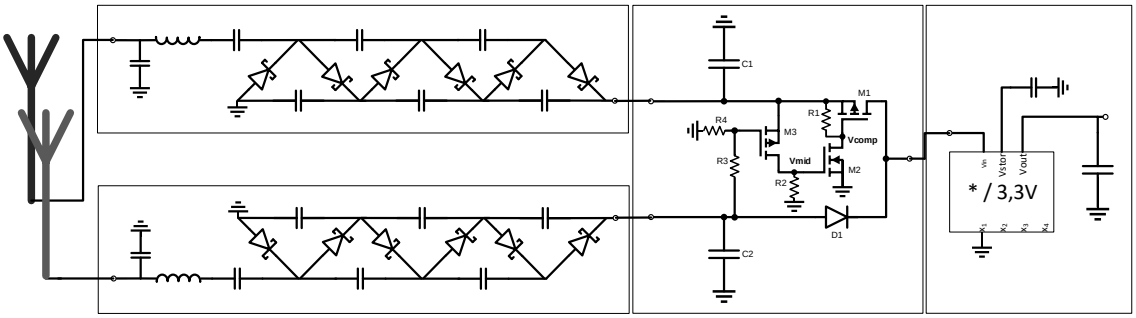

Fig. S1. Schematic of the whole harvesting system (no application unit). *Dc/dc converter simplified, see BQ25504 data-sheet for more details [30].*

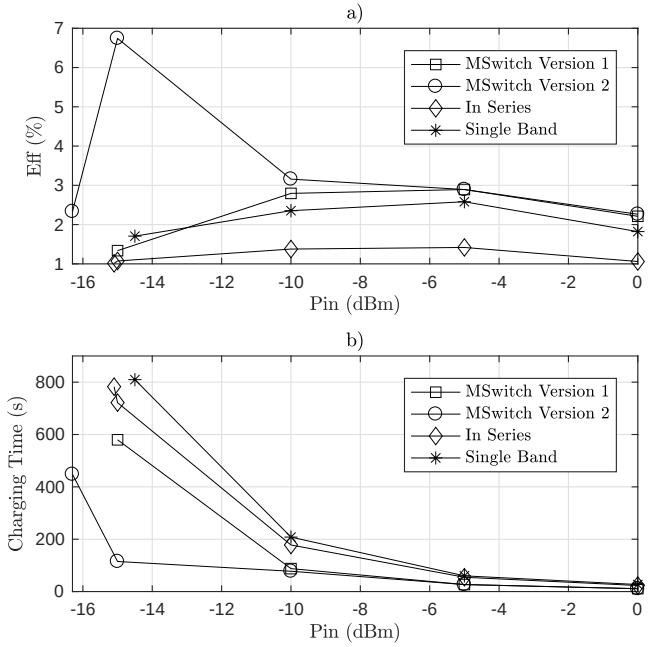

Fig. S2. Measurement of *MSwitch* efficiency (a) and charging time (b) in comparison with other solutions in cold-start operation.

2.2 Publication 2

"...pero es necesario que se pueda comunicar cualquier noticia,
que la electricidad pueda hablar..."
– Francesc Salvà Campillo

treNch: Ultra-Low Power Wireless Communication Protocol for IoT and Energy Harvesting

Fernando Moreno-Cruz[1,2], Víctor Toral-López[2], Antonio Escobar-Molero[1], Víctor U. Ruíz[3], Almudena Rivadeneyra[2] and Diego P. Morales[2]

[1] Infineon Technologies AG, Munich (Germany)
[2] Department of Electronics and Computer Technology, University of Granada, Granada (Spain)
[3] eesy-innovation GmbH, Munich (Germany)

MDPI Sensors

- Received September 2020, Accepted October 2020, Published October 2020 (volume 20, issue 21)
- DOI: 10.3390/s20216156
- Impact Factor: 3.275
- JCR Rank: 15/64 in category *Instruments & Instrumentation* (Q1) and 77/266 in *Engineering, Electrical & Electronic* (Q2)

sensors

MDPI

Article

treNch: Ultra-Low Power Wireless Communication Protocol for IoT and Energy Harvesting

Fernando Moreno-Cruz [1,2,*], Víctor Toral-López [2], Antonio Escobar-Molero [1], Víctor U. Ruíz [3], Almudena Rivadeneyra [2] and Diego P. Morales [2]

1 Infineon Technologies AG, 85579 Neubiberg, Germany; Antonio.Escobar@infineon.com
2 Department of Electronics and Computer Technology, University of Granada, 18004 Granada, Spain; vtoral@ugr.es (V.T.-L.); arivadeneyra@ugr.es (A.R.); diegopm@ugr.es (D.P.M.)
3 Eesy-Innovation GmbH, 82008 Unterhaching, Germany; ruiz.quero@eesy-innovation.com
* Correspondence: Fernando.MorenoCruz@infineon.com

Received: 21 September 2020; Accepted: 22 October 2020; Published: 29 October 2020

Abstract: Although the number of Internet of Things devices increases every year, efforts to decrease hardware energy demands and to improve efficiencies of the energy-harvesting stages have reached an ultra-low power level. However, no current standard of wireless communication protocol (WCP) can fully address those scenarios. Our focus in this paper is to introduce *treNch*, a novel WCP implementing the cross-layer principle to use the power input for adapting its operation in a dynamic manner that goes from pure best-effort to nearly real time. Together with the energy-management algorithm, it operates with asynchronous transmissions, synchronous and optional receptions, short frame sizes and a light architecture that gives control to the nodes. These features make *treNch* an optimal option for wireless sensor networks with ultra-low power demands and severe energy fluctuations. We demonstrate through a comparison with different modes of Bluetooth Low Energy (BLE) a decrease of the power consumption in 1 to 2 orders of magnitude for different scenarios at equal quality of service. Moreover, we propose some security optimizations, such as shorter over-the-air counters, to reduce the packet overhead without decreasing the security level. Finally, we discuss other features aside of the energy needs, such as latency, reliability or topology, brought again against BLE.

Keywords: Wireless Sensor Networks (WSN); Internet of Things (IoT); ultra-low power; Bluetooth Low Energy (BLE); energy harvesting

1. Introduction

The eruption of the Internet of Things (IoT) in our society has presented us with a scenario where every object is connected to the Internet for interaction. In this heterogeneous infrastructure, each intelligent point can communicate with the rest of the nodes, services or people through different topologies to substantially affect the user's experience and quality of life.

Under those circumstances, a challenge arises when powering the nodes without affecting the application quality of service (QoS). Generally, a power cord is excluded from the possible options because of its expenses, inconvenience or impracticability [1]. A common option is batteries; however, not only their cost in terms of their frequent replacement or recharge, but also their environmental impact play an important role: non-rechargeable chemical batteries (e.g., lithium) are a common choice, which are deeply contaminating [2]. Within this framework energy harvesting (EH) appears as a way of taking advantage of the diverse energy present in the environment, converting it into electricity for its use.

EH, however, encounters some difficulties in terms of the power capable of being extracted and its stability over time. Most of the EH sources are categorized as "ultra-low power (ULP)" (barely tens of microwatts) [3], see Figure 1. Moreover, the energy flow might unpredictably rise, drop, or directly stop, e.g., weather changes in solar, wind and thermal or lack of band use in RF. These force the applications over these technologies to be ULP as well, in addition to not presenting extremely low latency or high-dependability demands.

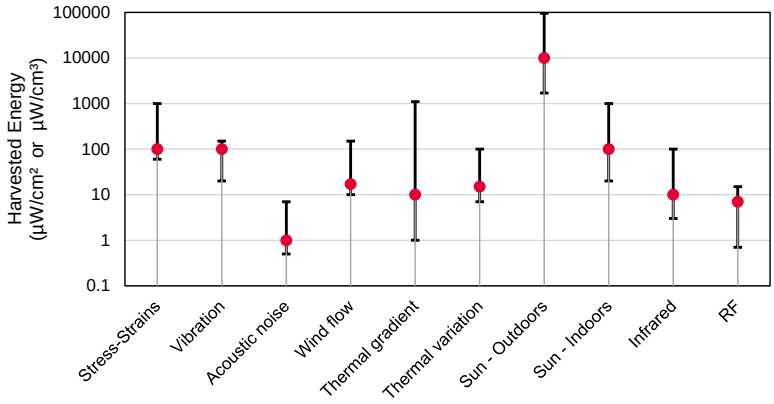

Figure 1. Power comparison of most common EH sources [3]. Typical range and most frequent value.

To address this, two fronts emerge:

1. Hardware, where every stage must be optimized. Starting from efficiency of energy gathering and conversion phases [4–7], and ending with consumption of the microcontroller (µC) and transceiver.
2. Software, where the operating system (OS) and the wireless communication protocol (WCP), often together, have the greatest influence. They are light and simple, and follow the ULP requirements without compromising the QoS [8–10].

An ULP IoT application generally operates in a duty-cycled fashion. This means remaining in a low energy consumption state (sleep phase) during most of the time and waking up to carry out measurements and communication (active phase). In recent years, a lot effort has been devoted to the improvement of the µCs and radio transceiver performance. Outstanding consumption figures have been achieved of less than 300 nW and 1 mJ for the sleep and active phases, respectively [5].

Meanwhile, low and ULP WCPs have emerged and extensively been deployed, although most of them are not suitable for EH use cases. Their operating principles and architectures do not always match these scarce energy profiles, often also burdened by legacy modes and the pursuit of broad interoperability. In particular, they often employ large packet-headers that lead to unnecessary communication overhead [11], normally due to the desire for more functionality or compatibility that other use cases can energetically afford, i.e., WCPs that first spotlight more energy-advantageous scenarios. Likewise, the bases of their operation, founded frequently on synchronous communications, imply the use of power consuming timers during the sleep phase or of the radio by the medium-sensing in asynchronous cases that make them more energy-demanding. Moreover, the cycle times are determined without considering the energy status, leading to more failures and therefore inefficiency [12]. The reception at the nodes, for its part, which represents a great sink of energy [13], is habitually realized indiscriminately, despite its necessity. Moreover, even the WCPs with ULP requirements are often designed to work with a constant power source, i.e., a battery, and are not efficient with abundant power drops, i.e., an EH supply [12].

1.1. Related Work

Table 1 summarizes the most extended WCPs for embedded systems and ultra-/low power use cases. Bluetooth Low Energy (BLE), after its last release in 2017, stands out for the ULP scenarios [14].

Its functionality without previous connection (advertising) and the more recent mesh option has achieved extraordinarily low energy requirements. The advertising mode, however, lacks the reception feature and does not count with security (besides some connection-based modes having weaknesses as well) [15]. In the mesh case, an ULP node needs a "friend" node for implementing receptions and security, which brings overhead and also vulnerabilities [16,17]. Solving this would require the establishment of a traditional master–slave connection with synchronous operation, leaving behind its benefits. Zigbee and Thread, both based on the IEEE 802.15.4 standard, exhibit excellent power consumption as well, and are a possible solution for the most energetic EH use cases. ANT and Z-Wave, besides being proprietary protocols, stand already on slightly higher energy levels, as does Wi-Fi, intended for higher data rates and not fitting in these ULP scenarios. EnOcean, on the other side, is the only one decidedly designed for EH, although with limited functionality and of proprietary use, which complicates its deployment.

Table 1. Most common ultra-/low power WCPs.

	Power Consumption	Range	Topology	Data Rate	Standard	Power Management Techniques
BLE [14,18,19]	Ultra-low 10 s of µW	WPAN 100 m	Star, Bus, Mesh	1 and 2 Mbps	Bluetooth SIG	Phy.-layer (FSK-based mod.) Periph. skip connections Mesh: Friendship, flooding
Wi-Fi [14,18]	Low power 10 s of mW	WLAN 250 m	Star, Mesh	11–300 Mbps	IEEE 802.11	-
Zigbee [14,18,19]	Ultra-low ∼50 µW	WPAN 100 m	Star, Mesh, Cluster	20, 40, 250 kbps	IEEE 802.15.4	Phy.-layer (O-QPSK mod., DSSS) Parent relationships Beacon-enabled/CSMA/CA
Z-Wave [14,20]	Low power ∼100 µW	WPAN 30 m	Mesh, Star	40 kbps	Proprietary	Low data rate Phy.-layer (FSK mod., sub-GHz) Asynch. TX, Synch. RX
ANT [21,22]	Ultra-low ∼80 µW	WPAN 30 m	Star, Bus, Mesh	60 kbps	Proprietary	Phy.-layer (FSK-based mod.) Isochro. + Medium-sensing
Thread [20,23]	Ultra-low ∼50 µW	WPAN 100 m	Mesh, Star	250 kbps	IEEE 802.15.4	Phy.-layer (O-QPSK mod., DSSS) Asynchronous CSMA/CA
EnOcean [24,25]	Ultra-low µW	WPAN 30 m	Star	125 kbps	Proprietary	Phy.-layer (ASK/FSK mod., sub-GHz) Low overhead Asynch. TX, Smart ACK
LoRaWAN [26–28]	Low power 100 s of µW	WWAN 10 km	Star	0.3–50 kbps	Proprietary	Phy.-layer (LoRa mod., sub-GHz) Low data rate Asynch. TX, Subsequent RX

WPAN, wireless personal area network; WLAN, wireless local area network; WWAN, wireless wide area network.

Other solutions not considered are NB-IoT (5G), LoRaWAN and Sigfox, as they are designed for long-range communications (WWAN) and have higher power consumptions. RFID (radio frequency identification) and near field communication (NFC) stay out of the scope as well, since they need express interaction for every transmission, as well as being proximity communication protocols.

Concerning the power management, the state-of-the-art WCPs address it with different energy-saving techniques, which make them fit with different use cases; see Table 1. Presuming duty-cyclic functionality for all of them, the trend is asynchronous transmissions, where the node decides when to wake up and transmit. However, some protocols also implement it synchronously, such as BLE (in its connection-based mode), with time slots, as WirelessHart (based on IEEE 802.15.4 too) [29], or even hybrid modes between them, such as ANT or Zigbee.

Furthermore, the physical layer plays an important part. Low data rates and FSK- and PSK-based modulations are commonly used, while some use sub-GHz bands as well in search of less interference and more signal integrity. Especially noteworthy are the IEEE 802.15.4-based protocols with spread spectrum (DSSS) [30] and LoRaWAN implementing it dynamically with its proprietary algorithm.

Other mechanisms include diverse medium access methods, such as the Zigbee beacons, synchronous protocols skipping events, such as BLE conn., the EnOcean "smart ACK", which employs the acknowledgment to send data to the node, or the parent/friendship relationship of Zigbee and BLE, respectively, where the gateway or an extra node saves the messages directed to a node while this node stays in sleep phase (saving energy), for later retransmitting when it wakes up.

Regarding custom protocols addressing this niche market, to the best of our knowledge there has not being any attempt during the last decade to standardize or disseminate a WCP which solves the issues described above. Nevertheless, the literature focuses on improving the current protocols, proposing new features or solving vulnerabilities. For instance, Zhang et al. [31] and Laurentiu et al. [32] reported security flaws in BLE and LoRaWAN, Sigfox and NB-IoT, respectively. Mao et al. [33] proposed a security configuration strategy for IEEE 802.15.4 that adapts its level depending on the network security threats, service requirements and harvested energy. Meka and Fonseca [34] introduced a procedure that improves the Zigbee route selections through a different route-cost calculation. To conclude, among many other successful examples, Bomfin et al. [35] proposed an extension for the LoRa modulation which leads to a more energy-efficient system.

1.2. Contribution

In this work, we propose a new WCP intended for the harshest EH scenarios of IoT, with the latter goal of public standardization and broad expansion. *treNch* solves the ULP wireless sensor network (WSN) use cases through the use of a light cross-layer architecture with asynchronous transmissions, synchronous (subsequent) and optional receptions, short frame sizes and by a dynamic operation adaption depending on the energy status. This cross-layer principle is reflected in the proposed energy-management algorithm that uses two different operation modes for the sleep phase depending on the power input.

For evaluating our design, we conduct a detailed experimental analysis of *treNch* under different realistic scenarios, comparing the results with BLE at the same conditions and for its different profiles. Our focus is the power consumption at the nodes, but we discuss other features as well, such as the security, latency or reliability, among others. In particular, we propose techniques to implement low-overhead secure mechanisms that reduce the packet size without decreasing the security level, such as shorter over-the-air counters.

The main features that make *treNch* succeed in comparison with the state-of-the-art WCPs mentioned before are outlined as follows:

1. Power management algorithm sensing the energy status (cross-layer).
2. Control in the nodes, responsibility in the gateway, complexity in the client.
3. Asynchronous transmissions, synchronous (subsequent) and optional receptions.
4. Low frame overhead (including optimized security).
5. Randomized and controlled medium access (without sensing).
6. No physical-layer definition: adaptive to conditions.
7. Dynamic nodes emitting power.

The remainder of this article is organized as follows. In Section 2, we provide an in-depth description of the new WCP and its operation. In Section 3, we analyze the performance achieved through a comparison with BLE and finally, Section 4 draws the main conclusions of this work and expounds the focus for future work.

2. "*treNch*"

treNch is a cross-layer WCP and OS designed for ULP conditions in the IoT area, meant to be used with embedded EH systems as part of an interconnected WSN.

The operation principle is based on the node best-effort: Their transmissions are carried out asynchronously around a defined period, while the receptions (optional and previously notified) are performed synchronously right after the transmission (see Figure 2). In this way, a node transmits

when its energy level allows it, not being forced to wake up to transmit/receive periodically by the risk of the connection being closed due to inactivity.

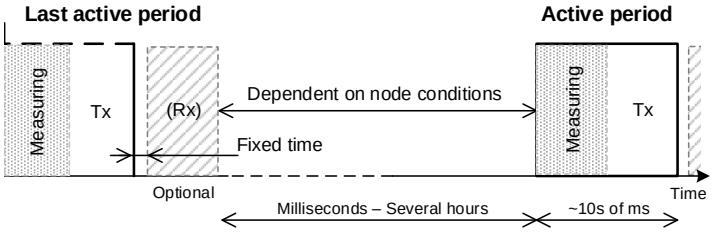

Figure 2. *treNch* principle of operation.

2.1. Network and Roles

In *treNch*, a network is formed by subnetworks in star topology; see Figure 3, where new nodes have to perform an automatic registering process in order to be part of it. The communication is connectionless, closed and private.

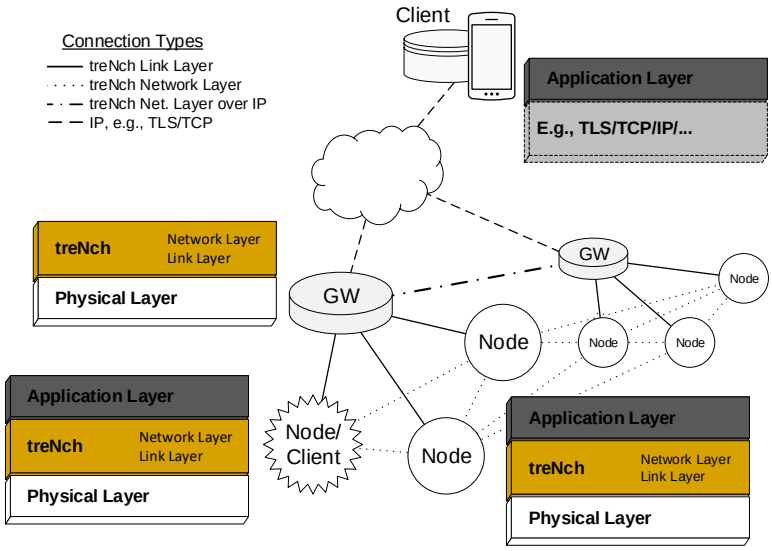

Figure 3. *treNch* network and protocol stack per device.

A network has three different device roles:

- Node: Usually a sensor running under ULP conditions.
- Gateway (GW): Always ready to receive the node messages and answer them if pertinent. With network/link-layer functionalities, but transparent at application level. It defines a sub-network. No power limitations.
- Client (back-/frontend): Server and data consumer and in direct communication with the gateways. Interprets/triggers the application services, but with no network/link-layer functionalities. It approves new nodes registrations. No power limitations.

Subnetworks (gateways) and clients are interconnected through an auxiliary communication protocol not defined by *treNch*. Nonetheless, secure standards which are widely spread as TLS are recommended.

2.2. Protocol Stack

At link-layer level, a node is exclusively connected with a gateway through a bidirectional communication link. In the general use case, the gateway solely forwards the information coming from a node to the client and vice versa, apart from the network/link-layer directives, as the registering,

acknowledgment or reception cycle, among others. This communication happens in the packet header but also in the payload with reserved parameters (see Sections 2.3 and 2.4).

However, network-layer level direct node-to-node/s communication is also allowed through the gateway, by means of "channel subscription" (permanent receptions) or momentary point-to-point transmission. A *channel* is defined by a parameter class and a specific origin node. This is configured by the client in both cases, since its functionality is defined at application level.

To this end, the gateway keeps a queue of parameters for each node, sending them together in the payload of the next node reception phase. In the event of inter-sub-network transmissions, the gateway of the emitting node forwards the payload to the gateway owner of the destination node through a broadcast over the auxiliary protocol, e.g., IP.

Following this principle, a node without power concerns could also work as a client, as seen in Figure 3, with no need for the auxiliary protocol.

Regarding the physical layer, *treNch* does not define it in the protocol stack, leaving it open for every use case conditions. In this way, the noise, path losses, interferences of the environment, energy conditions and available hardware can be considered.

2.3. Frame Format

Tables 2 and 3 introduce the frame formats for the two options within the bidirectional communication (node-to-gateway and gateway-to-node, respectively).

The frame encapsulates the packet structure with the *length* and *cyclic redundancy check (CRC)*. The physical-layer *preamble (preamb.)* needed by the radio is not defined, while the *sync word* is used as address. In the node-to-gateway transmissions, it indicates the node *origin ID*, whereas in the opposite case, it points out the node *destination ID (destin. ID)*. Since at link-layer level it is the only communication allowed; there is no need to include more address fields.

Table 2. treNch frame format for node-to-gateway transmissions (security Level 0).

PREAMB.	**ORIGIN** ID (SYNC)	LENGTH	PROT. VER.	PAYLOAD						CRC
				PARAM			PARAM 2	...	**CTR /NODE**	
				Type		Data				
				Class	Length				RX-Cycle **Reset** **ACK**	
X Bytes	2 Bytes	5 bits	3 bits	5 bits	3 bits	N Bytes	M Bytes	...	6 bits 1 bit 1 bit	2 Bytes
		1 Byte		1 Byte					1 Byte	

Table 3. treNch frame format for gateway-to-node transmissions (security Level 0).

PREAMB.	**DESTIN.** ID (SYNC)	LENGTH	PROT. VER.	PAYLOAD						CRC
				PARAM			PARAM 2	...	**CTR /GW**	
				Type		Data				
				Class	Length				RX-Cycle **RSSI**	
X Bytes	2 Bytes	5 bits	3 bits	5 bits	3 bits	N Bytes	M Bytes	...	6 bits 2 bits	2 Bytes
		1 Byte		1 Byte					1 Byte	

The packet is concluded with the *protocol version (prot. ver.)* and *CTR (treNch control)* fields. As seen in Tables 2 and 3, the *CTR* follows two structures depending on the direction, including four different subfield types (functionalities explained in Section 2.4):

- *RX-Cycle*. It indicates after how many operation cycles the node will perform a reception. 0 forces the gateway to answer or, sent by the gateway, asks the node to receive again.
- *Reset*. It signals that the node is coming from a brown out reset (1), giving valuable information about its energy conditions.
- *ACK*. It acknowledges the last node reception.
- *RSSI*. It gives instructions to the node about the required emitting power, adapting it according the needs.

The payload is composed of an array of "*params*", where a *param* is a group of two subfields: *type* and *data*. The *data* subfield carries the effective payload to transmit, while the *type* describes it with the data *class* and its *length*. Although some *classes* are reserved for the protocol, they do not follow any standardization, being defined by the user.

The bit assignation for every field sets the maximum *param-data* size in 7 Bytes and the maximum payload size in 27 Bytes. This gives a maximum theoretical throughput of 85.2%.

A message from a node is by default directed to the client and vice versa (only network configuration messages stay in the gateways). Nonetheless, the node-to-node communication use cases require special handling. In these scenarios, the header remains unchanged and the network recipient/origin is explicitly indicated with an address *param* in the payload, being the following *params* part of that connection. The payload, therefore, must be sequentially read. In this way, e.g., a node sending a packet with information to the client and to two different nodes would fill the payload with: client data *params*, address 1 *param*, node 1 data *param*, address 2 *param* and node 2 data *param*, in that order.

2.4. Workflow

Figure 4 represents the nodes active phase workflow. When a node enters *treNch_Start* (active phase), the different application profiles are executed, for later continuation to a transmission. In case the node is not registered yet, it proceeds first to registration (see Section 2.4.1).

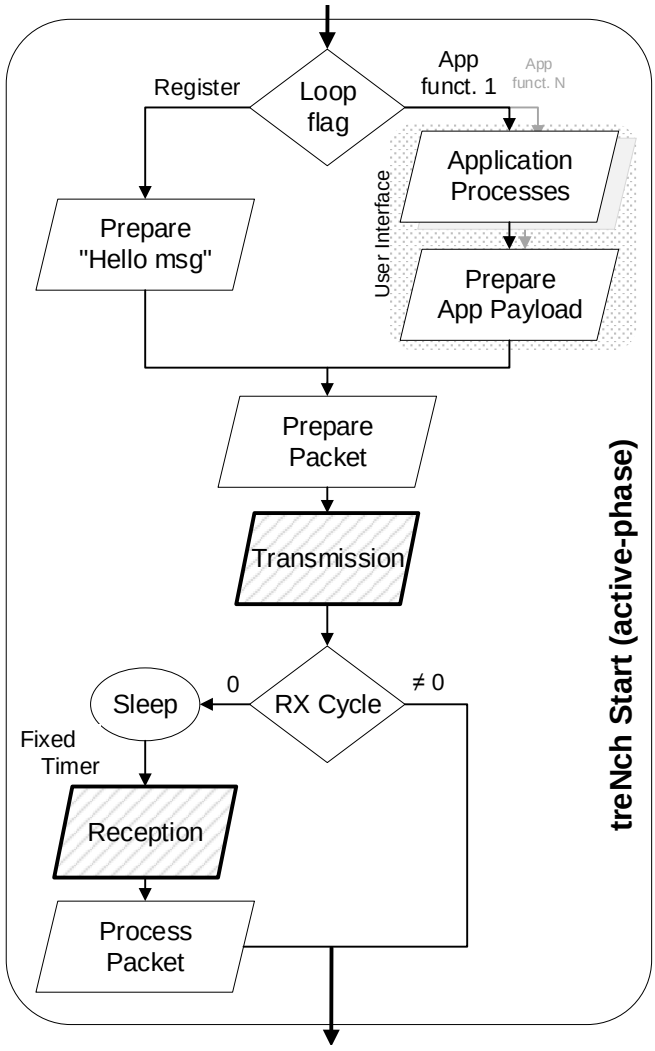

Figure 4. *treNch* node active phase workflow. Executed cyclically before and after a low power state (sleep).

Once the transmission is made, depending on the *RX-cycle*, the node executes the reception routine or goes directly to a low power consumption state for later waking up and starting the cycle again. The reception routine includes a sleep phase during a short and fixed time period, the packet reception and its processing at application- and network/link-layer levels.

The gateway workflow consists of a listening interface for the *treNch* node packets. It answers them with the data queue for each node when the *RX-cycle* indicates it and forwards the *params* to other nodes (queue) or through the auxiliary protocol interface to the clients or other gateways. Similarly, it includes forwarding the packets in the opposite direction or special actions regarding the network configuration, such as the registering or channel subscription, both described in the following.

2.4.1. Registering

Before a node can interact with a network, it must become part of it through registering. A node sends a *"Hello message"* until a gateway answers with the registration information, starting only then with its application functionality.

The *Hello message* includes the node hardware ID, type and application. The reply includes the same hardware ID and the *treNch* ID, a shorter identifier (2 Bytes) that will be used as address for the node. Up to this time, when the *treNch* ID is assigned, the address employed in the frames (origin and destination ID) is a reserved one for broadcasting.

The process concludes when the client approves the registration, while the node remains in a quarantine list in the gateway with limited functionality (although transparent for the node).

In the case of a network with more than one gateway, every gateway broadcasts first to the rest of them the hardware ID, the received RSSI and a random number (for ties). The gateway with the best conditions adds the node to its sub-network and continues the process.

2.4.2. Acknowledgments

treNch carries out acknowledgments at the link-layer level, not performing automatic re-sends (in the nodes) but notifying the application about incorrect transmissions. It is up to the application to decide if the message should be re-sent or ignored. In the case of the gateway, the retransmissions are automatic.

For transmissions in gateway-to-node direction, the correct reception is flagged with the *ACK* bit of the frame in the next cycle. For the opposite direction, the mere reception of a frame indicates implicitly the successful previous transmission, since it is the node who forces the gateway to send a packet. That means that a node application can request at any time an acknowledgment setting the *RX-cycle* to 0.

2.4.3. Node-to-Node Transmission/Channel Subscription

First, the client triggers the process (application level), since it is the one with the overall information. It sends a command to a node, setting the transmission/reception of a *param-class* (see Tables 2 and 3) to/from an specific node with several repetitions, a expiry date or certain circumstances as trigger. This might also change some other configuration parameters, such as the operation or reception periods according to the application. This process must be consistent with each node involved, since their applications have to be able to send/process a specific *param-class* as well as be realistic with the energy needs to fulfill the QoS.

The node then answers the command, acknowledging the client positively if applicable. Next, for the node-to-node transmission, it modifies at application level the destination of the messages for the following transmissions, indicating it on each frame. For the channel subscription, it sends with the same acknowledgment packet a network command to the gateway to set up the channel. Hereinafter, the gateway will forward automatically the configured *param-class* coming from the specified origin to the target node.

2.5. Power Management Algorithm and Energy Flag

The energy flag is an external binary signal informing about the status of the power capacitor/battery. It comes usually from the dc/dc converter required by the EH stage or even from the µC itself. The voltage levels between its thresholds for changing the value (with hysteresis) must encompass the worst case of the active phase energy needs and be above the minimum µC operation level.

After initiation or a reset, the hardware and the *treNch* directives are initialized; see Figure 5. The last one includes setting up the protocol configuration and the registering information stored in flash, if this applies. By default, the system follows the *Rhythm Mode*. This means entering after the active phase in a deep sleep state to be woken up by a timer with the *minimum cycle time*. This value is defined by the user and has a slight random factor to avoid continuous collisions.

While the energy allows it, the system stays in this mode. In case of a decrease in the power input (energy flag down at the wake-up), *treNch* first increases the timer and goes to power-down state. Once the capacitor is charged (energy flag high), it wakes up and directly enters the active phase. In the next cycle, it goes again to deep sleep, with the updated timer value. If after several rounds the rhythm timer reaches its maximum (set by default at 115% of the minimum), the system goes to *B-Effort Mode*.

B-Effort Mode largely decreases the power consumption (see measurements of Section 3.1), since it sends the µC to power-down state after each active phase. With no timer but a wake-up by the energy flag (high), this allows the nodes to operate under extreme energy-adverse circumstances, in the range of up to 400 nW and with high power input fluctuations.

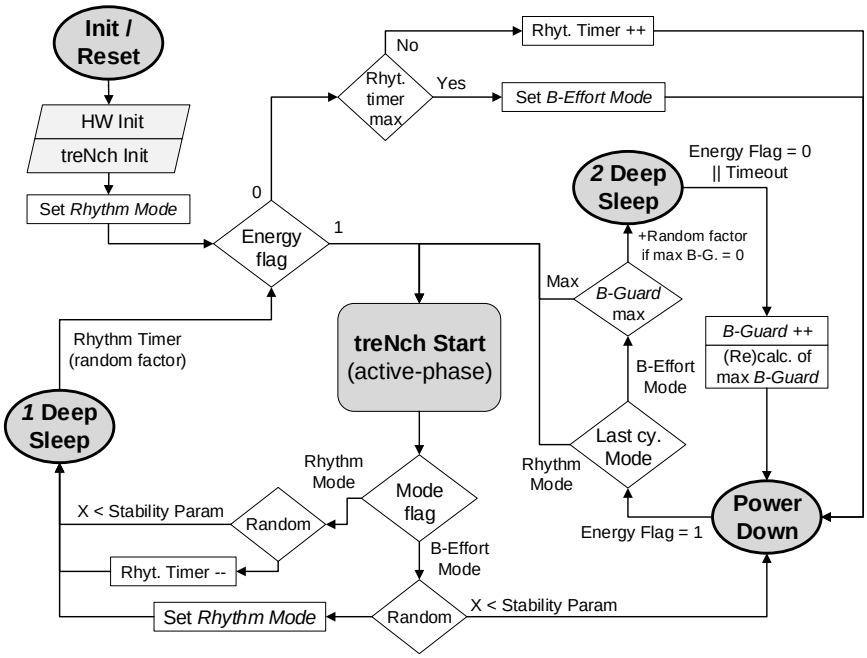

Figure 5. *treNch* node Sleep Modes and energy optimization algorithm workflow.

To avoid the violation of the *minimum cycle time* in the *B-Effort Mode*, *treNch* performs an estimation of the power input to set an approximation of a period without the wake-up timer. This is done with a second deep sleep state set with a clock that wakes up with the fall of the energy flag. The period is estimated with the time spent until the flag falls, knowing the sleep states power consumptions (µC data-sheet) and the energy needed for an active-cycle (value known by the user for the capacitor dimensioning and energy flag hysteresis configuration). The desired cycle time is achieved repeating the process according to the calculation until the maximum *B-Guard* value is reached, see Figure 5.

In the case of a maximum *B-Guard* resulting in less than one, the next operation cycle goes directly to the active phase (pure best-effort), performing randomly the estimation again. In the worst scenarios, this avoids a much bigger cycle time and waste of energy, due to the *B-Guard* calculation round.

treNch implements a procedure for returning cautiously to *Rhythm Mode* and to the *minimum cycle time*, through random attempts within the workflow. The periodicity of these attempts is configurable through the *stability parameter*, which incorporates in the method the expected power input fluctuation (set by the user).

The cross-layer energy management and usage defined by *treNch* achieves consequently great ULP operation while keeping the QoS, with brown out resets happening only in severe unexpected conditions.

2.6. Security

The existence of nodes with a very tight energy budget makes it complex to design a security concept without adding a significant overhead. Nevertheless, the criticality of security is such that compromises need to be introduced very carefully. We define four security levels:

- Level 0: no security. Packets are neither encrypted nor authenticated. For evaluation purposes. Not recommended for productive environments.
- Level 1: authentication. All packets are authenticated. For scenarios in which the exchanged data can be left public.
- Level 2: encryption and authentication. All packets are authenticated and encrypted.
- Level 3: encryption and authentication with extended *Message Integrity Check (MIC)*.

The secure modes have the following features:

2.6.1. Secure Device Provisioning

Nodes are programmed with a pre-shared commissioning key, shared with the gateway and used only during the registering. Alternatively, it may also use an out-of-band mechanism. The goal is to securely distribute the node ID and a newly generated communication key to a node, for the first commissioning or after the node goes back to an unregistered state (e.g., after too many unsuccessful communication attempts with the gateway). For this, we propose using a commissioning key, which is reserved for the registering, together with a 104 bits random value, acting as a nonce for the cryptographic engine and included in the *Hello message* generated by the node. The gateway stores the nonce used by the node during the registering request and replies with the {communication key, node ID} pair. It uses the nonce chosen by the node with its most significant bit toggled (to avoid nonce repetition) and the pre-shared commissioning key to authenticate and encrypt the response. Commissioning exchange is always done with security level 3.

2.6.2. Separation of Concerns

The gateway, during the registering, assigns different communication keys for the point-to-point communication with the different nodes, so if a communication key is exposed, only a particular link with a particular node is compromised.

2.6.3. Replay Attack Protection

Replay attacks are avoided during registering, since the gateway stores all the random 104 bits nonces ever used by the nodes with a particular commissioning key and silently rejects further commissioning attempts using the same nonce. 104 bits nonces are sufficiently large, and registering attempts are sufficiently rare that the probability of the node randomly repeating a nonce is extremely low. Replay attacks are also avoided after registering, since the nodes always employ an increasing 104 bits counter, acting as a nonce, of which only the least-significant byte is added in the packet. The most significant bit of the counter is always used as zero by the node. If the gateway needs to

reply, it will always use the last nonce received by the node, with the most significant bit set to one. If the gateway receives a counter equal to or lower than the last received counter, it will assume that a counter overflow occurred and will try to decode the packet adding one to the hidden (not transmitted over the air) most significant part of the counter. Gateways always store the last counter received from every node, while nodes only need to store in flash when the hidden most significant part is increased (e.g., every 255 packet transmissions). A loss of sync in the counter would be detected by the node, since no answer from the gateway would be received, and the node would react by going back to the unregistered state and trying a new commissioning attempt, which triggers a renewal of the key and reinitializes the associated counter. It might happen if an overflow is missed by the gateway (e.g., more than 255 successive packets are lost by the gateway) or if the node fails to properly store the most significant part of the counter in the flash (e.g., due to energy constraints).

In security levels 1 to 3, the whole packet is authenticated. The header is extended with the security level and counter fields and the *MIC* is appended before the CRC. In security levels 2 and 3, only the payload and the *CTR* field are encrypted (authenticated encryption with associated data).

In security level 1, *CBC-MAC* [36] authentication is proposed to generate the *MIC*, while in levels 2 and 3, *AES-CCM* [37] is proposed to get both authentication and encryption, using 128 bits keys and the AES-128 block cypher. *MIC* is truncated to the least-significant 4 Bytes in levels 1 and 2, and to the least-significant 8 Bytes in level 3. The length of the *MIC* field dictates how often a gateway or a node may trigger a key refresh. To avoid birthday attacks in levels 1 and 2, the key should be renewed before it has been used 2^{16} times, while in level 3 it should be renewed before it has been used 2^{32} times.

2.7. Other Features

2.7.1. Reliability

treNch offers acknowledgments if the application demands it, thus, the reliability of the network ultimately resides in the energy conditions of the nodes and their predictability (best-effort).

2.7.2. Latency

A node is configured with a *minimum cycle time* and, while the power input allows it remaining in *Rhythm Mode*, it operates asynchronously with that duty cycle up to a 15% higher value. If the power input decreases, the system enters in *B-Effort Mode*, where an estimation of that period is performed and ultimately follows the best-effort principle. The boundary case is where the *minimum cycle time* is set to 0, meaning this pure best-effort or operation by external interruptions.

2.7.3. Medium Access Control

The short frame size, the high typical operation period for EH systems and the randomness of the transmissions act as the medium access control mechanism; together with the above mentioned minimum period of activity (avoiding that a node saturates the medium when the power conditions are favorable). The packet losses because of medium access collisions are consequently expected to be irrelevant [38].

2.7.4. Emitting Power

In the *CTR-RSSI* field, the gateway gives instructions to the node in every reception to adjust the emission power. This helps to decrease the power consumption when the path losses are low or to reduce the wrong transmissions and increase the range in the contrary case.

2.7.5. Hardware

Concerning the hardware requirements, in the case of a node, the mentioned energy flag needs an external binary signal informing about the energy level, i.e., a dc/dc converter or µC with that

functionality. Moreover, the dimensioning of the capacitors must be realized together with the expected energy availability, device power consumption and the energy flag hysteresis [5].

In the case of a gateway, simply enough memory and computing power for fulfilling the above described activities are required.

3. Comparison with BLE

In this section, we analyze the performance of *treNch* through a detailed comparison with one of the main ULP protocols. We selected BLE considering not only its power consumption characteristics (one of the lowest, see Table 1), but also its wide spread and versatility within different scenarios. Hence, we analyzed BLE in connection, advertising and mesh low power modes.

The focus of the analysis is given to the power consumption of the nodes, since the main purpose of *treNch* is to address the requirements given by EH scenarios. Nonetheless, we also discuss other relevant aspects.

3.1. Power Consumption Analysis

The experiment was carried out with the first release of *treNch* in accordance with the characterization made in the previous section. The tested code includes the complete workflow of a node described in Figures 3–5 with a simple application returning a random number, and a lite version of the gateway for one sub-network administration. The security grade chosen was Level 0 for better performance isolation.

In the case of BLE, we used the S132 Softdevice version 7.0.1 of Nordic Semiconductor, which includes the three operation modes of interest. The application over the BLE stack was the same, changing accordingly for the studied scenarios, and the security was disabled as well. For that purpose, we used an adaption of the UART emulator with transmission characteristic set as *Notify* and reception as *Write without response*.

In terms of hardware, we used for both protocols Nordic nRF52 development kits [39] with SDK version 16. It consists of a board with an ARM Cortex M4 system on chip and a 2.4 GHz transceiver, including the antenna. We chose this option because the theoretical power consumption according to the data-sheet is within the required ULP range and because Nordic provides with the official BLE Softdevice, simplifying our development steps and allowing easy reproduction of the results.

In both cases, we used two devices, working as gateway, client and node, server, in the terminology of *treNch* and BLE, respectively, and a third one acting as *friend* only for BLE mesh. For *treNch*, the client role was played by a computer with an USB-UART interface to the gateway. Moreover, for BLE we employed a commercial sniffer in parallel for extra validation of the communication (without interference in the measurements).

For a proper comparison, we configured the radio transceiver of *treNch* with the same physical-layer characteristics of BLE. Additionally, the emitting power was set to 0 dBm in all the cases, except of the scenario where we analyze its impact.

The measurements were carried out at 3 V input power (given by the development kits) and with a Teledyne Technologies HD6054 oscilloscope for the active phases and an Agilent 34461A multimeter for the sleep phases. Figure 6 depicts an illustration of the measurements with a representation of the power consumption in time during the active phase for the most general cases of the protocols. The difference in frame sizes, processing time and peak power needed by the architectures can be clearly recognized. In particular, BLE already presents greater active-cycle times and a marked offset in consumption, seen during both the transmission and reception phases, due to the inherent software architecture processes.

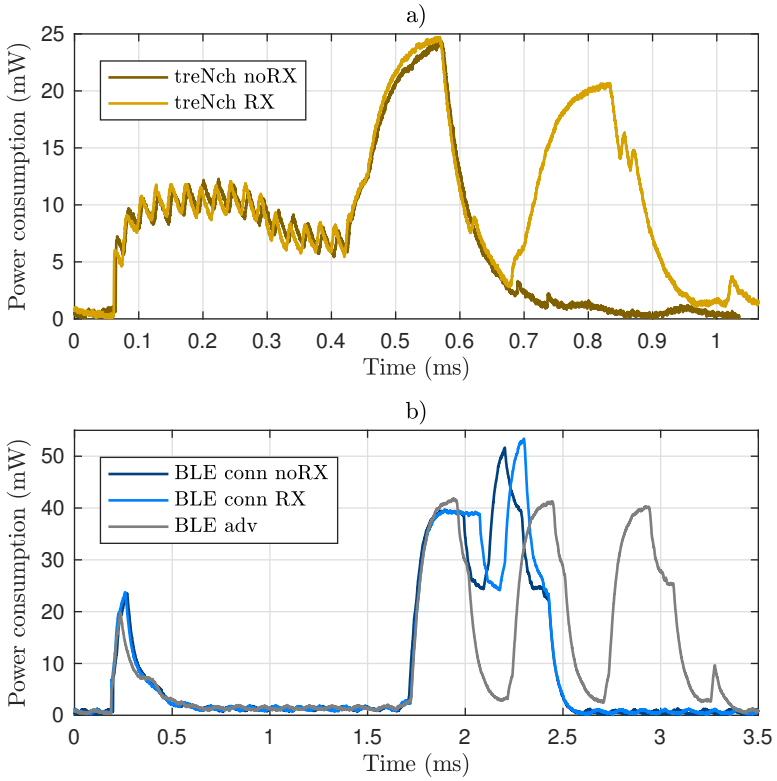

Figure 6. Measurement of power consumption in time during active phase. Most general cases of *treNch* (**a**) and BLE (**b**).

In Table 4, the average power consumption and duration time of every event in the protocols are summarized. In each case, the effective payload was of 1 Byte (except for the large payload scenario), no security was used and an error- and noise-free channel was assumed.

Table 4. Measurements of power consumption for every event.

Event	Duration (ms)	Avg. Power (mW)
treNch		
Start, TX (0 dBm)	15.7	3.9
TX (from DSleep)	700×10^{-3}	9.8
TX (from PDown)	819×10^{-3}	12.7
TX Max. Pay. (27 B)	1.5	10.7
+ RX	1.1	4.2
Registering Cycle	15.7	4.9
Deep Sleep	-	5.4×10^{-3}
Power Down	-	360×10^{-6}
BLE		
Conn.-TX (0 dBm)	2.6	12.3
Conn.-TX Max. Pay. (23 B)	2.7	18.9
Conn.-TX, RX	2.7	14.2
Conn.-Advertising, Pairing	5.6×10^{3}	1.1
Conn.-Keep Alive	2.4	11.0
Conn.-Sleep	-	5.4×10^{-3}
Adv. - Start, TX (0 dBm)	441.8	778×10^{-3}
Adv. & Mesh-TX	3.1	10.9
Adv. & Mesh-TX Max. Pay. (26 B)	3.8	15.2
Adv. & Mesh-Sleep	-	4.5×10^{-3}
Mesh-TX, RX	4.2	11.1
Mesh-Start, TX	518.3	2.9

After that, we evaluated different use cases where we compared the performance between *treNch* and the diverse BLE options, based on the characterized events. We join the corresponding event consumptions, satisfying the protocols workflow to determine their energy demands for every situation.

3.1.1. Transmitter

In this scenario, the nodes do not perform application data receptions. We analyzed the average power consumption over a cycle in a broad period spectrum, assuming that the power input was always sufficient and uninterrupted for the required operations.

Figure 7 reveals how *treNch* stays always below in the cycle average power consumption, thanks mostly to the energy-management algorithm described in Section 2.5. The figure includes for more detail the *treNch* consumption in the most power-demanding situation of the *Rhythm Mode* (dotted line), meaning this pure timer operation during the sleep phase. For a given cycle time, when the power input is distanced from that curve, *treNch* starts operating in *B-Effort Mode*, with the period estimated from the power input. As soon as the power rises, *Rhythm Mode* takes over again with a more precise cycle.

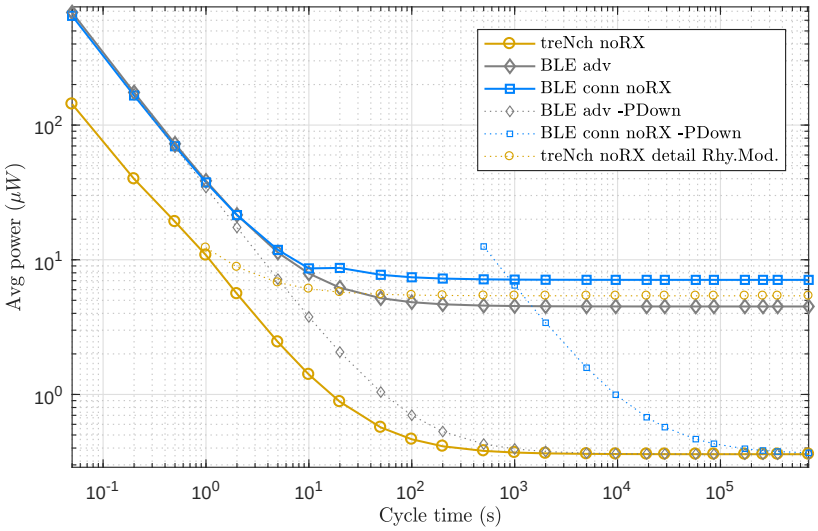

Figure 7. Use case of node with only transmission needs. Average power of a complete cycle over cycle time. *Note logarithmic scale in both axes.*

BLE adv. (same case as mesh) attends to only one operation principle, being the power consumption dominated by the transmission energy in the first part of the graph (done in three different channels) and by the sleep phase in the second, with the transmission negligible and tending to constant.

For BLE conn., the curve has two tendencies. This is because of the obligation of sending keep alive messages as the operation cycle increases, to keep the connection open. The consumption then stays constant, tending to the sleep phase consumption too. In contrast to *treNch*, both BLE cases have a fixed and stable cycle time.

In the BLE cases, although not implemented by the BLE functionality, we tested how the consumption would be if the application would set the µC into power-down state, for being later woken up by an external signal (dotted lines in the graph). For that, we used the power-down value consumption of *treNch* as reference. As result, despite the sleep consumption decreasing greatly, only in cycle times higher than an hour is beneficial for BLE conn., since the inactivity during the power-down means losing the connection and opening it in every cycle, aside of the security issues that arise. Likewise, it is still not enough for BLE adv. to overtake *treNch*, due to the three-channel transmission.

Notice that for this approach to follow a specific cycle time, an external clock not considered in the consumption would be needed, or the implementation of an algorithm similar to *treNch*.

3.1.2. With Reception

This scenario presents nodes with application data receptions over the same period spectrum as the previous one and again assuming sufficient and uninterrupted power input. Figure 8 depicts the tested protocols with a reception in every active-cycle and for the maximum allowed by *treNch* (62, i.e., maximum given by the *RX-Cycle* frame field). We also evaluated the hypothetical use of the power-down state by BLE and, again for reference, the *Rhythm Mode* of *treNch*.

The results are very similar to the previous scenario. The power consumptions of BLE conn. and *treNch* do not vary significantly, since for both protocols the methodology is equal and the extra energy needed for the reception is comparable to some more time in sleep state. BLE mesh, however, presents a big difference respect to BLE adv. and even higher consumption than BLE conn. in the low cycle times. This is due to the polling and reception to the *friend* device in three different channels. Nevertheless, it surpasses quickly BLE conn., although not *treNch*, due to the 96 h friend poll timeout and the lower sleep state consumption, where all finally tend.

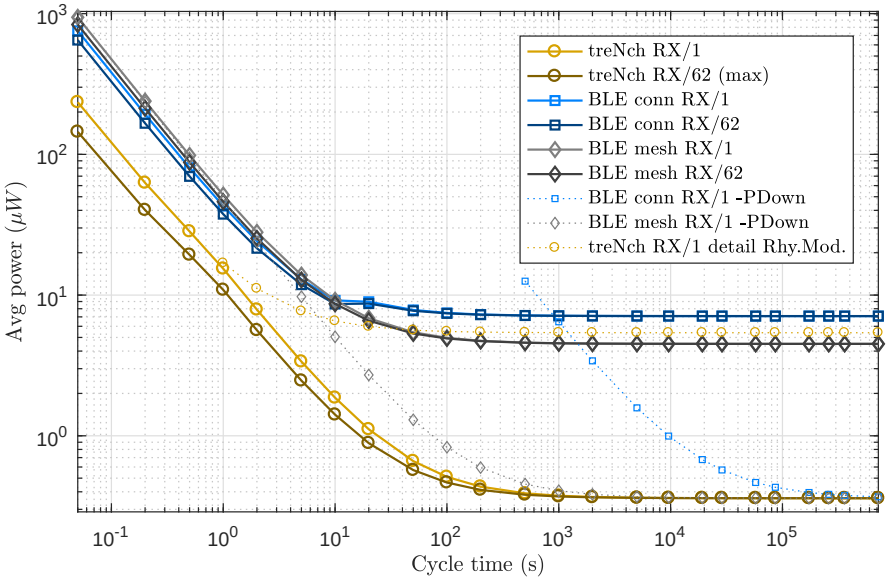

Figure 8. Use case of node with different reception period needs (every N active cycles: *RX-Cycle*). Average power of a complete cycle over cycle time. *Note logarithmic scale in both axes*.

3.1.3. Critical Energy

This use case assumes the worst situation where the power input allows only the active phase. We consider that the µC is turned off shortly after the end of every active cycle due to lack of energy and the sleep consumption, with the sleep phase having no effect in the analysis. This evaluation also contemplates the occasional situation after a brown out, often happening with EH devices.

Table 5 presents the results with and without reception. The consumption of BLE conn., 2 orders of magnitude above *treNch*, proves how highly inefficient the synchronous protocols are in this kind of scenarios, because of the need for re-connecting. BLE adv./mesh stays from 1 to 2 orders of magnitude above as well, due mostly to the initialization and guard time and in the reception case to the three channels polling at the *friend* device.

Table 5. Use case of node with critical power input.

	Energy of Active Phase (mJ)	
	No RX	**With RX**
treNch	61×10^{-3}	66×10^{-3}
BLE conn.	6.09	6.10
BLE adv./mesh	344×10^{-3}	1.54

3.1.4. Distance

In this scenario, we evaluated the energy needed for an active-cycle depending on the distance to the receiver. Again, the power consumption during the sleep time is not contemplated and we considered that the nodes are coming from a normal wake-up, not a reset (it would add a fixed energy consumption because of the startup). We analyzed for each protocol the case with and without reception.

For the analysis, we calculated the distance as the theoretical maximum range achieved according to [40]:

$$pathloss = 40 + 25 \times \log d, \tag{1}$$

with d the distance, assuming an isotropic antenna, a channel without obstacles, noise or reflections and given the sensitivity of the used hardware of -93 dBm.

Aside of the energy differences in the transmission cycle for the general case (due to the mandatory master/slave reception in BLE conn. and to the three-channel transmission in BLE adv. and mesh), BLE does not implement automatic emitting power adjustment apart from the power class election. Thus, as Figure 9 illustrates, their curves remain constant (0 dBm transmission). *treNch*, on the other side, provides feedback to the nodes depending on the received signal strength by the gateway (*CTR-RSSI* field), achieving in this experiment up to a 8 times lower energy consumption and a greater range (bounded in the graph by the minimum and maximum emitting power of the used hardware, -40–4 dBm).

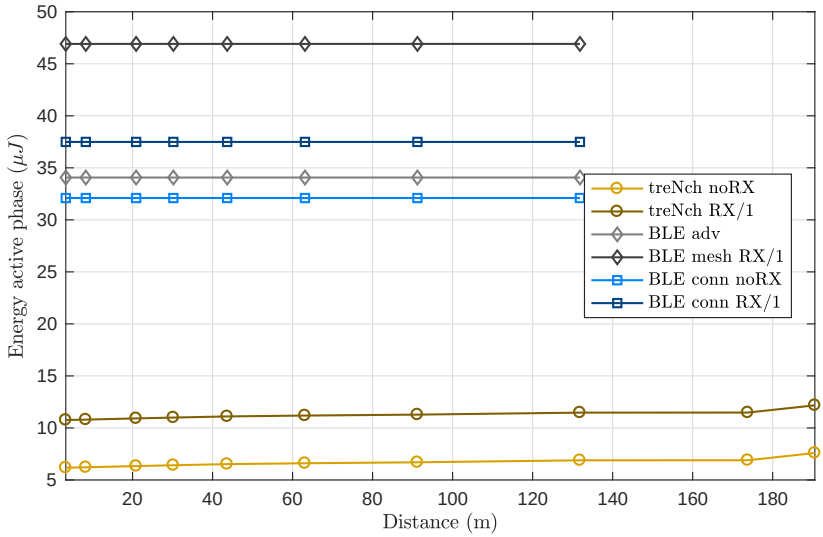

Figure 9. Use case of node at different distances from the gateway. Energy of active phase (no sleep time considered) over distance. Notice that BLE remains constant.

3.1.5. Large Payload

This use case analyzes the consumption of an application with large payload requirements. Since *treNch* does not implement data fragmentation in the current revision, we considered the

maximum payload size admitted for each protocol within one single frame, i.e., *treNch*, 27 Bytes; BLE conn., 23 Bytes and BLE adv./mesh, 26 Bytes.

The results, Figure 10, are very similar to the ones obtained in Section 3.1.1 (1 Byte of effective payload). The consumption gets increased around twice its value in every protocol at low cycle times, although remains dominated by the sleep phase, thus tending for higher cycle times to the same figures.

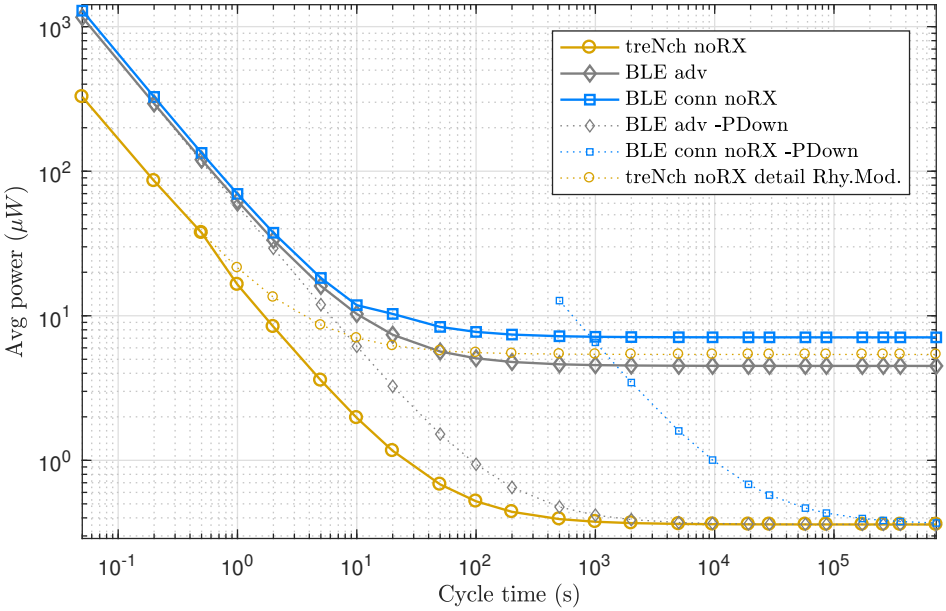

Figure 10. Use case of node with large payload needs. Average power of a complete cycle over cycle time. Maximum payload size for every WCP: *treNch*, 27 Bytes; BLE conn., 23 Bytes and BLE adv., 26 Bytes. *Note logarithmic scale in both axes*.

The larger payload size makes the existing differences in the frame overhead close to irrelevant. However, this matter is not enough to overcome the lighter architecture and processes of *treNch*, as reflected in Figure 6. Table 4 details the great contrast in the power and time demands of these events.

3.2. Other Aspects

3.2.1. Error Handling

After an error with a packet transmission, BLE conn. always re-sends it due to the layer-link intrinsic acknowledgments, normally in the next *connection interval*. This might be valuable in some applications, but it can also cause unnecessary overhead, delay and energy waste, in scenarios where an old message is outdated and no longer desired. BLE adv. operates in the opposite boundary: without possibility of acknowledgments. *treNch*, contrary to this, gives the opportunity of deciding to the application, also in the next cycle. This principle is shared with BLE mesh.

3.2.2. Latency

The average latency in BLE conn. in both directions is half the *connection interval*, being a complete cycle the worst case (synchronous). In the rest of BLE modes and *treNch*, an interruption in the node can trigger the transmission in any moment (asynchronous). In the opposite direction (not including BLE adv.), the latency cannot be predicted since it depends on the nodes.

3.2.3. Reliability

Giving the analyzed protocols the acknowledgment option (except BLE adv.) and using in the experiment the same physical layer, the differences in reliability come by the benefit of the BLE conn.

channel hoping algorithm and the triple transmission of BLE adv. and mesh, ensuring more robustness. *treNch* deals with noisy environments leaving the physical-layer characteristics open for every use case. Moreover, its best-effort principle and light architecture allow it to keep functioning under extreme lower power conditions.

3.2.4. Topology

Only BLE mesh supports the bidirectional communication between nodes as *treNch* does. Neither BLE conn. considers this topology only achievable at application level; nor BLE adv., which broadcasts unidirectionally.

3.2.5. Interoperability

One of the main features of BLE is its interoperability through standardized profiles (*services*) and *characteristics*. *treNch* seeks for more simplicity leaving to the application all the responsibility and setting up independent networks, which may operate even at different frequency bands.

3.2.6. Security

The total overhead of the packet by adding security is: 2-bits, to specify the security level; 1 Byte to specify the counter, and either 4 Bytes (security level 1 and 2) or 8 Bytes (security level 3) for the *MIC*. In comparison, the counter used in BLE is 3 Bytes long, since it transmits a larger part of the nonce over the air and in BLE Mesh the packet is authenticated and encrypted at two different levels (network and application), so two different *MIC*s (either 4 or 8 Bytes long each) are required.

4. Conclusions

This paper has introduced *treNch* for use in EH ultra-low-power WSN. We described its operation principles and compared it with the BLE modes in realistic ULP scenarios, demonstrating a better performance in each of them. Its proposed light architecture with asynchronous transmissions, synchronous and optional receptions, short frame sizes and the unique energy-management algorithm, make *treNch* achieve power consumptions from 1 to 2 orders of magnitude lower than BLE.

The proposed energy-management algorithm, exploiting the cross-layer paradigm in the WCP, entails a large advance concerning the power consumption without losing QoS. It achieves best-effort communications with defined periodicity control, without wasting energy in timers during the sleep phase. In addition, for more demanding applications, the switch to more reliable communication is carried out automatically, as soon as the energy conditions are favorable.

As a result of the described features, we set a new minimum operation threshold for the power input, opening the possibility for new EH scenarios within the IoT, where the application can operate automatically from pure best-effort to nearly real time, depending on the environment.

The experimental results have proven as well that the synchronous WCP as BLE conn. are highly inefficient for EH use cases, where the energy flow is not assured, neither predictable in most of the scenarios. On the other side, giving the control to the nodes for acting according to their needs, stands as a more efficient practice, since it does not waste energy in tedious protocol procedures. BLE adv. and BLE mesh advance in this direction too. Although BLE adv. does not implement receptions, nor security option, and BLE mesh, more focused on the mesh nodes than in the low power ones, resolves it in a more burdened way.

We also proposed a security scheme that uses standard and proven mechanisms and are straightforward to integrate, in addition to being seamless enough that it does not increase the processing time (assuming most transceivers have an AES accelerator) or the frame size significantly, i.e., the power consumption.

In other respects and future work, we envision an out-of-band registering process, over NFC/RFID or a low-frequency receiver, enabling the use of radio transmitters (hardware without reception capabilities). This would boost the use of low-cost nodes, without compromising privacy and security. Moreover, we plan to design data fragmentation, currently only possible at application layer.

Author Contributions: Conceptualization, F.M.-C., A.E.-M. and V.U.R.; methodology, F.M.-C. and V.T.-L.; software, V.T.-L., F.M.-C. and V.U.R.; validation, F.M.-C.; formal analysis, F.M.-C.; investigation, F.M.-C.; resources, F.M.-C.; data curation, F.M.-C. and V.T.-L.; writing—original draft preparation, F.M.-C. and A.E.-M.; writing—review and editing, A.R. and D.P.M.; supervision, A.R. and D.P.M.; project administration, F.M.-C.; funding acquisition, F.M.-C., A.R. and D.P.M. All authors have read and agreed to the published version of the manuscript.

Funding: This work was partially supported by the ECSEL Joint Undertaking through CONNECT project under grant agreement No 737434. This Joint Undertaking receives support from the German Federal Ministry of Education and Research and the European Union's Horizon 2020 research and innovation program and Slovakia, Netherlands, Spain, Italy. It was also supported in part by the Spanish Ministry of Education, Culture and Sport (MECD)/FEDER-EU through the Predoctoral Grants under Grant FPU18/01376, in part by the BBVA Foundation through the 2019 Leonardo Grant for Researchers and Cultural Creators, and in part by the University of Granada through its Projects for Junior Researchers.

Conflicts of Interest: The authors declare no conflict of interest.

References

1. Jayakumar, H.; Lee, K.; Lee, W.S.; Raha, A.; Kim, Y.; Raghunathan, V. Powering the internet of things. In Proceedings of the 2014 International Symposium on Low Power Electronics and Design, La Jolla, CA, USA, 11–13 August 2014; pp. 375–380.
2. Zhou, G.; Huang, L.; Li, W.; Zhu, Z. Harvesting ambient environmental energy for wireless sensor networks: A survey. *J. Sens.* **2014**, *2014*, 815467.
3. Moreno-Cruz, F.; Escobar-Molero, A.; Castillo, E.; Becherer, M.; Rivadeneyra, A.; Morales, D.P. Why Use RF Energy Harvesting in Smart Grids. In Proceedings of the 2018 IEEE 23rd International Workshop on Computer Aided Modeling and Design of Communication Links and Networks (CAMAD), Barcelona, Spain, 17–19 September 2018; pp. 1–6.
4. Liu, X.; Sánchez-Sinencio, E. A highly efficient ultralow photovoltaic power harvesting system with MPPT for internet of things smart nodes. *IEEE Trans. Very Large Scale Integr. (Vlsi) Syst.* **2015**, *23*, 3065–3075.
5. Moreno-Cruz, F.; Toral-López, V.; Cuevas, M.R.; Salmerón, J.F.; Rivadeneyra, A.; Morales, D.P. Dual-Band Store-and-Use System for RF Energy Harvesting with Off-the-Shelf DC/DC Converters. *IEEE Internet Things J.* **2020**, doi:10.1109/JIOT.2020.3024017.
6. Sandhu, M.M.; Geissdoerfer, K.; Khalifa, S.; Jurdak, R.; Portmann, M.; Kusy, B. Towards Optimal Kinetic Energy Harvesting for the Batteryless IoT. *arXiv* **2020**, arXiv:2002.08887.
7. Deng, F.; Yue, X.; Fan, X.; Guan, S.; Xu, Y.; Chen, J. Multisource energy harvesting system for a wireless sensor network node in the field environment. *IEEE Internet Things J.* **2018**, *6*, 918–927.
8. Nikoukar, A.; Raza, S.; Poole, A.; Güneş, M.; Dezfouli, B. Low-power wireless for the Internet of Things: Standards and applications. *IEEE Access* **2018**, *6*, 67893–67926.
9. Zikria, Y.B.; Kim, S.W.; Hahm, O.; Afzal, M.K.; Aalsalem, M.Y. Internet of Things (IoT) operating systems management: Opportunities, challenges, and solution. *Sensors* **2019**, *19*, 1793.
10. Zikria, Y.B.; Yu, H.; Afzal, M.K.; Rehmani, M.H.; Hahm, O. Internet of things (IoT): Operating system, applications and protocols design, and validation techniques. *Future Gener. Comput. Syst.* **2018**, *88*, 699–706.
11. Freschi, V.; Lattanzi, E. A Study on the Impact of Packet Length on Communication in Low Power Wireless Sensor Networks Under Interference. *IEEE Internet Things J.* **2019**, *6*, 3820–3830.
12. Aripriharta, A.; Firmansah, A.; Yazid, M.; Wahyono, I.; Horng, G. Modelling of adaptive power management circuit with feedback for self-powered IoT. *J. Phys. Conf. Ser. Iop Publ.* **2020**, *1595*, 012023.
13. Amirinasab, M.; Shamshirband, S.; Chronopoulos, A.T.; Mosavi, A.; Nabipour, N. Energy-efficient method for wireless sensor networks low-power radio operation in internet of things. *Electronics* **2020**, *9*, 320.
14. Al-Turjman, F.; Abujubbeh, M. IoT-enabled smart grid via SM: An overview. *Future Gener. Comput. Syst.* **2019**, *96*, 579–590.

15. Figueroa Lorenzo, S.; Añorga Benito, J.; García Cardarelli, P.; Alberdi Garaia, J.; Arrizabalaga Juaristi, S. A comprehensive review of RFID and bluetooth security: Practical analysis. *Technologies* **2019**, *7*, 15.
16. Álvarez, F.; Almon, L.; Hahn, A.S.; Hollick, M. Toxic Friends in Your Network: Breaking the Bluetooth Mesh Friendship Concept. In Proceedings of the 5th ACM Workshop on Security Standardisation Research Workshop, London, UK, 11 November 2019; pp. 1–12.
17. Ghori, M.R.; Wan, T.C.; Anbar, M.; Sodhy, G.C.; Rizwan, A. Review on Security in Bluetooth Low Energy Mesh Network in Correlation with Wireless Mesh Network Security. In Proceedings of the 2019 IEEE Student Conference on Research and Development (SCOReD), Perak, Malaysia, 15–17 October 2019; pp. 219–224.
18. Feng, X.; Yan, F.; Liu, X. Study of wireless communication technologies on Internet of Things for precision agriculture. *Wirel. Pers. Commun.* **2019**, *108*, 1785–1802.
19. Mahmoud, S.M.; Mohamad, A.A.H. A study of efficient power consumption wireless communication techniques/modules for internet of things (IoT) applications. *Adv. Internet Things* **2016**, doi:10.4236/ait.2016.62002.
20. Unwala, I.; Lu, J. IoT protocols: Z-Wave and Thread. *Int. J. Future Rev. Comput. Sci. Commun. Eng. (IJFRSCE)* **2017**, *3*, 355–359.
21. ANT Web Site. Available online: https://www.thisisant.com (accessed on 26 August 2020).
22. Dementyev, A.; Hodges, S.; Taylor, S.; Smith, J. Power consumption analysis of Bluetooth Low Energy, ZigBee and ANT sensor nodes in a cyclic sleep scenario. In Proceedings of the 2013 IEEE International Wireless Symposium (IWS), Beijing, China, 14–18 April 2013; pp. 1–4.
23. Thread Group Web Site. Available online: https://www.threadgroup.org (accessed on 26 August 2020).
24. enOcean Alliance Web Site. Available online: https://www.enocean-alliance.org (accessed on 27 August 2020).
25. Sharma, H.; Sharma, S. A review of sensor networks: Technologies and applications. In Proceedings of the 2014 Recent Advances in Engineering and Computational Sciences (RAECS), Chandigarh, India, 6–8 March 2014; pp. 1–4.
26. Sornin, N.; Luis, M.; Eirich, T.; Kramp, T.; Hersent, O. *Lorawan Specification*; LoRa Alliance: San Ramon, CA, USA, 2015.
27. San Cheong, P.; Bergs, J.; Hawinkel, C.; Famaey, J. Comparison of LoRaWAN classes and their power consumption. In Proceedings of the 2017 IEEE Symposium on Communications and Vehicular Technology (SCVT), Leuven, Belgium, 14 November 2017; pp. 1–6.
28. Bäumker, E.; Garcia, A.M.; Woias, P. Minimizing power consumption of LoRa® and LoRaWAN for low-power wireless sensor nodes. *J. Phys. Conf. Ser. Iop Publ.* **2019**, *1407*, 012092.
29. Collotta, M.; Ferrero, R.; Rebaudengo, M. A Fuzzy Approach for Reducing Power Consumption in Wireless Sensor Networks: A Testbed with IEEE 802.15. 4 and WirelessHART. *IEEE Access* **2019**, *7*, 64866–64877.
30. Detterer, P.; Erdin, C.; Huisken, J.; Jiao, H.; Nabi, M.; Basten, T.; De Gyvez, J.P. Trading sensitivity for power in an IEEE 802.15. 4 conformant adequate demodulator. In Proceedings of the 2020 Design, Automation & Test in Europe Conference & Exhibition (DATE), Grenoble, France, 9–13 March 2020; pp. 1674–1679.
31. Zhang, Y.; Weng, J.; Dey, R.; Jin, Y.; Lin, Z.; Fu, X. On the (In) security of Bluetooth Low Energy One-Way Secure Connections Only Mode. *arXiv* **2019**, arXiv:1908.10497.
32. Coman, F.L.; Malarski, K.M.; Petersen, M.N.; Ruepp, S. Security issues in internet of things: Vulnerability analysis of LoRaWAN, sigfox and NB-IoT. In Proceedings of the 2019 Global IoT Summit (GIoTS), Aarhus, Denmark, 17–21 June 2019; pp. 1–6.
33. Mao, B.; Kawamoto, Y.; Liu, J.; Kato, N. Harvesting and threat aware security configuration strategy for IEEE 802.15. 4 based IoT networks. *IEEE Commun. Lett.* **2019**, *23*, 2130–2134.
34. Meka, S.; Fonseca, B. Improving route selections in ZigBee wireless sensor networks. *Sensors* **2020**, *20*, 164.
35. Bomfin, R.; Chafii, M.; Fettweis, G. A Novel Modulation for IoT: PSK-LoRa. In Proceedings of the 2019 IEEE 89th Vehicular Technology Conference (VTC2019-Spring), Kuala Lumpur, Malaysia, 28 April–1 May 2019; pp. 1–5.
36. FIPS. *113 Computer Data Authentication*; National Institute of Standards and Technology, Federal Information Processing Standards: Gaithersburg, MD, USA, 1985; p. 29.
37. Whiting, D.; Housley, R.; Ferguson, N. Counter with cbc-mac (ccm). In *Internet Engineering Task Force Report*; IETF: Fremont, CA, USA, 2003.
38. Liu, X.; Goldsmith, A. Wireless medium access control in networked control systems. In Proceedings of the 2004 American Control Conference, Melbourne, Victoria, Australia, 20–23 July 2004; Volume 4, pp. 3605–3610.

39. Nordic Semiconductor. *nRF52 DK for Bluetooth LE, Bluetooth Mesh, ANT and 2.4 GHz Applications. nRF52 Product Brief*; Nordic Semiconductor: Trondheim, Norway, 2019.
40. Tosi, J.; Taffoni, F.; Santacatterina, M.; Sannino, R.; Formica, D. Performance evaluation of bluetooth low energy: A systematic review. *Sensors* **2017**, *17*, 2898.

2.3 Publication 3

"There is poetry in science and the cultivation of the imagination is an essential prerequisite to the successful investigation of nature."
– Joseph Henry

Screen Printed Security-Button for Radio Frequency Identification Tags

Almudena Rivadeneyra[1], Andreas Albrecht[2], **Fernando Moreno-Cruz**[1,3], Diego P. Morales[1], Markus Becherer[2] and José F. Salmerón[2]

[1] Department of Electronics and Computer Technology, University of Granada, Granada (Spain)
[2] Institute for Nanoelectronics, Technical University of Munich, Munich (Germany)
[3] Infineon Technologies AG, Munich (Germany)

IEEE Access

- Received February 2020, Accepted March 2020, Published March 2020 (volume 8)
- DOI: 10.1109/ACCESS.2020.2979548
- Impact Factor: 3.745
- JCR Rank: 35/156 in category *Computer Science, Information Systems* (Q1) and 61/266 in *Engineering, Electrical & Electronic* (Q1)

IEEE Access
Multidisciplinary ⋮ Rapid Review ⋮ Open Access Journal

Received February 14, 2020, accepted March 3, 2020, date of current version March 19, 2020.

Digital Object Identifier 10.1109/ACCESS.2020.2979548

Screen Printed Security-Button for Radio Frequency Identification Tags

ALMUDENA RIVADENEYRA[1], ANDREAS ALBRECHT[2], FERNANDO MORENO-CRUZ[3], DIEGO P. MORALES[4], MARKUS BECHERER[2], AND JOSÉ F. SALMERÓN[2]

[1]Pervasive Electronics Advanced Research Laboratory (PEARL), Department of Electronics and Computer Technology, University of Granada, 18071 Granada, Spain
[2]Institute for Nanoelectronics, Technical University of Munich, 8033 München, Germany
[3]Infineon Technologies AG, 85579 Munich, Germany
[4]Biochemistry and Electronics as Sensing Technologies Group, University of Granada, 18071 Granada, Spain

Corresponding author: Almudena Rivadenerya (arivadeneyra@ugr.es)

This work was supported by the fellowship under Grant 2020-MSCA-IF-2017-794885-SELFSENS.

ABSTRACT Radio frequency identification (RFID) security is a relevant matter. The wide spread of RFID applications in the general society and the persistent attempts to safeguard it confirm it, especially since its use involves payments and the store or transmission of sensitive information. In this contribution, we present an innovative solution for improving the security of RFID passive tags through the use of a screen printed button, that allows the reception and transmission only when a certain level of physical pressure normal to its plane is applied. The materials and fabrication technology used demonstrate an easy to implement and cost-effective system, valuable in several scenarios where the user has straight contact with the tags and where its usage is direct and intentional.

INDEX TERMS Flexible, force sensor, high-frequency band, pressure, printed electronics.

I. INTRODUCTION

Radio frequency identification (RFID) tags or systems are increasingly used in day-to-day situations to provide information or handles to information stored elsewhere. In many use cases, this information stored within the tag can be sensitive; implying payments, access to restricted zones or privacy matters. Security concerns arise when not-authorized entities are able of tracking the location of tags or the person carrying it, eavesdropping on tag-to-reader communication, misuse of the information or identity theft through tag cloning [1]. In the case of users carrying RFID-tagged objects, the threat to people's privacy relies in companies, governments and crooks, tracking people without their knowledge and consent; and potentially exploiting this private information. Criminals may also fabricate fake products or duplicate identities to take advantage of its illegal use [2]. Thus, it would be desirable to add some extra control to the wireless data transfer, while maintaining it transparent to the user and not interfering in its utilization.

The associate editor coordinating the review of this manuscript and approving it for publication was Yanjiao Chen.

A lot of effort has gone into RFID privacy. To mention the most relevant solutions of the literature, Juels proposes one-time pads transmitted across multiple authentication protocols [3]. Their successful use depends on the attacker not being able to eavesdrop for a number of consecutive transmissions, appearing this as its main limitation. Garfinkel proposes a strict regulation for the customer tracking (RFID Bill of Rights) [4]. Nevertheless, this set of laws may be only viable for some use cases, since it relies entirely on legislation. Molnar and Wagner [5] for their part, propose to decrease the tag identification time with a tree-based tag scheme, even at the expense of considerably less privacy guarantees. More recently, Tu and Piramuthu [6] and Korak and Hutter [7] addressed the relay attack, consisting on the non-authorized use of the tag (identity theft) through a man in the middle attack, resending the tag communication while physically far from the target.

A common assumption in every proposed solution is that the attacker, in his pursuit of breaking the privacy of the protocol, is not capable to physically manipulate and tamper the tags. Accessing the tags' memory would mean accessing secret keys, relevant state information and hence, the ability

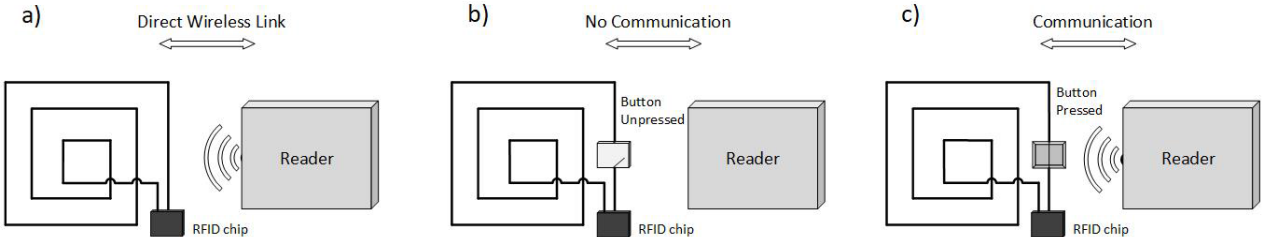

FIGURE 1. Scheme of operation: (a) Normal RFID tag; (b) Proposed Open tag; (c) Proposed Shorted tag.

of indistinguishably forge the tag. These situations are not considered, or directly assumed that physically compromised tags are out of the system. In this way, the RFID privacy concerns of these models deal only with algorithmic attacks, seeing the tag as a ''black-box''. The adversarial then has prohibited to tamper with tags' private information or to use side-channel information to break the RFID security.

On the other side, Gassend *et al.* extended the RFID privacy model to include hardware tampering attacks with minimal hardware by means of physical unclonable functions (PUFs) [8]. PUFs exploit physical characteristics of the circuit, which are difficult to model even allowing the attacker to have contact with the system.

In this paper, we focus on the high frequency (HF) band (13.56 MHz) that can be implemented in many portable devices, such as smartphones, tables or dataphones [9]. In fact, this broad use is a double-edged sword. On one side, it generalizes the use of such technology and thus, the emergence of new applications, contributing to the maturity of the technology. On the other side, it makes easier the access to the transmitted information through the wireless link, arising methods to hack the protocols and/or devices. Therefore, it is mandatory to come up with new and sophisticated strategies to cope with these potential security risks.

In this contribution, we describe an extra hardware security level for HF RFID tags. In particular, we include a force sensor between the chip and antenna, so that the tag is unreadable until it touches the reader with enough pressure normal to its surface. In this direction, Marquardt *et al.* [10] described different simple approaches to give awareness of the RFID operation to the user. Specifically, they developed three kinds of designs providing either visual, audible or vibro-tactile feedback, although the last two options needed an extra battery.

II. MATERIALS AND METHODS

A. DESCRIPTION OF OUR APPROACH

Our idea was to implement a button into the RFID antenna that is open by default and closes the loop antenna on pressure. To accomplish this, we modified the connection layer between the inductor and the RFID chip, which is normally developed by an insulator layer among the conductive traces and on top a conductive line through insulator as well, as the two points that are connected (see Figure 1a). In this work, we did not place directly a conductive line between these connections but instead, we deposited a matrix of cubes made of silicone and glued to it a silver trace printed of a polymeric foil (see Figure 1b). Therefore, once we want to activate our RFID tag we need to press on this array with a certain pressure value to create the connection between chip and antenna that allows the communication (see Figure 1c).

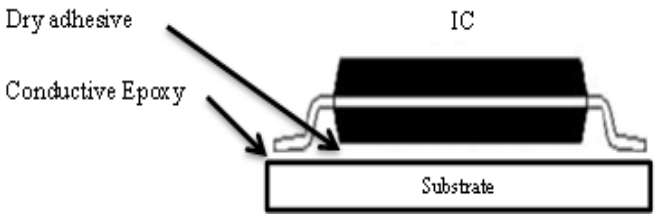

FIGURE 2. Schematics of the chip assembly process.

B. TAG FABRICATION

The silver (Ag) screen printing paste employed in this work to print the antenna was LOCTITE ECI 1010 0.2KG E&C by Henkel (Germany) used without modifications. The array of cubes was made of screen-printed polydimethylsiloxane (PDMS). The isolating paste used to isolate the bridge connecting the two ends of the inductor was TD-642 of AppliedInkSolutions (US).

All pastes were printed onto thermally pre-heated (100°C for 30 min) polyethylene terephthalate (PET) Melinex 506 of DuPont of a thickness of 100 μm. A manual screen printer (Nino from Coruna, Switzerland) was used to print with a screen with a mesh density of 120 Threads/cm. After printing, the pastes were dried at 100°C for 30 min in an oven before printing the next type of paste.

The assembly of the RFID chip to the foil was done in a three-step process as depicted in Figure 2. First, H20E conductive resin (Epoxy Technology Inc., Billerica, United States) was deposited to interconnect the integrated circuit (IC) and the screen printed silver pads. Double layer 50 μm-thick dry adhesive (AR Clear 8932 from Adhesives Research, Inc. Glen Rock, Pennsylvania, United States) was located on the bottom part of the IC to fix it to the substrate. Finally, a heating step was performed in an oven at 120 °C for 20 min to cure the conductive resin. Additionally, the dry film adhesion is enhanced with temperature, so the heat treatment served also to fix it better to the substrate.

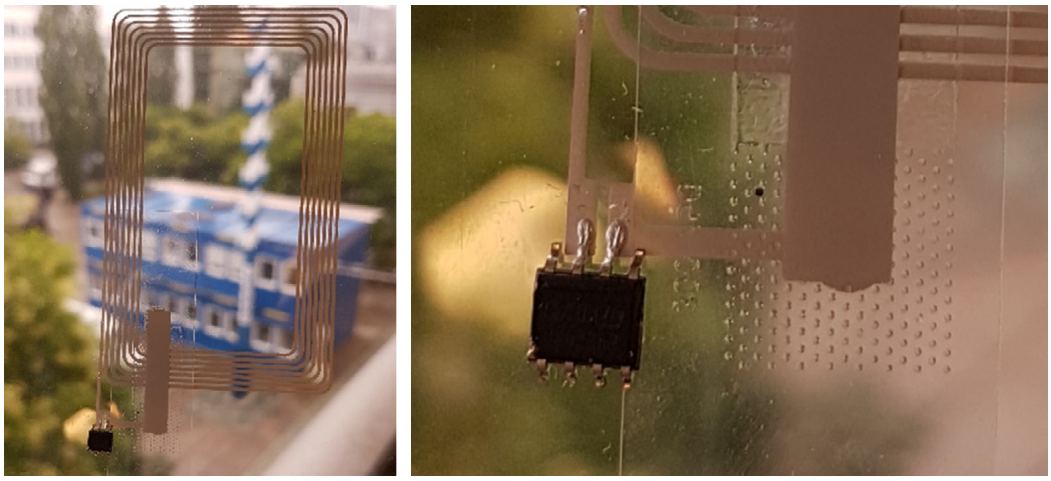

FIGURE 3. a) Screen-printed one-chip RFID tag with a pressure-activated button. b) Magnification of chip and pressure-sensing button.

C. TAG CHARACTERIZATION

A Keithley 2700 multimeter with 20 input channels was used for measuring the resistances and open-circuit voltages in the bending setup and in the thermocouple setup. A Keithley 2602B source meter was employed in the thermocouple setup. The LCR meter E4982A of Keysight was employed for all capacitance measurements at an amplitude of 1 V at a frequency of 100 kHz, if not indicated otherwise. A calibration of the wires was done after each change of the setup. The impedance analyzer E4990A was employed to measure the frequency dependent response of the wireless tags and an E5061B ENA Vector Network Analyzer of Keyight for the S_{11} parameter measurements.

Sheet resistance measurements were conducted on a printed 5 × 10 mm^2 area with a self-made linear four-point probe in combination with a Keysight B2900 source meter or a Keithley 2700 multimeter. A correction factor of 0.651 was calculated for the 5 × 10 mm^2 areas and applied to compensate the effect of limited boundaries according to Smits [11]. Profilometer studies were done with a Dektak XT of Bruker (US) with the micro-porous vacuum chuck that holds flexible samples flat.

III. RESULTS AND DISCUSSION

We investigated the use of our thin pressure sensors without a dielectric as they are pressed at a certain pressure. The implementation in a HF RFID tag is shown in Figure 3a with a magnification of the RFID chip and the sensor in Figure 3b. The latter shows the structured dielectric as dots around and between the contact areas of the bridge to the bottom contact wired to the chip, closing the circuit.

Preliminary results show that the button works as intended and changes from a capacitance of about 17.5 pF to a resistor of about 0.8 Ω at the desired frequency of 13.56 MHz (see Figure 4). The latter should not have a large influence on the antenna behavior as intended, working close to an ideal closed switch even for HF signals. The first one however,

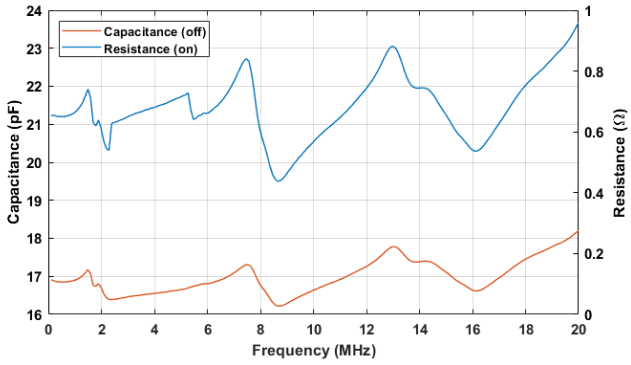

FIGURE 4. Capacitance (when the button is OFF) and resistance (when the button is pressed at 10 mN), over the frequency range from 100 Hz to 20 MHz.

introduces a second large capacitance next to the internal one into the microcontroller and leads to a decoupling between the reader and antenna. Thus, it acts in practice as an ideal open switch, not allowing the signal to get in the microcontroller and therefore not permitting the communication.

We used a FR4 antenna as reader, resonating at approximately 13.56 MHz, and brought the safe tag close to it, pressing the button with a plastic clamp at two different distances (as shown in Figure 5). We tested two copper antennas as well as reference, whose responses with the reader can be seen in Figure 5 (copper1 and copper2) with a resonance frequency in both cases about 14 MHz.

When the HF tag is placed in the reader surroundings, the antiresonance of the reader antenna disappears. In particular, when the button was pressed, the matching of the characteristic impedance was achieved at resonance frequency of 13.56 MHz. On the other side, if the clamp was removed and the button was not pressed, a shift in the resonance frequency of the circuit appeared of more than 1 MHz. This should reliably inhibit the coupling of the reader and the tag and not permit non-intended communications, since the RFID chip would not be able to operate.

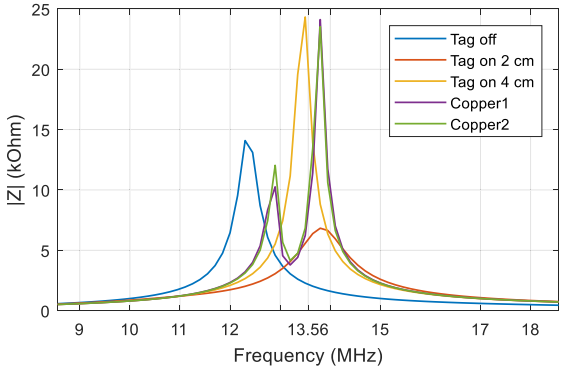

FIGURE 5. Coupling of a copper HF reader with two reference copper antennas and the printed tag. Tag without (off) and with (on) pressure in the button at distances of 2 and 4 cm.

Apart from providing extra hardware security to the RFID communication, our developed switch gives a threshold pressure value of around 10 mN. New use-cases emerge from tags that only activate when certain pressure is applied to the objective, security aside. Goods differentiation or energy savings in case of battery-assisted tags can be as well achieved.

IV. CONCLUSION

We demonstrated how a pressure-sensitive button implemented in an RFID tag can increase its security by inhibiting unwanted readings. In other words, through the combination of a NFC tag with an imperceptible printed security button, we allow data transfers only when the button is pressed with a certain level of pressure. This merges the comfort of a wireless tag like a credit card or an access batch, with additional security against tracking, relay attack or eavesdropping. The inclusion on current solutions as the mentioned ones would be indubitably straightforward. Besides, adding that antenna, circuitry and button are screen printed, results in a greatly convenient and inexpensive solution for a security boost in several use cases, not implying changes in the firmware or communication protocols, nor the inclusion of more components to the system.

To conclude, we enhanced the security and, in last term privacy, of RFID tags. Although still assuming that the attacker is not able to physically manipulate the tag as most of the literature; we went further than most of the current solutions not considering only the protocol algorithmic, but as well its physical nature and interaction in realistic scenarios, without compromising the energetic autonomy of the tag.

REFERENCES

[1] N. Marquardt, A. S. Taylor, N. Villar, and S. Greenberg, "Rethinking RFID: Awareness and control for interaction with RFID systems," in *Proc. SIGCHI Conf. Hum. Factors Comput. Syst.*, 2010, pp. 2307–2316.

[2] P. Kitsos, *Security in RFID and Sensor Networks*. New York, NY, USA: Auerbach, 2016.

[3] A. Juels, "Minimalist cryptography for low-cost RFID tags," in *Proc. Int. Conf. Secur. Commun. Netw.*, 2004, pp. 149–164.

[4] S. Garfinkel, "An RFID bill of rights," *Technol. Rev.*, vol. 105, no. 8, p. 35, 2002.

[5] D. Molnar and D. Wagner, "Privacy and security in library RFID: Issues, practices, and architectures," in *Proc. 11th ACM Conf. Comput. Commun. Secur. (CCS)*, 2004, pp. 210–219.

[6] Y.-J. Tu and S. Piramuthu, "On addressing RFID/NFC-based relay attacks: An overview," *Decis. Support Syst.*, vol. 129, Feb. 2020, Art. no. 113194.

[7] T. Korak and M. Hutter, "On the power of active relay attacks using custom-made proxies," in *Proc. IEEE Int. Conf. RFID (IEEE RFID)*, Apr. 2014, pp. 126–133.

[8] B. Gassend, D. Clarke, M. van Dijk, and S. Devadas, "Silicon physical random functions," in *Proc. 9th ACM Conf. Comput. Commun. Secur. (CCS)*, 2002, pp. 148–160.

[9] N. Chhabra, "Comparative analysis of different wireless technologies," *Int. J. Sci. Res. Netw. Secur. Commun.*, vol. 1, no. 5, pp. 3–4, 2013.

[10] N. Marquardt, A. S. Taylor, N. Villar, and S. Greenberg, "Visible and controllable RFID tags," in *Proc. 28th Int. Conf. Extended Abstr. Hum. Factors Comput. Syst.*, 2010, pp. 3057–3062.

[11] F. Smits, "Measurement of sheet resistivities with the four-point probe," *Bell Syst. Tech. J.*, vol. 37, no. 3, pp. 711–718, 1958.

ALMUDENA RIVADENEYRA received the master's degrees in telecommunication engineering, environmental sciences, and electronics engineering from the University of Granada, Spain, in 2009, 2009, and 2012, respectively, and the Ph.D. degree in design and development of environmental sensors from the University of Granada, in 2014. Since 2015, she has been with the Institute for Nanoelectronics, Technical University of Munich, where her work is centered in printed and flexible electronics with a special focus on sensors and RFID technology.

ANDREAS ALBRECHT received the master's degree in electrical engineering and information technology and the Ph.D. degree in printed electronics and printed sensors for the Internet of Things from the Technical University of Munich, in 2014 and 2018, respectively. He is currently with Cicor Technologies in the industrialization of aerosol jet printed electronics for mass and niches markets.

FERNANDO MORENO-CRUZ received the M.S. degree in telecommunications engineering from the University of Granada, Spain, in 2013, with the maximum grade obtained on his senior thesis. After two years in development and test in the automotive sector and two years in research and development in the IoT field, he is currently pursuing the Ph.D. degree with Infineon Technologies AG and Grupo de Investigación en Dispositivos Electrónicos,Granada. He has been rewarded with first prizes in the contests; Intel IoT Solutions 2017 and Embedded Wireless Systems and Networks 2018. His research interests include wireless power for sensor nodes, energy harvesting, antennas, and low-power network protocols.

DIEGO P. MORALES received the M.Sc. degree in electronic engineering and the Ph.D. degree in electronic engineering from the University of Granada, Spain, in 2001 and 2011, respectively. He was an Associate Professor with the Department of Computer Architecture and Electronics, University of Almería, Spain. He joined the Department of Electronics and Computer Technology, University of Granada, where he currently serves as a Tenured Professor. His current research interest includes developing reconfigurable applications.

MARKUS BECHERER was born in Bühl, Germany. He received the Diploma and Ph.D. degrees from the Technical University of Munich (TUM), Germany, in 2005 and 2010, respectively. He is currently a Full Professor with the Chair of Nanoelectronics, TUM.

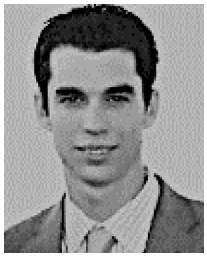

JOSÉ F. SALMERÓN received the degrees in telecommunication engineering and electronics engineering from the University of Granada, Granada, Spain, in 2009 and 2011, respectively, and the master's degree in computer and network engineering and the Ph.D. degree in development of sensing capabilities in RFID technologies from the University of Granada, in 2012 and 2014, respectively. He is currently a Postdoctoral Researcher with the Institute for Nanoelectronics, Technical University of Munich, Germany, where he is involved in the design and development of smart RFID labels with sensing capabilities.

2.4 Publication 4

"Nature is our kindest friend and best critic in experimental science if we only allow her intimations to fall unbiased on our minds."
– Michael Faraday

Why Use RF Energy Harvesting in Smart Grids

Fernando Moreno-Cruz[1,2], Antonio Escobar-Molero[1], Encarnación Castillo[2], Markus Becherer[3], Almudena Rivadeneyra[2] and Diego P. Morales[2]

[1] Infineon Technologies AG, Munich (Germany)
[2] Department of Electronics and Computer Technology, University of Granada, Granada (Spain)
[3] Institute for Nanoelectronics, Technical University of Munich, Munich (Germany)

IEEE 23rd International Workshop on Computer-Aided Modeling, Analysis, and Design of Communication Links and Networks (CAMAD)

- Barcelona, 2018
- DOI: 10.1109/CAMAD.2018.8514966

Why Use RF Energy Harvesting in Smart Grids

Fernando Moreno Cruz
Infineon Technologies AG
Munich, Germany
Fernando.MorenoCruz@infineon.com

Antonio Escobar Molero
Infineon Technologies AG
Munich, Germany
Antonio.Escobar@infineon.com

Encarnación Castillo
Dept. of Electronics & Computer Tech.
University of Granada
Granada, Spain
Encas@ugr.es

Prof. Dr. Markus Becherer
Institute for Nanoelectronics
Technical University of Munich
Munich, Germany
Markus.Becherer@tum.de

Almudena Rivadeneyra
Institute for Nanoelectronics
Technical University of Munich
Munich, Germany
Almudena.Rivadeneyra@tum.de

Diego P. Morales
Dept. of Electronics & Computer Tech.
University of Granada
Granada, Spain
DiegoPM@ugr.es

***Abstract*—Smart Grid is a promising new paradigm for the next generation power grid that aims at a more efficient generation, transformation, distribution and consumption of electricity and at the integration of the new renewable energies in the equation. For its development, extraordinary two-way communication and great sensorization are required and at this point emerges the wireless sensor networks with energy harvesting technologies. In this article, we present an innovative technique for energy harvesting in the area of smart grid at the wireless sensor nodes through radio frequency (RF) electromagnetic waves: RF energy harvesting, making them energetically autonomous. Several specific use-cases and applications are proposed where nodes with RF energy harvesting have advantages respect batteries, wires or other methods. A general node hardware structure for their development and a special wireless communication protocol for energy optimization in this kind of nodes are proposed as well.**

***Index Terms*—Energy efficient communication protocol, internet of things, node, RF energy harvesting, smart grid, use-cases, wireless sensor networks.**

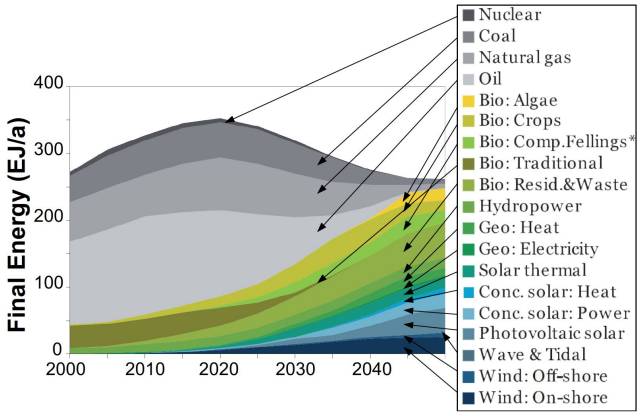

Fig. 1. World final energy supply [5].

I. Introduction

As the world population increases, the energy needs of the planet do it at the same time. With a world population currently at about 7.5 billion people, most of the studies conclude that by 2050 that figure will be above 9 billion, with an uninterrupted tendency of general industrial development [1]. This is directly related with the consumer demand for energy, since it depends on the level of development of a country [2]. Household consumption contributes to almost 30% of the total final energy consumption (electricity) and normally grows at the same radio as the gross domestic product (GDP). Just in the last fifteen years, the real per capita GDP in the EU-27 member states has increased around one quarter and for the period through 2020 it is expected to increase approximately at a rate of 2–3% annually. The related energy demand is increasing more rapidly than any other sector except for transportation [3], traditionally using fossil fuels, but which also is planned to contribute greatly to the increase of the electricity demand with the irruption of the electric car.

Although it is expected that renewable energy will play a more important role in the power generation while fossil fuels get depleted (see Fig. 1), the environmental impact of the energy generation nowadays is alarming: greenhouse (mainly CO_2, NO_x) and toxic gases emissions (SO_2, particulates), depletion of natural resources, rise of wastes, visual and noise pollution, among others [4]; that eventually affect to the global warming and habitability on Earth.

The actual trends make unsustainable the present model and urge to seek for new technologies and a change of paradigm that solves this negative tendency. In an attempt of tackling these issues *Smart Grid* (SG) emerges as a step forward to the increase of the efficiency, reliability, safety, sustainability and flexibility of the electrical energy generation, transmission, distribution and consumption systems and to the integration of the renewable energies within them.

In order to achieve enough intelligence in the system, reliable and updated information is essential. Sudden changes on the structure that cause power disturbances and outages must be managed, such as equipment failures, capacity overload or natural accidents, and solved. Although in a future grid, these failures or changes on the system might be predicted through the use of machine learning and artificial intelligence (AI), and

therefore, corrected before they occur or before they turn into major defects. For that, constant and long-term information is needed.

In this context arise wireless sensor networks (WSNs), providing the communication demands for the information and data gathering and control or response actions. Traditional electric-power monitoring systems have been typically realized through wire, requiring expensive deployment and maintenance costs, however, with wireless communication these issues are overcome. Besides, the collaborative operation of WSNs brings added advantages as rapid deployment, low cost, flexibility, reliability and aggregated processing power via parallel and distributed operations [6].

Given that, *radio frequency energy harvesting* (RFEH) appears as an innovative and advantageous technique for powering network nodes in several scenarios, avoiding the use of any wires or the inconvenience of recharging or changing batteries. The use of this technology seems a logic way to take advantage of the energy present in electromagnetic signals, when their energy suffice for feeding broad node types where other energy harvesting methods are unviable or less favorable.

This paper is organized as follows: Section II brings the general concepts of SG (II-A) and RFEH (II-B), keeping a perspective adjoining WSNs, since it is the common linker. Section III introduces and analyzes some innovative use-cases for RFEH within WSNs for SG and describes the proposed solutions in terms of hardware and an ultra-low power standardized communication protocol. Finally, section IV presents conclusions.

II. Background

A. Smart Grid

The traditional term grid refers to a system that supports all or some of the following operations: electricity generation, transmission, distribution and control [5]. It was developed through a centric approach where relatively few high-power ac plants (hundreds of kW at 50 or $60\,\mathrm{Hz}$) were interconnected by ac or dc high-voltage transmission systems (e.g. $400\,\mathrm{kV}$). Several substations afterward would reduce the voltage to a distribution level (e.g. $20\,\mathrm{kV}$ or $400\,\mathrm{V}$ depending on the load power needed) and deliver it through a huge number of distribution lines [7].

Lately, the inclusion of distributed renewable energy generators such as solar panels or wind generators (producing between some kW and some MW depending on the deployment) has already modified the initial architecture of the grid, although their heterogeneous nature makes the integration arduous and inefficient so far, added to the age of today's infrastructure that has remained unchanged for about a hundred years [8] and to the concentration of the network intelligence in central locations and only partially in substations, being remote locations almost or totally passive (one-way communication).

Alternatively, *SG* is an electric system that integrates distributed intelligence and control (information and related actions from a two-way communication system) with the electrical generation, transmission, distribution, consumption and business applications, including new renewable energy sources; with the objective of achieving a system *sustainable, efficient, clean, reliable, resilient, safe and secure* [5], [7]. In Table I a summary of the main differences between smart and traditional grid is pointed out.

TABLE I
Brief comparison between existing grid and smart grid [5].

Existing Grid	**Smart Grid**
Electromechanical	Digital
One-way communication	Two-way communication
Centralized generation	Distributed generation
Few sensors	Sensors throughout
Manual monitoring	Self-monitoring
Manual restoration	Self-healing
Failures and blackouts	Adaptive and islanding
Limited control	Pervasive control
Few customer choices	Many customer choices

In pursuance of the mentioned objectives, a new concept comes up as shows Fig. 2, where SG can be divided in three mayor systems [5]:

1) *Smart infrastructure system:* Energy, information and communication two-way infrastructure.
2) *Smart management system:* Advanced control and management system of services and functionalities.
3) *Smart protection system:* Failure, security and privacy protection and reliability analysis subsystem.

As consequence of the evolution and new principles, new actors arise as well, as microgrids, a bounded combination of generators, storages and loads able to work independently and in conjunction with the main grid [5]; or the methodologies for the management of the vast electric-car deployment, all conforming an heterogeneous new paradigm.

B. RF Energy Harvesting

An energy harvester is a system that converts energy from ambient sources such as thermal, solar, vibrational or radio frequency (RF) electromagnetic waves into electrical energy. The inclination for the use of one of these sources will depend on their presence in the vicinity of the system and the device needs in terms of power. RFEH specifically, makes use of the energy present at the signal carriers in the far field region, whose frequencies normally are between some kHz and hundreds of GHz.

RFEH offers in most of the cases clear advantages in regard to practically everywhere and every-time availability, predictability and stability over time, wireless nature, low cost implementation and small form factor [10], [11]. Nonetheless, the mayor drawbacks are the amount of power that can be harvested (refer to Table II) as a result of the inverse square relation with the distance to the radiation source (Friis equation [12]). Besides, in some cases the availability of the signal is not permanent due to duty-cycle or random use of the service (e.g. Wi-Fi router or mobile phone) and in other cases (e.g. AM radio), the size of the antenna needed makes the system impracticable for small nodes [13], [14].

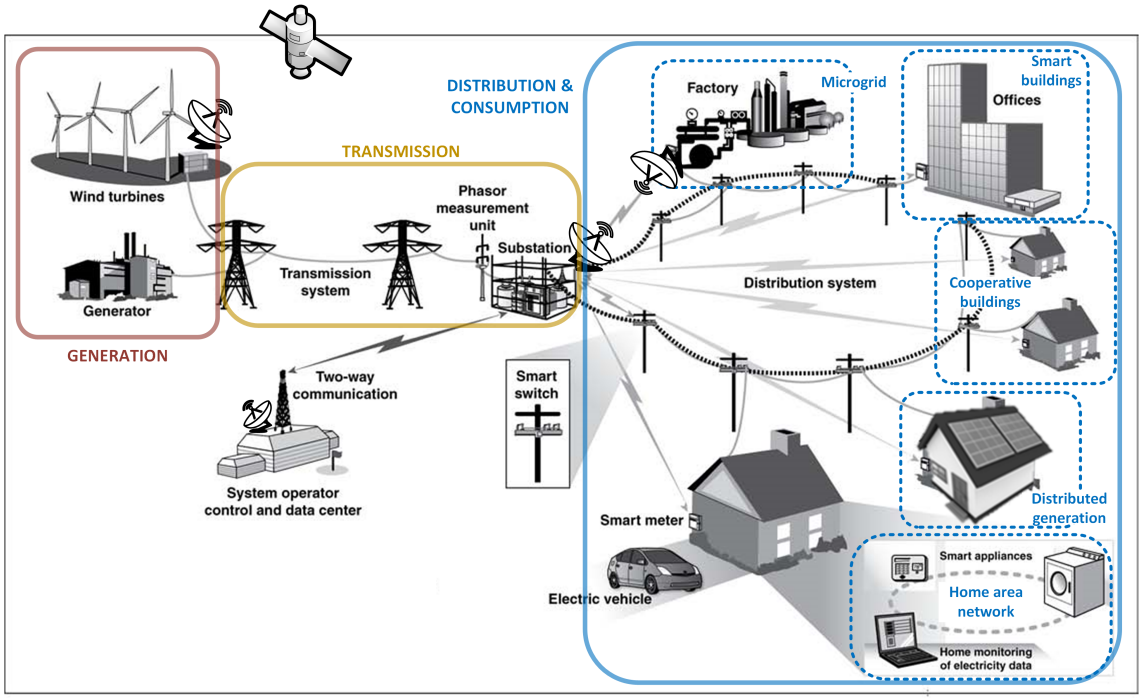

Fig. 2. Smart grid conceptual model (graphic based on [9]).

TABLE II
DENSITY POWER VALUES FOR DIFFERENT ENERGY HARVESTING SOURCES (NOTICE THE CHANGE IN UNITS).

Source	Power density *Harvested – Available*	Comments
Solar–outdoors	0.15–15 mW/cm^3	Cloudy/sunny day [15]
Solar–indoors	10–100 µW/cm^2	[15]
Vibrations	0.021–330 µW/cm^3	10–105 Hz [15]
Thermoelectric	40 µW/cm^3	5 °C gradient [15]
Wind flow	16.2 µW/cm^3	5 m/s [15]
Acoustic noise	1 µW/cm^3	100 dB [15]
Magnetic field	130 µW/cm^3	200 µT, 60 Hz [15]
GSM base station	8 µW/m^2	100 W at 1 km [11]
Mobile phone	1.6 mW/m^2	0.5 W at 5 m [11]
Wi-Fi router	3.2 mW/m^2	1 W at 5 m [11]
AM radio station	159 µW/m^2	50 kW at 5 km [11]
Isotropic RF transmitter	5.5 µW	902–928 MHz, 4 W at 5 m [16]

RFEH might be seen as a wireless energy transfer technique as well together with inductive coupling (including resonant inductive)[1]. The difference with respect to harvesting is the use of a dedicated energy source for the supply. Resonant inductive coupling and inductive coupling methods have been deeply researched and already used (e.g. radio frequency identification [RFID] and phone charging respectively), however, their transfer ranges are limited from a few millimeters to a few meters, since the power strength for near field propagation is attenuated with the cube of the distance [17]. RF energy transfer has clear advantage in the effective distance reached (20 dB attenuation per decade versus 60 dB for near field [11]); although, nowadays it has low RF-to-dc energy conversion efficiency, especially when the power is small.

The power losses from the RF source until the load, no matter if through harvesting or a dedicated source, are spread between the path and presumable obstacles and the rectifier-converter efficiency. The electrical power received is

$$P_{rec}^{DC} = P_{RF} \cdot \eta_{RF-DC}, \tag{1}$$

where P_{RF} is given by the Friis transmission equation and depends favorably on antenna gains and unfavorably on the squares of the signal frequency and distance, and where η_{RF-DC} is the rectifier-converter efficiency.

According to several studies [18]–[21], the present energy levels in cities open-spaces go to maximums around -30 dBm and less commonly of -20 dBm at bands of high utilization such as the cellular network (global system for mobile communications [GSM] or its successors), TV broadcasting, private mobile radio or wireless local networks; although the duty-cycle also varies. These levels are a direct consequence of the limitation on RF emissions given by the region regulation (e.g. 500 mW effective radiated power in the 868 MHz band for Europe [22]). In terms of frequency ranges, generally the part of the spectrum that shows the biggest interest goes from some hundreds MHz up to a few tens of GHz, depending the specific frequency band on again the country regulation and of course on the specific scenario.

Despite the limited energy available, even with data reception sensitivity some orders of magnitude higher (-60 dBm typically), with the current state of the art these levels might

[1]Capacitive coupling has several disadvantages and it is not used.

suffice. The power demand of WSN nodes vary broadly depending on the application and assuming a favorable environment and an efficient energy management and storage, RFEH can be the perfect solution for numerous applications where others energy sources fail, as demonstrate the already existing applications [11].

III. Use Cases and Proposed Solutions

The incipient development of novel technological concepts (e.g. Internet of Things, smart home) expands and attracts further the areas and applications where SG and RFEH-WSNs can work together. The integration with smart home and smart city eases the data acquisition and control due to the shared infrastructure (e.g. gateways, access points, extra sensorization and automatization), in addition to the multiplication of use-cases and thus, multiplication of use-cases as well where RFEH stands out among other power sources.
The progress and implementation of machine learning techniques and AI contributes likewise to the great need of sensors of innumerable types, in order to gather the bigger and more heterogeneous amount of information, which can lead in extraordinarily accurate patterns and predictions for their use in SG.

Some proposed use-cases where RFEH appears energetically as an interesting option for the power source and where provides an added value are:

- Transformation and distribution stations, especially close to point-to-point antennas as microwave direct communications or satellite communications (abundant in the new SG, see Fig. 2). These stations need commonly plenty of sensors as temperature, humidity, atmospheric pressure, motor speed, noise, among others. The deployment of autonomous RFEH-nodes contributes to lower costs related to set up and maintenance.
- Unapproachable points as pylons and chimneys, where values as gases/particles emissions, structural health or weather must be monitored. In remote locations far from the civilization the environmental energy available might not suffice, here the principle of energy transfer instead of harvesting can be used where the case lets no choice for other sources, emitting only when the information is needed.
- Unapproachable points within power plants or (smart) cities where a huge sensor deployment is demanded. Broad variety of sensors likewise are in the scope and due to the considerable size of the locations and the amount of nodes, RFEH-nodes characteristics make them a very suitable solution for such locations with a rich electromagnetic spectrum, impacting again in costs reduction and convenience.
- Integration in smart home and smart office systems where some RF bands are highly utilized. New building designs already include the projection for the telecommunication systems and automatization. Including on these plans nodes where the RF coverage is high enough, even embedded in walls or in not reachable places, can facilitate and reduce the price of their deployment and maintenance.

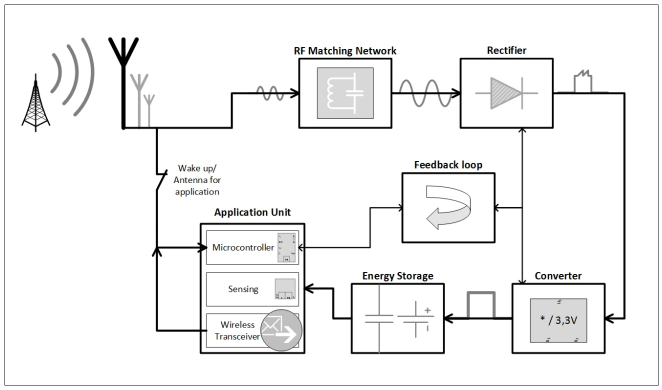

Fig. 3. RFEH node block diagram.

A. Node Structures

The proposed node hardware architecture is shown in Fig. 3 and follows the actual lines of other approaches from the literature [10]–[12], [23], gathering several advances in a generic way.

The blocks that compose the architecture are:

- *Antenna(s).* Transducer that captures the electromagnetic waves and converts them into electricity. The frequency range chosen must attend to the most utilized band of the spectrum at the specific location and time of use. Several bands can be harvested if a multi-band antenna or several ones in parallel are used.
- *Matching network.* Adapts the impedance from the antenna to the next stage in order to maximize the power transmission. Again, it must be designed for a specific frequency range, acting as an infinite impedance for the frequencies out of it.
- *Rectification stage.* Converts the electrical signal from ac (normally in a range of very, ultra or super high frequency) to dc, commonly using a Schottky diode or diode-connected transistor out of a complementary metal–oxide–semiconductor (CMOS) integrated circuit.
- *Conversion stage.* Regulates and shifts to a proper and stable voltage level the rectified signal for a correct storage and further use. The level used must be coherent with the energy needed during the active phase and the size of the storage element.
- *Energy storage.* Due to the duty-cyclic working principle, the energy is accumulated until it is enough for the active period. A battery or a (super)capacitor can be used depending on the leakages, losses, time of storage and voltage levels.
- *Application unit.* The load of the system which includes the microcontroller (μC), sensing/acting elements and the transceiver, that may use the same antenna for receiving/transmitting than the harvesting.

- *Feedback loop.* Virtual block that includes the optimizations that can emerge from the interrelation of blocks, as the voltage level adaption depending on the load or available energy to harvest; the usage of wake-up receivers (WUR) or any other wake-up method that enhance the energy saving (e.g. signal of objective battery-voltage reached); usage of intermediate switches that isolate different stages while some voltage levels are achieved; among others.

B. Communication Protocols

The objective is to fulfill the whole application requirements while integrating the new RFEH-WSNs with the actual (and coming) SG communication infrastructures, despite the restriction of hardware and energy availability. Due to the power constraints, every detail of the RFEH nodes communication workflow should be designed to be ultra-low power, to work potentially with a duty-cycle, whose maximum period will depend on the application (always assured by the energy density), and to make use of a gateway or a bridge for accessing the next level of the network. A mesh topology would be also possible, provided that either the ambient RF density is high enough or that there are other node-profiles employing more abundant energy sources, establishing the referred ones a special node kind of "ultra-low power *trench-nodes*". As regards the covered area, the nodes could be adapted to work within a local area network coverage or a wider one, depending again on the energy availability.

In respect to the current protocol standards, Bluetooth Low Energy, ZigBee, ANT, LoRaWAN, among others[2] might suffice in some scenarios due to the great energy availability or the application needs, but generally they are high power consuming protocols *in comparison* with the energy harvested; cause of not only the frequency band, packet size, emitting power and other basic characteristics, but also of the communication establishment phase, specific duty-cycle, protocol operation and so forth [24]. Therefore, a greater optimization by simplification and customization whether possible is needed for most of the cases.

With that aim in view, the development of the application firmware and the communication protocol must be done together, as well as with the usage of the hardware resources: *cross-layer design*. In this way, the optimization of active modes of μC, radio and sensing or acting units is maximized, going to ultra-low power modes (deep-sleep) the rest of the time, where the consumption is close to null (less than $800\,\mathrm{nW}$ in some μCs) and where the batteries or capacitors are charged again until the trigger of the next cycle: duty-cycle working principle.

Nonetheless, energy efficient packet reception is complicated with long duty-cycles: first, due to the clocks precision to wake up the receivers effectively, and second, because the mere fact of having that clock activated during the whole sleep time-slot costs too much energy. As solution three options are proposed:

1) *Establishment of the communication always by the RFEH-nodes*, followed by a defined time-slot for reception and a second reply (see Fig. 4). The easiest use-case is a star topology where the communication is done with a gateway, but in more complicated situations as mesh networks this gateway role would be carried out by non-RFEH-nodes. Here the period widths would depend on the energy availability and would be managed by the RFEH-nodes, although generally the availability of energy for RFEH is stable and predictable, as mentioned in Section II-B.
2) *Establishment of a highly synchronized mesh network to avoid collisions*. In high-density networks, unsuccessful transmissions are very likely to appear. Nodes based on energy harvesting cannot afford classical collision detection/avoidance mechanisms that rely on further increasing reception slots (CSMA/CD, CSMA/CA, ACK-based mechanisms) since reception is a very expensive operation in terms of required energy. Furthermore, packet collisions are fatal for the network performance, since nodes usually have enough energy for only one transmission and are not capable of further repeating the packet in case of error, or even being aware of its existence. Complexity increases exponentially in mesh networks, where several hops are needed and relays are introduced. A need for designing challenging protocols, in which successful transmission rate is optimized while the reception and routing overhead is kept to a minimum is a reality. Time-synchronized protocols based on flooding [25] are a promising alternative when these energy losses surpass the energy needed for maintaining this working principle, since simplicity and reliability are at the core of their design. In case the nodes do not have enough energy to maintain a low-power timer running, keeping the network-wide scheduling and enabling the synchronization, novel concepts like opportunistic networking can be used as alternative.
3) *Use of an ultra-low power WUR*, triggering the change from deep-sleep to reception mode. This second radio with a specific reception pattern per node would increase slightly the costs and would have to be used with a specific criteria that allows the node energy recovery, but makes the network more dynamic and flexible.

In consequence and in order to achieve a spread deployment of this type of nodes, the development of a "lite" wireless communication protocol standard with the features described urges. This protocol would define the basic communication functionality and architecture assuring the compatibility, but leaving room as well for a greater customization.

IV. Conclusions

In this article the inclusion of RFEH for the development of autonomous nodes within WSNs in the new paradigm of

[2]Not including RFID or Near Field Communication (NFC) which have already energy transfer, being consequently a source of energy and not a sink; but imply other requirements at the same time, like the small distance or the physical alignment with the emitter.

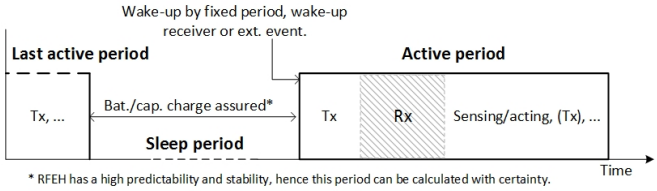

Fig. 4. Proposed workflow of communication protocol for simple RFEH-nodes.

SG has been introduced. Several use-cases and applications have been proposed where RFEH has outstanding advantages against other harvesting methods and batteries. Besides the general costs reduction due to the no need of wires and battery-recharge or substitution, the use of autonomous nodes with a new powering technique opens the deployment of nodes where before no other harvesting methods allowed it, likewise new sensoric possibilities for their use with machine learning and AI in advance pattern recognition and actuation methods, contributing to a smarter grid.

A generic hardware architecture has been presented in Section III-A, based on the literature and seeking for its best configuration for SG. In addition, the basics of a wireless communication protocol for ultra-low energy environments and nodes has been proposed. This protocol must be able to let a great level of customization for the workflow and management of the hardware resources for each case, in order to optimize the energy consumption. The proposed working principle is duty-cycled, assuring the recharge of the energy storage device for each period, and the proposed methodology for the packet reception includes options with a WUR, exclusively node-pairing-start or high/dynamic synchronization for mesh networks.

The future work embraces the optimization of each hardware block (Fig. 3) for a better efficiency and the development of a standard communication protocol that fulfills the presented requirements.

ACKNOWLEDGMENT

This project was partially funded by the Electronic Component Systems for European Leadership Joint Undertaking under grant agreement No 737434. This Joint Undertaking receives support from the European Union's Horizon 2020 research and innovation program and Germany, Slovakia, Netherlands, Spain, Italy.

REFERENCES

[1] W. Lutz, W. P. Butz, and K. e. Samir, *World Population & Human Capital in the Twenty-First Century: An Overview*. Oxford University Press, 2017.

[2] J. Lippelt and M. Sindram, *Global energy consumption*. Spring, 2011, vol. 12, no. 1.

[3] K. Rennings, B. Brohmann, J. Nentwich, J. Schleich, T. Traber, and R. Wüstenhagen, *Sustainable energy consumption in residential buildings*. Springer Science & Business Media, 2012, vol. 44.

[4] T. Tsoutsos, N. Frantzeskaki, and V. Gekas, "Environmental impacts from the solar energy technologies," *Energy Policy*, vol. 33, no. 3, pp. 289–296, 2005.

[5] X. Fang, S. Misra, G. Xue, and D. Yang, "Smart grid—the new and improved power grid: A survey," *IEEE communications surveys & tutorials*, vol. 14, no. 4, pp. 944–980, 2012.

[6] V. C. Gungor, B. Lu, and G. P. Hancke, "Opportunities and challenges of wireless sensor networks in smart grid," *IEEE transactions on industrial electronics*, vol. 57, no. 10, pp. 3557–3564, 2010.

[7] V. C. Gungor, D. Sahin, T. Kocak, S. Ergut, C. Buccella, C. Cecati, and G. P. Hancke, "A survey on smart grid potential applications and communication requirements," *IEEE Transactions on industrial informatics*, vol. 9, no. 1, pp. 28–42, 2013.

[8] ——, "Smart grid technologies: Communication technologies and standards," *IEEE transactions on Industrial informatics*, vol. 7, no. 4, pp. 529–539, 2011.

[9] G. C. Wilshuse and D. C. Trimble, "Cybersecurity challenges in securing the modernized electricity grid," United States Government Accountability Office, Tech. Rep., 2012.

[10] P. Kamalinejad, C. Mahapatra, Z. Sheng, S. Mirabbasi, V. C. Leung, and Y. L. Guan, "Wireless energy harvesting for the internet of things," *IEEE Communications Magazine*, vol. 53, no. 6, pp. 102–108, 2015.

[11] X. Lu, P. Wang, D. Niyato, D. I. Kim, and Z. Han, "Wireless networks with rf energy harvesting: A contemporary survey," *IEEE Communications Surveys & Tutorials*, vol. 17, no. 2, pp. 757–789, 2015.

[12] P. Nintanavongsa, "A survey on rf energy harvesting: circuits and protocols," *Energy Procedia*, vol. 56, pp. 414–422, 2014.

[13] X. Liu and E. Sánchez-Sinencio, "A highly efficient ultralow photovoltaic power harvesting system with mppt for internet of things smart nodes," *IEEE transactions on very large scale integration (vlsi) systems*, vol. 23, no. 12, pp. 3065–3075, 2015.

[14] H. Jayakumar, K. Lee, W. S. Lee, A. Raha, Y. Kim, and V. Raghunathan, "Powering the internet of things," in *Proceedings of the 2014 international symposium on Low power electronics and design*. ACM, 2014, pp. 375–380.

[15] G. Zhou, L. Huang, W. Li, and Z. Zhu, "Harvesting ambient environmental energy for wireless sensor networks: a survey," *Journal of Sensors*, vol. 2014, 2014.

[16] D. Pavone, A. Buonanno, M. D'Urso, and F. Della Corte, "Design considerations for radio frequency energy harvesting devices," *Progress In Electromagnetics Research B*, vol. 45, pp. 19–35, 2012.

[17] J. Park, Y. Kim, Y. J. Yoon, J. So, and J. Shin, "Rectifier design using distributed greinacher voltage multiplier for high frequency wireless power transmission," *Journal of electromagnetic engineering and science*, vol. 14, no. 1, pp. 25–30, 2014.

[18] M. Russo, P. Šolić, and M. Stella, "Probabilistic modeling of harvested gsm energy and its application in extending uhf rfid tags reading range," *Journal of Electromagnetic Waves and Applications*, vol. 27, no. 4, pp. 473–484, 2013.

[19] M. Yılmaz, D. G. Kuntalp, and A. Fidan, "Determination of spectrum utilization profiles for 30 mhz–3 ghz frequency band," in *Communications (COMM), 2016 International Conference on*. IEEE, 2016, pp. 499–502.

[20] A. Palaios, J. Riihijarvi, and P. Mahonen, "From paris to london: Comparative analysis of licensed spectrum use in two european metropolises," in *Dynamic Spectrum Access Networks (DYSPAN), 2014 IEEE International Symposium on*. IEEE, 2014, pp. 48–59.

[21] A. Palaios, V. Miteva, J. Riihijärvi, and P. Mähönen, "When the whispers become noise: A contemporary look at radio noise levels," in *Wireless Communications and Networking Conference (WCNC), 2016 IEEE*. IEEE, 2016, pp. 1–7.

[22] H. Yan, J. M. Montero, A. Akhnoukh, L. C. De Vreede, and J. Burghartz, "An integration scheme for rf power harvesting," in *Proc. STW Annual Workshop on Semiconductor Advances for Future Electronics and Sensors*, 2005, pp. 64–66.

[23] S. S. Chouhan, M. Nurmi, and K. Halonen, "Efficiency enhanced voltage multiplier circuit for rf energy harvesting," *Microelectronics Journal*, vol. 48, pp. 95–102, 2016.

[24] A. Dementyev, S. Hodges, S. Taylor, and J. Smith, "Power consumption analysis of bluetooth low energy, zigbee and ant sensor nodes in a cyclic sleep scenario," in *Wireless Symposium (IWS), 2013 IEEE International*. IEEE, 2013, pp. 1–4.

[25] A. Escobar, J. Garcia-Jimenez, F. J. Cruz, J. Klaue, A. Corona, and D. Tati, "Competition: Redfixhop with channel hopping," in *Proceedings of the 2017 International Conference on Embedded Wireless Systems and Networks*. Junction Publishing, 2017, pp. 264–265.

2.5 Publication 5

"That's the paper that Ashenden handed out to the other members of the group."
– S. Lewis (Colin Dexter's book)

Low-Cost Energy-Autonomous Sensor Nodes Through RF Energy Harvesting and Printed Technology

Fernando Moreno-Cruz[1,2], Francisco J. Romero-Maldonado[2], Noel Rodríguez Santiago[2], Diego P. Morales[2] and Almudena Rivadeneyra[2]

[1] Infineon Technologies AG, Munich (Germany)
[2] Department of Electronics and Computer Technology, University of Granada, Granada (Spain)

ALLSENSORS 2020: The Fifth International Conference on Advances in Sensors, Actuators, Metering and Sensing

- Valencia, 2020
- ISBN: 978-1-61208-766-5

Use of Low-Cost Printed Sensors with RF Energy Harvesting for IoT

Fernando Moreno-Cruz, Infineon Tech. AG, BEX, Munich, Germany
Víctor Toral López, University of Granada, Granada, Spain
Francisco J. Romero, University of Granada, Granada, Spain
Christian Hambeck, eesy-innovation GmbH, Munich, Germany
Diego P. Morales, University of Granada, Granada, Spain
Almudena Rivadeneyra, University of Granada, Granada, Spain

1 Introduction

The massive deployment of smart sensor nodes within the Internet of Things (IoT) world is an upcoming reality, where the expenses, security and energy sources will be the most critical issues to be addressed. In this context, the employment of low-cost printed sensors and RF energy harvesting (RFEH) appear as a solution for both costs and energy supply affairs toward the series production of intelligent systems.
The proven capability of RF energy harvesting of feeding ultra-low power sensor nodes as part of a wireless sensor network (WSN) fits with the novel and emerging development of diverse printed sensors with ultra-low power requirements, showing both technologies low costs in production and maintenance (no battery needs), besides other advantages.

In this paper, we demonstrate the combination of both growing technologies for a use in IoT with a novel under-development smart transceiver, fulfilling the requirements of real applications in terms of functionalities and costs.

1.1 RF Energy Harvesting

The term energy harvesting refers to the process of capturing, converting into electrical energy and storing small amounts of ambient energy, such as thermal, solar, vibrational or RF electromagnetic waves, for its further use in, normally, wireless autonomous devices like nodes part of a WSN. Which source will be used depends on the ambient conditions around the application device and on the device energy requirements itself, i.e. amount of energy needs, part of the day of operation, among others.
In the case of RFEH, the energy present at the signal carriers in the far field region is captured through an antenna and later on converted to dc. The frequencies of operation are between some kHz and hundreds of GHz [1].

There are some clear advantages to using RFEH: practically everywhere and every-time availability, predictability and stability over time, wireless nature, low-cost implementation and small form factor [1] [2] [3]. However, as the Friis equation anticipates [4], the biggest drawback is the amount of power received and therefore harvested, due to the inverse square relation with the distance to the radiation source and to the efficiency of the rectifying and converting processes. In addition, frequently the availability of the signal is not constant, e.g. Wi-Fi router duty-cycle or mobile phone random use [5] [6].

RFEH can be also used as a wireless energy transfer technique, just as the well-known inductive coupling (including resonant inductive). The difference with respect to harvesting is the use of a dedicated signal emitter and the advantage against the other wireless methods is the effective distance reached (20 dB attenuation per decade versus 60dB for near field [3]); although, it has much lower RF-to-dc energy conversion efficiency.

1.2 Printed Sensors Technology

As well as RFEH, flexible electronics is an auspicious field for diverse scientific and industrial areas, such as wearables or electronic skin (e-skin) [7] [8]. In this context, printed sensors technology is expected to satisfy the requirements of this kind of applications, which are not affordable with the current rigid silicon-based solutions (flexibility, lightness, transparency, etc.). Among the different printing technologies, the sensors presented in this work were developed by inkjet-printing, which offers the following advantages: ***i)*** contactless (nozzle-substrate), ***ii)*** high resolution and small thickness, ***iii)*** no mask required and ***iv)*** no wasted material. Besides, it is also compatible with the roll-to-roll techniques, enabling the mass-production of sensors in a cost-effective way [9].

1.3 Smart Transceiver

Every node from a WSN needs a component to perform logic tasks, control and data processes, likewise the wireless communication. We have chosen the TreuFunk chip, an ultra-low power smart transceiver under development with an innovative sensor interface including amperometry, voltametry and impedance spectroscopy. The core consists on an ARM Cortex M0 and the transceiver is based on the sub-GHz TDA5340 from Infineon. In addition, it includes radio frequency identification (RFID) and near field communication (NFC) capabilities with a standalone peripheral. See Figure 1 for a more detailed overview on its structure.

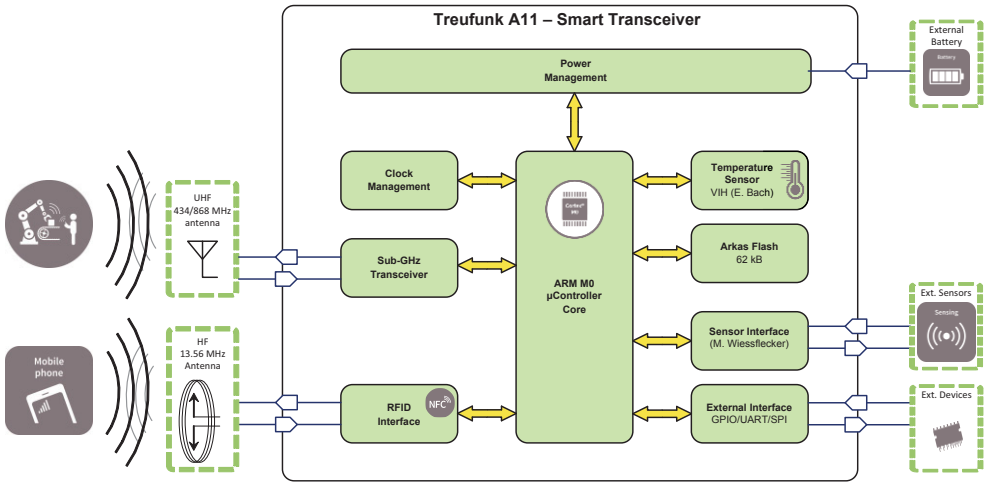

Figure 1. TreuFunk chip structure overview.

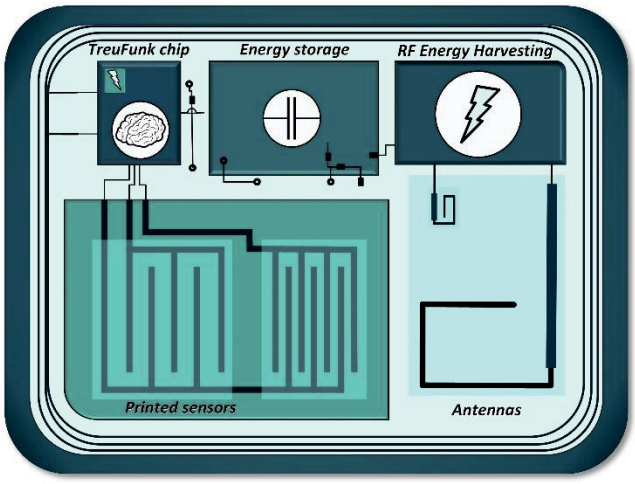

Figure 2. Complete system: Node with printed sensor and RFEH, plus RFID/NFC.

2 Merging Technologies

Combining ultra-low power sensors, logic and communication ends up in the best composite for RFEH, especially if the application demands are not too critical and if the surrounding environment enhances its usage. In Figure 2 the complete system is sketched, consisting of: *i)* smart transceiver TreuFunk chip, being also able to be manufactured in bendable technology; *ii)* printed sensor, in this case a capacitive structure for measuring the relative humidity (RH) of the air; *iii)* different antennas for communication (868 MHz), harvesting from global system for mobile communications (GSM) (949 MHz) and RFID/NFC usage (13.56 MHz) and *iv)* RFEH block, outputting directly regulated dc voltage to a *v)* storage capacitor.

2.1 Working Principle

The system works with a duty-cycled operation where most of the time the logic, including radio, will be in sleep mode (ultra-low power consumption) and where meanwhile the harvesting procedure will charge the storage capacitor. Once a certain level is reached and if the application requires it, it will make a measurement and send it to the next node or gateway depending on the communication scheme (points that do not work with energy harvesting). The minimum period depends only on the richness of the spectrum, i.e. how much energy is available around the node, but will be in last instance the application who determines how often the measurements are carried out.

2.2 Energy Availability

Nowadays the energy levels in cities open-spaces go to maximums around -30 dBm (although -20 dBm is also commonly found) at high utilization bands as GSM or its successors, TV broadcasting or wireless local networks (Wi-Fi); going the frequency range from some hundreds MHz to a few tens of GHz [1]. Additionally, within indoor environments or with active emitting, the present energy can reach more than -3 dBm at averaged distances [3].

From the source of energy until its final use, the losses are divided between the path and presumable obstacles and the rectifier-converter-storage efficiency, where the path losses are given by the Friis transmission equation (depends favorably on antenna gains and unfavorably on the squares of the signal frequency and distance) [1]. With the actual state of the art in rectification, conversion and storage, these levels can satisfy the power requirements for some applications as the one presented. For the favorable scenarios, the power harvested varies from some μW to hundreds of them [3]. Making use as well of the store and use principle, this can be utilized in more energetic bursts during the duty-cycle.

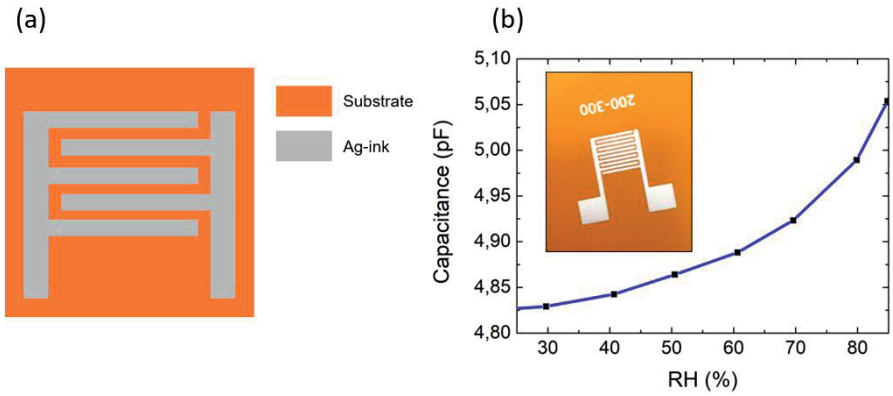

Figure 3. (a) Planar IDE capacitor layout. (b) Example of capacitance response as a function of the RH. Inset shows a real view of an Ag-inkjet printed RH sensor.

2.3 Sensor Description

The presented node is intended for RH monitoring. For that, we inkjet-printed a planar interdigitated electrodes (IDE) capacitor with silver nano particles on a Kapton® HN flexible substrate, as depicted in Figure 3a. The dependency with respect to the moisture of the dielectric constant of this thin-film substrate makes the capacitance of these structures sensitive to humidity changes (an example of response curve is shown in Figure 3b), which allows the manufacturing of inexpensive flexible RH sensors.

3 Conclusions

We have presented a suitable solution for developing RFEH autonomous nodes for WSNs with a great variety of variables to measure, thanks to the use of innovative and low-cost printed sensors. Furthermore, the employment of an ultra-low power smart transceiver along with the added value of RFID/NFC communication gives the possibility of secure and wireless performance, promoting IoT applications with low costs and longer life-time for the next generation of smart-home and –city.

4 References

[1] F. Moreno-Cruz, A. Escobar-Molero, E. Castillo, M. Becherer, A. Rivadeneyra und D. P. Morales, „Why Use RF Energy Harvesting in Smart Grids," in *2018 IEEE 23rd International Workshop on Computer Aided Modeling and Design of Communication Links and Networks (CAMAD)*, 2018.

[2] P. Kamalinejad, C. Mahapatra, Z. Sheng, S. Mirabbasi, V. C. M. Leung und Y. L. Guan, „Wireless energy harvesting for the internet of things," *IEEE Communications Magazine,* Bd. 53, pp. 102-108, 2015.

[3] X. Lu, P. Wang, D. Niyato, D. I. Kim und Z. Han, „Wireless networks with RF energy harvesting: A contemporary survey," *IEEE Communications Surveys & Tutorials,* Bd. 17, pp. 757-789, 2015.

[4] P. Nintanavongsa, „A survey on RF energy harvesting: circuits and protocols," *Energy Procedia,* Bd. 56, pp. 414-422, 2014.

[5] X. Liu und E. Sánchez-Sinencio, „A highly efficient ultralow photovoltaic power harvesting system with MPPT for internet of things smart nodes," *IEEE transactions on very large scale integration (vlsi) systems,* Bd. 23, pp. 3065-3075, 2015.

[6] H. Jayakumar, K. Lee, W. S. Lee, A. Raha, Y. Kim und V. Raghunathan, „Powering the internet of things," in *Proceedings of the 2014 international symposium on Low power electronics and design*, 2014.

[7] S. Kim, R. Vyas, J. Bito, K. Niotaki, A. Collado, A. Georgiadis und M. M. Tentzeris, „Ambient RF energy-harvesting technologies for self-sustainable standalone wireless sensor platforms," *Proceedings of the IEEE,* Bd. 102, pp. 1649-1666, 2014.

[8] A. Nathan, A. Ahnood, M. T. Cole, S. Lee, Y. Suzuki, P. Hiralal, F. Bonaccorso, T. Hasan, L. Garcia-Gancedo, A. Dyadyusha und others, „Flexible electronics: the next ubiquitous platform," *Proceedings of the IEEE,* Bd. 100, pp. 1486-1517, 2012.

[9] S. Khan, L. Lorenzelli und R. S. Dahiya, „Technologies for printing sensors and electronics over large flexible substrates: a review," *IEEE Sensors Journal,* Bd. 15, pp. 3164-3185, 2015.

[10] M. Russo, P. Šolić und M. Stella, „Probabilistic modeling of harvested GSM energy and its application in extending UHF RFID tags reading range," *Journal of Electromagnetic Waves and Applications,* Bd. 27, pp. 473-484, 2013.

2.6 Publication 6

"I do not think that the radio waves I have discovered will have any practical application."
– Heinrich Hertz

Custom Tri-Band Antenna within RF Energy Harvesting

Fernando Moreno-Cruz[1,2], Marina Ramos Cuevas[2], Pablo Padilla de la Torre[3], Diego P. Morales[4] and Almudena Rivadeneyra[4]

[1] Infineon Technologies AG, Munich (Germany)
[2] Technical University of Munich, Munich (Germany)
[3] Department of Signal Theory, Telematics and Communications, University of Granada, Granada (Spain)
[4] Department of Electronics and Computer Technology, University of Granada, Granada (Spain)

Submitted to IEEE Transactions on Antennas and Propagation

Custom Tri-Band Antenna within RF Energy Harvesting

Fernando Moreno-Cruz, Marina Ramos Cuevas, Pablo Padilla de la Torre, Diego P. Morales and Almudena Rivadeneyra

***Abstract*—The ongoing deployment of Internet of Things and 5G in our society makes more necessary to find green solutions for its powering and, concurrently, more fruitful the employment of radio frequency energy harvesting (RFEH) in an every time more populated RF spectrum. In this work, we present a tri-band antenna customized for the most energetic frequency bands of our particular environment and the general required features for RFEH, and propose three different use-cases for its efficient utilization in this modality of harvesting. Two of them, make use of the power management stage *MSwitch*, that mixes two dc signals, and utilize the third one for the application communication in one case and for energetically assisting the power management in the other. Besides, we introduce in a third use-case the novel under development *MSwitch-X3*, a tri-band dc mixing power management stage. In addition, we developed two different adaption boards including the needed signal splitting, rectification, impedance matching and connectors. The results bear clear benefits in terms of costs, space and amount of energy harvested, with respect to single band structures or arrays of them.**

***Index Terms*—Radio frequency energy harvesting (RFEH), Antennas, Internet of Things (IoT), Wireless sensor networks (WSN), Ultra-low power, Multi-band.**

I. Introduction

WHILE the number of Internet of Things (IoT) devices keeps growing and more applications emerge, some challenges still persist, such as the powering of the nodes. Batteries have been proven to be impractical in large deployments because of their recharging and replacement needs, in addition to their undoubtedly enormous environmental impact [1]. In pursuit of solving this, energy harvesting (EH) stands as a suitable solution. EH devices capture ambient energy in a green fashion, converting it to electricity for its use. The sources are of a broad nature, such as thermal, solar, vibrational or electromagnetic waves; while their uses depend on their availability in the specific space where they are used and on the requirements of the application.

Radio frequency energy harvesting (RFEH) in particular, captures the energy from the signal carriers in the far field region of ambient electromagnetic radiation, coming from bands of high utilization such as the cellular network (global system for mobile communications [GSM] or its successors), TV broadcasting, private mobile radio or wireless local networks. This radiation may reach in cities open-spaces up to $-30\,\mathrm{dBm}$ and less commonly of $-20\,\mathrm{dBm}$ [2]–[5].

The system operational viability depends on the amount of energy able to capture. This is conditioned to a great extend by the structure, orientation and frequency of the antenna, finally culminating in its efficiency at the operational frequencies. Nowadays, most of the designed antennas for RFEH present a planar printed structure. From Yagi-Uda [6] to fractal [7] designs, they can all be manufactured by applying common printed circuit board (PCB) techniques, resulting finally in two-dimensional low-profile low-cost microstrip geometries.

Depending on the circumstances in which the device will operate, the design should consider critical parameters such as the band and number of them, the substrate material, the configuration or the directivity [8].

Along the literature, the designs of single band antennas have been based mostly on standard antenna structures. For instance, patch antennas at different configurations [9]–[11]; dipole antennas, either alone or combined in the same structure [12], [13]; inverted-F monopoles [14], [15] or utra-wide band (UWB) antennas, as Vivaldi or spiral geometries [16], [17], to cite some.

Depending on the parameters to be adapted, they include special shapes or dielectrics, variations in the ground plane structure or in the feeding technique [18]–[22]. In this way, by introducing parasitic elements inside the patch (generally slots or shorting pins) or in its vicinity and modifying the signal feeding, other resonance frequencies can be obtained [23]. Modifying the shape of the ground plane (or just eliminating it) motivates the presence of back radiation lobes, which contributes to a more omnidirectional radiation pattern [24]. Alongside of compound structures, arrays or changes in the symmetry, among others, that adjust the polarization or radiation schemes.

The simplest assumption is that the harvesting is done in one frequency band and with one single antenna, but that might be unfruitful in real scenarios where the emission is not constant or powerful enough. Harvesting from more than one band stands clearly as a more profitable practice [13], [14], [25]–[31], although the energy management gets more complicated, besides the need of an extra antenna or a multi-band one. The methods for combining the energy of the diverse bands address it at either one of two different stages: at the matching network or once the the signal is rectified [32].

When the energy leaves the antenna, the next stages take

Manuscript received September XX, 2020; revised ZZ XX, 2020.

F. Moreno-Cruz is with Infineon Technologies AG, Germany, e-mail: Fernando.MorenoCruz@infineon.com

M. Ramos Cuevas is with the Technical University of Munich, Germany.

P. Padilla de la Torre is with the Signal Theory, Telematics and Communications Department, University of Granada, Spain, e-mail: pablopadilla@ugr.es

A. Rivadeneyra and D.P. Morales are with the Department of Electronics and Computer Technology, University of Granada, Spain, e-mail: (see http://electronica.ugr.es/index.php?sec=personal).

on the rectification, voltage level adaption and storage. The rectification is formed by Schottky diodes or CMOS structures in diode configuration, due to the requirements on low turn-on voltage and high switching speed. They usually implement voltage multipliers, since the electronics of the next stages need a minimum voltage to operate [25]. Once the signal is rectified, a level adaption is needed, not only for the value (that depends directly on the power input), but also for the stabilization over time. This is done by a dc/dc converter that charges a capacitor or battery from where the application is powered.

A. Contribution

In this work, we present a novel tri-band (868, 949 and 2159 MHz) microstrip asymmetric stacked-patch antenna for being used in RFEH devices as part of a wireless sensor network (WSN). We analyze the antenna requirements for a general RFEH case, describe the selected design characteristics and evaluate its viability through simulations, for later manufacturing it and examining its measurements.

In addition, we propose three different concepts for taking advantage of its three bands and that solve its energy management stage in diverse RFEH use-cases. Each of them with different advantages regarding costs, size and amount and efficiency of energy captured.

The remainder of this article is organized as follows. In Section II, we describe the novel tri-band antenna developed, its simulation and experimental results. In Section III, we propose three different use-cases for its utilization with RFEH and finally, Section IV, draws the main conclusions of this work and expounds the focus for future work.

II. Tri-Band Antenna Development

Starting with the requirements, in this section we describe the designed antenna, analyzing its simulation results that guided us for its manufacturing and comparing the measurements with the expected values.

A. Specifications

1) Frequency requirements: Since the energy presence in the spectrum depends on the service providers and the base stations nearby, we performed a spectrum analysis to find the most favorable frequencies. The results exhibit the most powerful bands located at 868, 949 and 2159 MHz (hereinafter referred as bands I, II and III, respectively), corresponding with the 935–960 MHz GSM band and the 2110–2170 MHz international mobile telecommunications (IMT) band (i. e., 2G and 3G). We also selected the open short range devices (SRD) 863–876 MHz band considering our purpose of including the final system in an existing WSN operating at this band.

Our test environment consisted of an office area on the outskirts of Munich (Germany) of around $0.2\,\mathrm{km}^2$, from which the half is free space and the other half three-floors buildings. We utilized a Keysight FieldFox Handheld N9917A spectrum analyzer.

2) Polarization requirements: Because of the unknown polarization of the signals reaching the system, circular polarization is desired for the antenna. The electric field X and Y components at the antenna output present then equal magnitude but a $90°$ phase difference for a given frequency. This allows to capture energy with all polarization schemes: linear, circular and elliptical.

3) Directivity requirements: As stated previously, the signal sources are unknown in the general case. Therefore, the antenna directivity (and thus its gain) should take a relatively low value placed around 3–5 dBi, for achieving the closest to an omni-directional radiation characteristic.

4) Technology requirements: There are no particular requisites for the type of antenna. However, easy integration and low-cost manufacturing are preferable. Thus, a printed planar structure, such as common PCB techniques, stands out.

5) Efficiency requirements: The final goal and most critical requirement is the efficiency. Due to the low energy available to be harvested, this parameter must be prioritized in order to obtain the maximum energy input. As the structures considered include all a dielectric layer, only materials with low loss tangent are desired.

B. Antenna Design

Attending at the detailed requirements, we designed the antenna with the assistance of HFSS, a 3-D electromagnetic simulation software by ANSYS based on the finite element method.

The chosen structure is a patch antenna operating at each of the target frequency bands. These geometries have high radiation efficiency and low directivity, in addition to performing robustly with changes in its surroundings (e. g., presence of physical objects). Additionally, their natural bigger size and linear polarization can be compensated with different techniques, such as cut outs or the feeding configuration.

The common FR-4 material is considered a lossy unstable material, besides of most of the manufacturers not assuring specific characteristics. Therefore, we selected AD600L, whose parameters make it nearly lossless ($\varepsilon_r = 6.15$, $\tan\delta = 0.003$ [33]) and assist as well to decrease the antenna size.

A rectangular shape is selected because of its flexibility in terms of multi-band design. Besides, a stacked-patch structure will conform the final design, as it makes easier the resonance at distanced frequencies. The patch associated to bands I and II is immersed in the dielectric material, while the patch on top of the structure resonates at band III. The top patch presents a smaller size than the bottom one and is shifted from the center of the substrate, so the optimal feeding position for both patches are coincident. The detailed antenna structure and its physical dimensions can be found in Figure 1 and Table I.

The chosen feeding configuration is a single coaxial structure, positioned in a way that allows exciting orthogonal current modes in the radiators. The upper patch is directly connected to it, while the lower one is excited by electromagnetic coupling. The result is dual polarization, although linear for each band.

TABLE I
DIMENSIONS OF THE STACKED-PATCH STRUCTURE

Patch	f_R (MHz)	L_X (mm)	L_Y (mm)	d_{hole} (mm)	d_{offX} (mm)	d_{offY} (mm)	L_{SX} (mm)	L_{SY} (mm)	(d_X, d_Y) (mm)	d_P (mm)	H_S (mm)
Bottom	868.1	53.07	60.29	4.02	2.75	2.75	85.00	85.00	(7.25,7.25)	6.096	13.716
	945.2										
Top	2158.3	24.47	26.84	-	-	-					

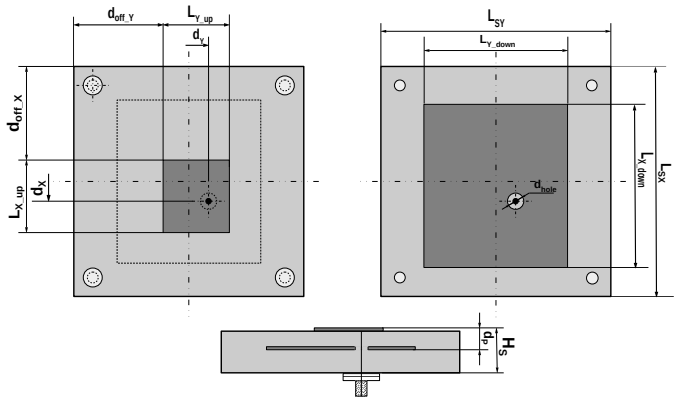

Fig. 1. Asymmetric dually-polarized multi-band stacked-patch antenna outline.

Fig. 2. Photo of the manufactured antenna.

C. Simulations & Measurements

Following, we analyze the proposed design through simulations with HFSS and compare them with the measurements of the manufactured antenna. We manufactured the antenna with the selected AD600L substrate material, stacking several layers of $1.524\,\mathrm{mm}$ between the copper patches according the above described dimensions and using a $50\,\Omega$ SMA connector (see Figure 2).

The results, first indicated with the simulations and checked with the measurements later, demonstrate efficient radiation and resonance and quasi omni-directional behavior at the frequencies of interest. The feeding method, exciting simultaneously two orthogonal current modes on each patch, achieves resonance at two different frequencies; while the asymmetric placement of the upper patch with respect to the center of the structure allows the input impedance matching at every band. The ground plane size chosen in the design contributes for its omni-directivity, mostly for the lower frequencies.

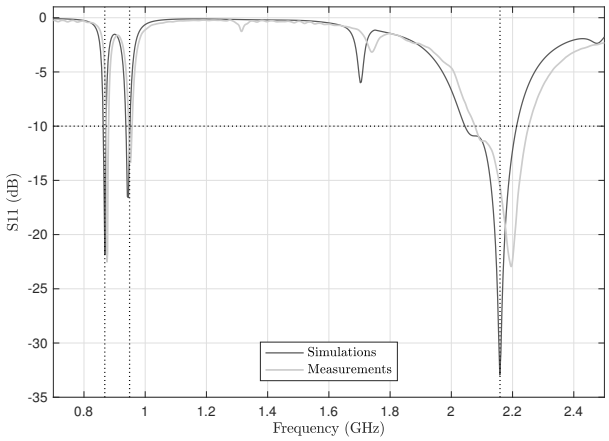

Fig. 3. Simulation and measurement of return losses (S11 parameter) for tri-band antenna. *Dotted the* $-10\,\mathrm{dB}$ *line and the center frequencies of interest for reference.*

Figure 3 depicts the resonant behavior of the antenna over the frequency at $50\,\Omega$ characteristic impedance. In the simulation, the three bands see fulfilled their bandwidth requirements with fractional bandwidth values of 1.04, 1.41 and 7.93%, respectively. The impedance bandwidth characteristics of the antenna for both simulation and measurement results are detailed in Table II, being f_1 and f_2 the $-10\,\mathrm{dB}$ threshold frequencies and f_R and f_0 the resonance (minimum value) and center of the bandwidth frequencies, respectively. The measurements follow the simulation as expected, achieving the bandwidth and return loss expectations. We see however a slight shift upwards in frequency, negligible for bands II and III, but that takes part of band I out of the $-10\,\mathrm{dB}$ threshold. The possible reasons of this are explained at the end of this section.

Regarding the radiation patterns, the simulations exhibit an efficiency over 85% at the lower bands, while for band III, it reaches even higher values with reduced back radiation lobes. Figure 4 represents the directivity at every plane for the three center frequencies. The radiation peak is found to be orthogonal to the plane where the antenna lays. As seen in the figure, the front-to-back ratio in band III is remarkably

TABLE II
SIMULATION AND MEASUREMENT RESULTS OF BANDWIDTH FOR TRI-BAND ANTENNA

	Patch	Band	f_1 (MHz)	f_2 (MHz)	f_R (MHz)	f_0 (MHz)	**-10dB-BW** (MHz **(%)**)
Sim.	**Bottom**	I	862.6	871.6	868.1	867.1	9.0 (1.04)
		II	936.8	950.2	945.2	943.5	13.4 (1.41)
	Top	III	2044.4	2213.3	2158.3	2128.6	168.9 (7.93)
Meas.	**Bottom**	I	872	881	875	876	9 (1.03)
		II	946	957	952	951	11 (1.16)
	Top	III	2077	2252	2196	2164	175 (8.09)

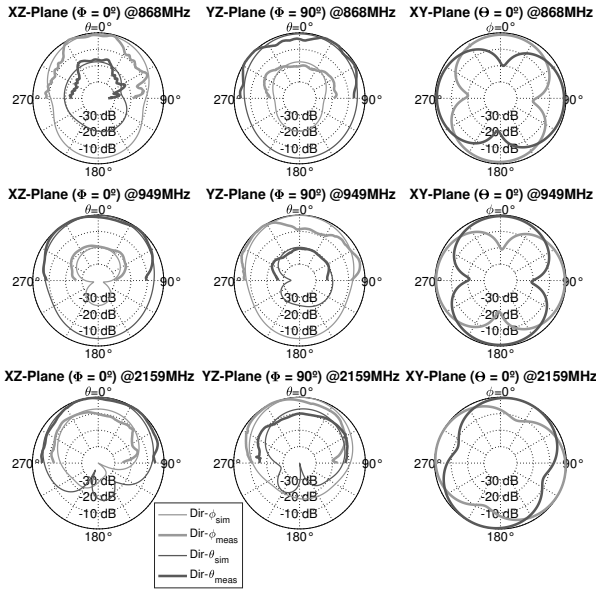

Fig. 4. Simulation and measurements of radiation pattern for tri-band antenna (directivity).

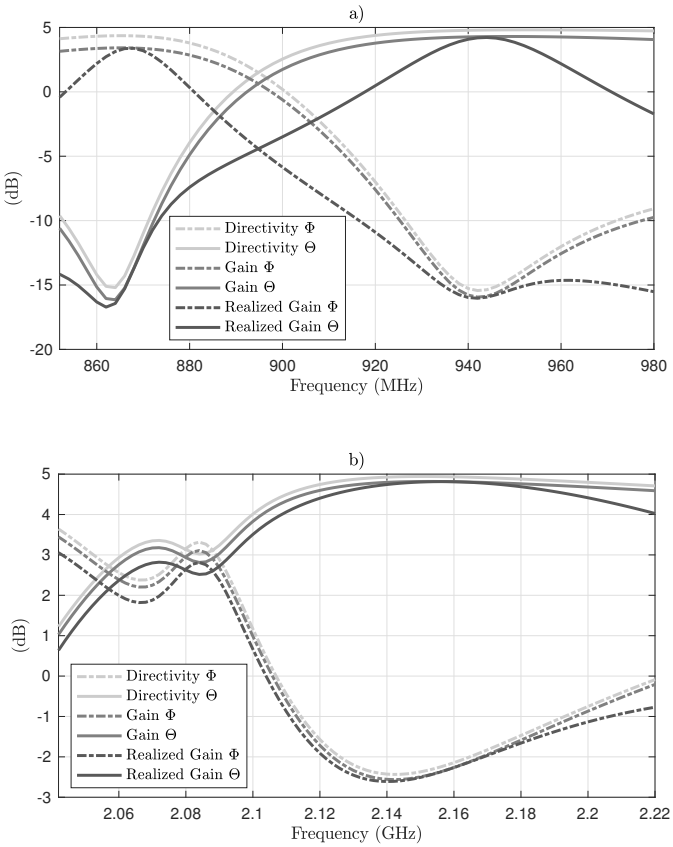

Fig. 5. Simulation of directivity, gain and realized gain for bands I and II (a) and band III (b) in $\Phi = \Theta = 0°$.

low, as its radiating patch is electrically smaller with respect to the ground plane. For bands I and II, directivity is quasi omni-directional in the vertical direction, since in this case the patch size is comparable with the ground plane, not containing the back-radiated waves.

The measurements, also illustrated in Figure 4, follow correctly the simulations. Although the back lobes and XY plane could not be measured because of the available equipment within the employed anechoic chamber; the manufactured antenna is proven to achieve the expected radiation patterns.

As no electric or magnetic field planes can be defined because of the dual polarization, cross-polarization cannot be clearly evaluated. However, we can analyze the evolution of the directivity over the bands for the different planes, e. g., $\Phi = 0°$ and $\Phi = 90°$. In the first case, the directivity in Θ becomes dominant for bands II and III, being the counter case for band I. In the plane $\Phi = 90°$, the situation is exactly the opposite, coinciding this with expected behavior for the patches designed structure.

Figure 5 gives as well more insights about the polarization at the objective bands with the directivity along the frequency, in addition to presenting the gain and realized-gain. The first, only slightly lower than the directivity due to the substrate low loss-factor; and the second, with also negligible difference with the gain around the -10dB-bandwidth, due to the achieved impedance matching.

Furthermore, we carried out simulations to check how the performance is affected by the variation of different structure parameters. We considered realistic variations that can occur during the fabrication process (between 5–10%). We concluded that the variation of the patches size, the feeding probe position, the distance between patches and the top patch relative position are not critical, neither for the radiation patterns, although both lower bands may eventually move out of the impedance bandwidth by cause of its narrower width. In the case of the ground plane size, the substrate height and the substrate relative electric permittivity, the impact is higher. Resonant frequencies might be shifted reducing the

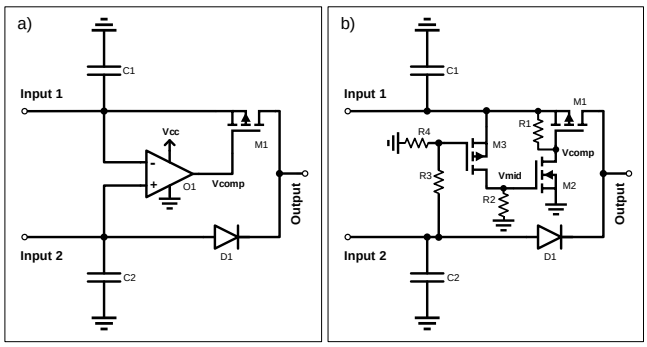

Fig. 6. Schematics of both versions of *MSwitch* stage: *Version 1* (with comparator) (a) and *Version 2* (with MOSFETs) (b) [25].

quality of the matching for band III and losing completely the frequency of interest for bands I and II. This explains the slight upward shift in frequency of our measurements. The manual manufacture of the antenna with several layers of substrate might affect the substrate height and electric permittivity, in our case, noticeable although not yet critical in band I.

III. RFEH Application

Following, we introduce three different use-cases of the designed tri-band antenna for RFEH. In each of them, we propose their operation with diverse versions of *MSwitch* [25], a stage within the energy harvester that manages the mixing of the signals once they are rectified. Therefore, a previous stage that separates and rectifies each band is required, also described for every use-case.

MSwitch is an autonomous dual-input circuit based on the store-and-use and switched capacitor principles, that regulates the mixing of the two energy inputs. With its analog algorithm, see Figure 6, it is capable of reducing the minimum average input power needed per RF band for an IoT application [25].

It performs three functions: stores energy in time until the level is high enough for running the electronics of the next stage, mixes both input lines in a dynamic manner and isolates the energy sources from the load, in order to not let the voltage drop.

Version 1 benefits more long store-and-use cycles in extreme low power scenarios. It has a first cold-start mode with only one input line delivering power, because of the need of a power supply by the comparator O1, which is meant to come from the next stage once it is operating. *Version 2*, on the other side, follows a dual and simultaneous conduction operation with quick dynamic self-adaption of the currents. This version replaces the comparator by two MOSFETs, not requiring an extra energy input.

We intend to utilize for the third of the use-cases the still in development *MSwitch-X3*, which incorporates a third signal input. Its objective is mixing the three rectified signals in a single output, in a similar way to the dual *Version 2*. Actually, the circuit of this variant is based on *Version 2* and counts with two sub-versions yet in analysis, adding the third level in parallel or cascade, respectively, see Figure 10.

The adaption boards are formed by a signal splitter 1-to-3 and two rectifiers and a microstrip line or three rectifiers,

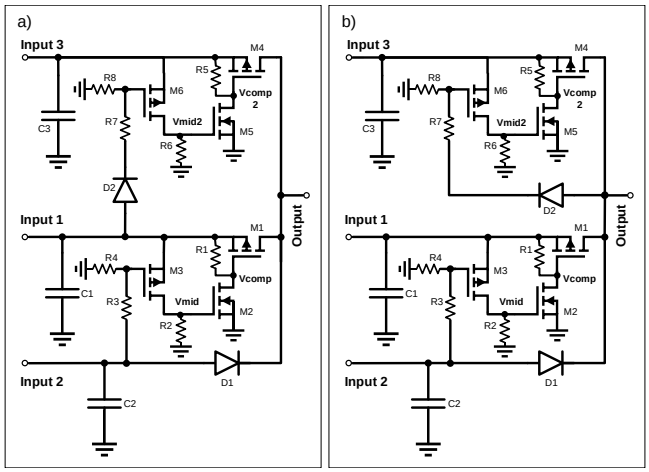

Fig. 7. Schematic of both versions of *MSwitch-X3* prototype. Version in parallel (a) and cascade (b).

depending on the version. In this way, the antenna is plugged through an SMA connector to the board, which is physically aligned with it (the boards have the same shape than the antenna, in order to be screwed together). The multi-band signal encounters then the signal splitter with three matching networks at the end of it for each of the frequencies. This splitter goes progressively from a line with characteristic impedance of $50\,\Omega$ until an impedance value of $50/3\,\Omega$, ending in a circular shape where $50\,\Omega$ lines begin. Right after the matching networks, 3-stage cockcroft-walton circuits rectify the signals already divided, for their output to the *MSwitch* stage. Only in the communication use-case, a second SMA connector is used instead of the rectifier, that connects the antenna to the radio transceiver.

A. Dual Mixing and Communication

This scheme targets the environments where only two of the bands are utilized by external devices, and therefore, only two bands have energy to be harvested. The third frequency of the antenna is employed for the communication needs of the IoT application, i. e., it is connected to the application radio transceiver, see Figure 8. For legal reasons, the communication band is fixed to $868\,\mathrm{MHz}$, part of the SRD band where the transmission is allowed.

Consequently, the adaption board incorporates two rectifiers and a second $50\,\Omega$ SMA connector that bonds the antenna with the radio transceiver. The communication path results thus, in the $50\,\Omega$ cable coming from the application board, connected to the SMA connector and a microstrip line, followed by the signal splitter and the connection to the antenna through the main SMA connector.

Aside of the RFEH utilization, the principal advantage of this setup is the cost and space savings of the application antenna, where the space savings include the separation between antennas and the no need of reserving a second radiation-capable area at its installation.

Fig. 8. Photo of the dual-harvester design, *MSwitch Version 2* and *IoT* application connected (radio transceiver).

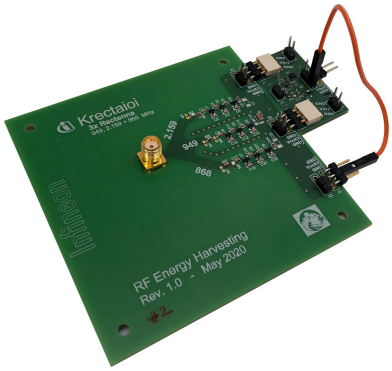

Fig. 9. Photo of the tri-harvester design and *MSwitch Version 1*.

B. Dual Mixing and Extra Supply

Directed to scenarios where the three bands can be harvested, this use-case rectifies the three signals after their matching networks (i. e., independently) and utilizes two of them for the *MSwitch Version 1* inputs and the remaining one for powering its comparator.

This setup potentially obtains a diminution of the minimum RF power input per line for staring to operate, due to the elimination of the *MSwitch Version 1* cold-start phase, where only one line conducts until the converter stage is able to power the comparator. In this way, the comparator runs from the beginning, performing the cyclic mixing of *MSwitch Version 1*.

C. Triple Mixing

Again for scenarios with three energetic bands, this setup mixes the three signals for their direct use at the application. With the same adaption board as the previous case, the three dc sources are connected to *MSwitch-X3*, the under development form of *MSwitch* with three inputs, based on *Version 2*.

Having its basis in a more efficient version of *MSwitch*, this scheme potentially increases the amount of energy delivered to the dc/dc converter, since it mixes dynamically three power sources. This allows the use of more power demanding applications or instead, its deployment in environments where the duty cycle of the signals to harvest is smaller, meaning this that the system would operate occasionally with only two bands.

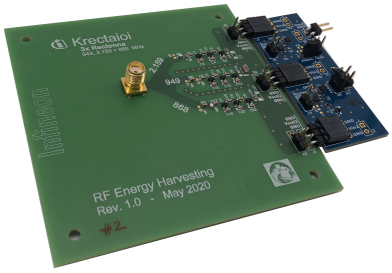

Fig. 10. Photo of the tri-harvester design and the prototype of *MSwitch-X3*.

IV. Conclusion

In this work, we have developed a custom tri-band antenna with purpose of gaining further advantages within its use in RFEH, against the case of a single band structure or several ones of them; in terms of number of bands to harvest from and diminution of space and costs. In addition, we proposed three use-cases to exploit its features, with different benefits under different scenarios and introduced the concept of a new power management stage for the mixing of three different dc signals.

After simulating several structures in pursuance of our specific requirements and frequency bands, we reached the final design consisting in a microstrip asymmetric stacked-patch structure in AD600L dielectric material of $85 \times 85\,\mathrm{mm}$, tailored for the frequencies 868, 949 and $2159\,\mathrm{MHz}$, which were the most energetic ones in our environment. We finally manufactured the antenna and measured it in the laboratory examining its properties. The results revealed great $50\,\Omega$ resonance and radiation at the target bands and quasi omni-directional behavior, i. e., fulfilling the RFEH demands.

Regarding the proposed use-cases, they make use of the power management stage *MSwitch*, efficiently mixing two of the bands after their rectification. Besides, they employ the third one, in one case, for powering the comparator of *MSwitch Version 1*, and in the other case, which utilizes *Version 2*, for the application communication. For this, we also developed two adaption boards, which included the rectification and signal splitting circuits, matching networks and needed connectors.

For the third use-case, we introduced *MSwitch-X3*, an under development power management stage based on *MSwitch Version 2* that mixes directly the three dc signals and which also encompasses our future work. This includes its complete characterization in its two variants (cascade and parallel) and the performance comparison with the rest of proposed use-cases.

In conclusion, the presented applications for the tri-band antenna, not only decrease the costs and needed space of a multi-band harvester, but also ease its deployment, since it can be offered as a plug-and-play module, which enhances in any case the features of a single band one. Moreover, the methodology described for the antenna design, guides for the customization of the bands for every specific case.

ACKNOWLEDGMENT

This work was partially supported by the ECSEL Joint Undertaking through CONNECT project under grant agreement No 737434. This Joint Undertaking receives support from the German Federal Ministry of Education and Research and the European Union's Horizon 2020 research and innovation program and Slovakia, Netherlands, Spain, Italy.

REFERENCES

[1] F. Moreno-Cruz, A. Escobar-Molero, E. Castillo, M. Becherer, A. Rivadeneyra, and D. P. Morales, "Why use rf energy harvesting in smart grids," in *2018 IEEE 23rd International Workshop on Computer Aided Modeling and Design of Communication Links and Networks (CAMAD)*. IEEE, 2018, pp. 1–6.

[2] M. Russo, P. Šolić, and M. Stella, "Probabilistic modeling of harvested gsm energy and its application in extending uhf rfid tags reading range," *Journal of Electromagnetic Waves and Applications*, vol. 27, no. 4, pp. 473–484, 2013.

[3] M. Yılmaz, D. G. Kuntalp, and A. Fidan, "Determination of spectrum utilization profiles for 30 mhz–3 ghz frequency band," in *Communications (COMM), 2016 International Conference on*. IEEE, 2016, pp. 499–502.

[4] A. Palaios, J. Riihijarvi, and P. Mahonen, "From paris to london: Comparative analysis of licensed spectrum use in two european metropolises," in *Dynamic Spectrum Access Networks (DYSPAN), 2014 IEEE International Symposium on*. IEEE, 2014, pp. 48–59.

[5] A. Palaios, V. Miteva, J. Riihijärvi, and P. Mähönen, "When the whispers become noise: A contemporary look at radio noise levels," in *Wireless Communications and Networking Conference (WCNC), 2016 IEEE*. IEEE, 2016, pp. 1–7.

[6] H. Sun, Y. Guo, M. He, and Z. Zhong, "A Dual-Band Rectenna Using Broadband Yagi Antenna Array for Ambient RF Power Harvesting," *IEEE Antennas and Wireless Propagation Letters*, vol. 12, pp. 918–921, 2013.

[7] Z. Zhou, W. Liao, Q. Zhang, F. Han, and Y. Chen, "A multi-band fractal antenna for RF energy harvesting," in *2016 IEEE International Symposium on Antennas and Propagation (APSURSI)*, Jun. 2016, pp. 617–618.

[8] M. Mrnka, P. Vasina, M. Kufa, V. Hebelka, and Z. Raida, "The RF Energy Harvesting Antennas Operating in Commercially Deployed Frequency Bands: A Comparative Study," 2016. [Online]. Available: https://www.hindawi.com/journals/ijap/2016/7379624/

[9] S.-E. Adami, P. Proynov, G. S. Hilton, G. Yang, C. Zhang, D. Zhu, Y. Li, S. P. Beeby, I. J. Craddock, and B. H. Stark, "A flexible 2.45-ghz power harvesting wristband with net system output from- 24.3 dbm of rf power," *IEEE Transactions on Microwave Theory and Techniques*, vol. 66, no. 1, pp. 380–395, 2017.

[10] P. Kamalinejad, C. Mahapatra, Z. Sheng, S. Mirabbasi, V. C. Leung, and Y. L. Guan, "Wireless energy harvesting for the internet of things," *IEEE Communications Magazine*, vol. 53, no. 6, pp. 102–108, 2015.

[11] A. M. Jie, M. F. Karim, K. T. Chandrasekaran *et al.*, "A wide-angle circularly polarized tapered-slit-patch antenna with a compact rectifier for energy-harvesting systems [antenna applications corner]," *IEEE Antennas and Propagation Magazine*, vol. 61, no. 2, pp. 94–111, 2019.

[12] Minhong Mi, M. H. Mickle, C. Capelli, and H. Swift, "RF energy harvesting with multiple antennas in the same space," *IEEE Antennas and Propagation Magazine*, vol. 47, no. 5, pp. 100–106, Oct. 2005.

[13] M. Piñuela, P. D. Mitcheson, and S. Lucyszyn, "Ambient rf energy harvesting in urban and semi-urban environments," *IEEE Transactions on microwave theory and techniques*, vol. 61, no. 7, pp. 2715–2726, 2013.

[14] S. Shen, Y. Zhang, C.-Y. Chiu, and R. Murch, "An ambient rf energy harvesting system where the number of antenna ports is dependent on frequency," *IEEE Transactions on Microwave Theory and Techniques*, vol. 67, no. 9, pp. 3821–3832, 2019.

[15] Y. Tawk, J. Costantine, F. Ayoub, and C. G. Christodoulou, "A communicating antenna array with a dual-energy harvesting functionality [wireless corner]," *IEEE Antennas and Propagation Magazine*, vol. 60, no. 2, pp. 132–144, 2018.

[16] T. Peter, T. A. Rahman, S. W. Cheung, R. Nilavalan, H. F. Abutarboush, and A. Vilches, "A Novel Transparent UWB Antenna for Photovoltaic Solar Panel Integration and RF Energy Harvesting," *IEEE Transactions on Antennas and Propagation*, vol. 62, no. 4, pp. 1844–1853, Apr. 2014.

[17] A. Alex-Amor, Á. Palomares-Caballero, J. M. Fernández-González, P. Padilla, D. Marcos, M. Sierra-Castañer, and J. Esteban, "Rf energy harvesting system based on an archimedean spiral antenna for low-power sensor applications," *Sensors*, vol. 19, no. 6, p. 1318, 2019.

[18] A. Eid, J. Costantine, Y. Tawk, A. Ramadan, M. Abdallah, R. ElHajj, R. Awad, and I. Kasbah, "An efficient rf energy harvesting system," in *2017 11th European Conference on Antennas and Propagation (EUCAP)*. IEEE, 2017, pp. 896–899.

[19] H. Sun, Y.-x. Guo, M. He, and Z. Zhong, "Design of a high-efficiency 2.45-ghz rectenna for low-input-power energy harvesting," *IEEE Antennas and Wireless Propagation Letters*, vol. 11, pp. 929–932, 2012.

[20] G. A. Vera, A. Georgiadis, A. Collado, and S. Via, "Design of a 2.45 ghz rectenna for electromagnetic (em) energy scavenging," in *2010 IEEE Radio and Wireless Symposium (RWS)*. IEEE, 2010, pp. 61–64.

[21] B. L. Pham and A.-V. Pham, "Triple bands antenna and high efficiency rectifier design for rf energy harvesting at 900, 1900 and 2400 mhz," in *2013 IEEE MTT-S International Microwave Symposium Digest (MTT)*. IEEE, 2013, pp. 1–3.

[22] A. Georgiadis, G. V. Andia, and A. Collado, "Rectenna design and optimization using reciprocity theory and harmonic balance analysis for electromagnetic (em) energy harvesting," *IEEE Antennas and Wireless Propagation Letters*, vol. 9, pp. 444–446, 2010.

[23] C. A. Balanis, *Antenna theory: analysis and design*. Wiley-Interscience, 2005.

[24] Z. W. Sim, R. Shuttleworth, M. J. Alexander, and B. Grieve, "compact patch antenna design for outdoor rf energy harvesting in wireless sensor networks," 2010.

[25] F. Moreno-Cruz, V. Toral-López, M. R. Cuevas, J. F. Salmerón, A. Rivadeneyra, and D. P. Morales, "Dual-band store-and-use system for rf energy harvesting with off-the-shelf dc/dc converters," *IEEE Internet of Things Journal*, pp. 1–1, 2020.

[26] M. Mattsson, C. I. Kolitsidas, and B. L. G. Jonsson, "Dual-band dual-polarized full-wave rectenna based on differential field sampling," *IEEE Antennas and Wireless Propagation Letters*, vol. 17, no. 6, pp. 956–959, 2018.

[27] V. Palazzi, J. Hester, J. Bito, F. Alimenti, C. Kalialakis, A. Collado, P. Mezzanotte, A. Georgiadis, L. Roselli, and M. M. Tentzeris, "A novel ultra-lightweight multiband rectenna on paper for rf energy harvesting in the next generation lte bands," *IEEE Transactions on Microwave Theory and Techniques*, vol. 66, no. 1, pp. 366–379, 2017.

[28] E. Khansalee, K. Nuanyai, and Y. Zhao, "A dual-band rectifier for RF energy harvesting," *Engineering Journal*, vol. 19, no. 5, pp. 189–197, oct 2015.

[29] J.-w. Zhang, X. Bai, W.-y. Han, B.-h. Zhao, L.-j. Xu, and J.-j. Wei, "The design of radio frequency energy harvesting and radio frequency-based wireless power transfer system for battery-less self-sustaining applications," *International Journal of RF and Microwave Computer-Aided Engineering*, vol. 29, no. 1, p. e21658, 2019.

[30] Y. Shi, Y. Fan, Y. Li, L. Yang, and M. Wang, "An efficient broadband slotted rectenna for wireless power transfer at lte band," *IEEE transactions on Antennas and Propagation*, vol. 67, no. 2, pp. 814–822, 2018.

[31] V. Palazzi, M. Del Prete, and M. Fantuzzi, "Scavenging for energy: A rectenna design for wireless energy harvesting in uhf mobile telephony bands," *IEEE Microwave Magazine*, vol. 18, no. 1, pp. 91–99, 2016.

[32] M. Wagih, A. S. Weddell, and S. B. Beeby, "Rectennas for rf energy harvesting and wireless power transfer: a review of antenna design," *IEEE Antennas and Propagation Magazine*, 2019.

[33] "AD600a™, AD1000™," accessed: 2019-05-29. [Online]. Available: https://www.rogerscorp.com/acs/products/80/AD600A-AD1000.aspx

2.7 Publication 7

"If you cannot measure it,
you cannot improve it."
– William Thomson (L. Kelvin)

Facile Manufacturing of Sub-mm Thick CNT-Based RC Filters

Florin C. Loghin[1], Aniello Falco[2], **Fernando Moreno-Cruz**[3,4], Paolo Lugli[2], Diego P. Morales[4], José F. Salmerón[4] and Almudena Rivadeneyra[4]

[1] Institute for Nanoelectronics, Technical University of Munich, Munich (Germany)
[2] Faculty of Science and Technology, Free University of Bolzano-Bozen, Bolzano (Italy)
[3] Infineon Technologies AG, Munich (Germany)
[4] Department of Electronics and Computer Technology, University of Granada, Granada (Spain)

Submitted to Flexible and Printed Electronics

Facile Manufacturing of Sub-mm Thick CNT-Based RC Filters

Florin C. Loghin[1], Aniello Falco[2], Fernando Moreno-Cruz[3,4], Paolo Lugli[2], Diego P. Morales[4], José F. Salmerón[4] and Almudena Rivadeneyra[4]

[1] Institute for Nanoelectronics, Technical University of Munich, Munich, Germany
[2] Faculty of Science and Technology, Free University of Bolzano-Bozen, Bolzano, Italy
[3] Infineon Technologies AG, Munich, Germany
[4] Department of Electronics and Computer Technology, University of Granada, Granada

E-mail: arivadeneyra@ugr.es

Received 5 November 2020
Accepted for publication xxxxxx
Published xxxxxx

Abstract

Even three decades after their discovery, Carbon Nanotubes (CNTs) keep offering novel application opportunities, thanks to their extraordinary properties still being examined. In this letter, we realize CNT-Based RC networks with the purpose of showing empirical findings on the influence of the interdigitated electrodes (IDE) spacing, the dispersant compound and the number of deposited layers, on the impedance magnitude and phase of the CNTs. Additionally, we propose use-cases for these networks, applying them to the realization of filters of second order with easily tunable cut-off frequency, and with the inherent advantages of CNTs and printed technologies, rendering them a prime choice for applications where thin and flexible second order filters are necessary.

Keywords: spray deposition, single walled carbon nanotubes, interdigitated electrodes, frequency response, filters

1. Introduction

Since their discovery by Iijima in 1991 [1], Carbon Nanotubes (CNTs) have being extensively studied for a broad spectrum of applications due to their unique characteristics in geometry, morphology and electrical properties [2]. Such applications include nanobalances, with a resolution up to 1.7 yoctogram (mass of one proton) [3]; identification of different species of atoms or molecules, specifically noble gas atoms or DNA molecules [4]; composites as electrode material for rechargeable Li-ion batteries, which enhance the energy conversion and storage capacity due to their high electrical and thermal conductivities and extremely large surface area [5, 6]; among others. Their detection principle is based on measuring the shift in the resonant frequency or the wave velocity in CNT nano-resonator structures, caused by the attachment of foreign atoms or molecules on the surface of the sensors [7].

CNTs belong to the family of fullerene structures, being a 1D material with a length-to-diameter ratio in excess of 1000 [8, 5]. They are nanometer-scale cylinders composed of rolled-up graphene sheets around a central hollow core and end caps with a hemisphere of fullerene structure [5]. They can be classified depending on their physical characteristics, being one of the possible categorizations the thickness of the carbon atomic wall. It is then possible to distinguish between single-walled CNTs (SWCNTs), with a one-atom thick graphene layer and multiwalled CNTs (MWCNTs) [9], consisting of two or more layers with van der Waals forces between adjacent layers.

Depending on the rolling angle of the graphene sheet against the tube axis, we define the chirality, represented by an integer pair (n, m). CNTs are called “armchair” and

"zigzag", for $n=m$ and $m=0$ respectively and "chiral" otherwise [10]. The chirality has significant impact on the CNTs electrical properties. Nanotubes with $n-m = 3j$ (with j being a non-cero integer) are metallic, while all the other cases are semiconducting [7]. In any manner, CNTs have exceptional physical and chemical properties, being the strongest and stiffest materials currently known on earth and having high thermal stability in both vacuum and air [11].

For their fabrication, there are three main techniques: arc-discharge, which was the first technique to be used; laser ablation and chemical vapor deposition (CVD) [12, 13]. While the first two are unsuitable for mass production [14], CVD can synthesize CNTs at relatively low temperature, being more efficient and allowing to scale up growth of both SWCNTs and MWCNTs [2]. In all these growth methods, impurities in the fabrication may affect negatively the CNTs properties. For that reason, a purification process is important to obtain high-quality nanotubes. So far, samples of up to 99.6% purity can be obtained [2].

Once the CNTs are grown, they need to be transferred to the target surface, which could be structured or flat, and can then be employed as conductors or semiconductors depending on their physical and chemical characteristics. Solution processing by means of spray deposition is one of the methods that showed the most reliable and significant results in the cost effective deposition of CNT networks. It consists on the deposition of (usually) a material in liquid state, with the aid of a gas stream and offers a reproducible coating of the desired surface by using shadow mask with a controllable thickness [15, 16].

The result ultimately is a material with outstanding properties that can be brought quickly into solution, which facilitates their use in processing techniques commonly employed in emerging technologies [17]. Such techniques have inherent advantages in comparison to conventional silicon-based processes in terms of processing condition, resulting features (like flexibility and stretchability) and potential throughput [18, 19].

Concerning the costs, the mentioned integrated solutions and more complex ones, like hybrid-acoustic filters or digital filters, place themselves in another level of prices. In addition to the straightforward and economic integration with other printable technologies, the cost itself of the production and development is far lower.

In this letter, we demonstrate the feasibility of designing analog circuits and RC networks based on CNT devices by only tuning the spacing of interdigitated electrodes (IDE) or the number of deposited layers. In particular, we deposit the CNT layer by spray deposition. We study the influence of the dispersant employed for the CNT solution and the spacing among consecutive fingers of IDE layouts. Finally, we show some applications where different of such elements are utilized.

2. Materials and Methods

For the device fabrication, Si wafers with a 200 nm thermally grown oxide of 65 nm thickness were used as substrates. IDE structures were photolithographically patterned with a subsequent physical vapor deposition of Cr/Au (5 nm/40 nm) as contacts. The resist and excess Cr/Au film was removed via lift-off. Commercially bought CNTs (Carbon Solution Inc.) (0.03 wt%) were dispersed in deionized water (DI H2O) with the aid of a dispersant. Two solutions were fabricated, one based on sodium carboxymethyl cellulose (CMC) and one on sodium dodectyl sulfate (SDS). The corresponding weight percentage of dispersants were 0.5 wt% for CMC and 1% for SDS. The solution was then deposited by spray deposition onto the substrates. The deposition parameters were adapted from [20]. Post deposition treatment is dispersant dependent. The dispersant needs to be removed as it, in both cases, inhibits charge carrier transport. For CMC the substrates are placed in dilute nitric acid (1:4) (65% HNO3:DI H2O) for 12+h while the SDS samples are placed in DI H2O for 30 min. For the investigation in this paper, both CNT thickness, more specifically number of layers deposited, as well as varying electrode spacing, were investigated. Such samples were fabricated with varying number of layers deposited (1, 2 and 3 layers) for both dispersants, while keeping the electrode spacing constant (200 µm). The subsequent experiment fixed the CNT layer in terms of dispersant and layer number while varying the electrode spacing (100 µm, 200µm and 500µm).

The impedance response of the fabricated devices was measured with a Keysight E4990A Impedance Analyzer with an impedance probe kit (42941A). The excitation voltage applied in all measurements was VDC=0 and VAC=500 mV and the frequency ranged from 100 Hz to 100 MHz.

3. Results and Discussion

In the following section, we present the results obtained of our experiments, conducted varying different device parameters, such as the thickness, the dispersant compound and the spacing. Next, we propose an application use for the innovation.

3.1 Number of Layers

The change in the thickness of the CNT devices through the variation of the number of layers was studied and we proved, as seen in **Error! Reference source not found.**, how it influences their impedance magnitude and phase in the frequency domain. For higher number of layers, i.e., higher thickness, the impedance magnitude decreases at low frequencies, converging later on the same values. In the same way, higher number of layers means more stable phase along the frequency axis, following all the same pattern, and with less pronounced lobes.

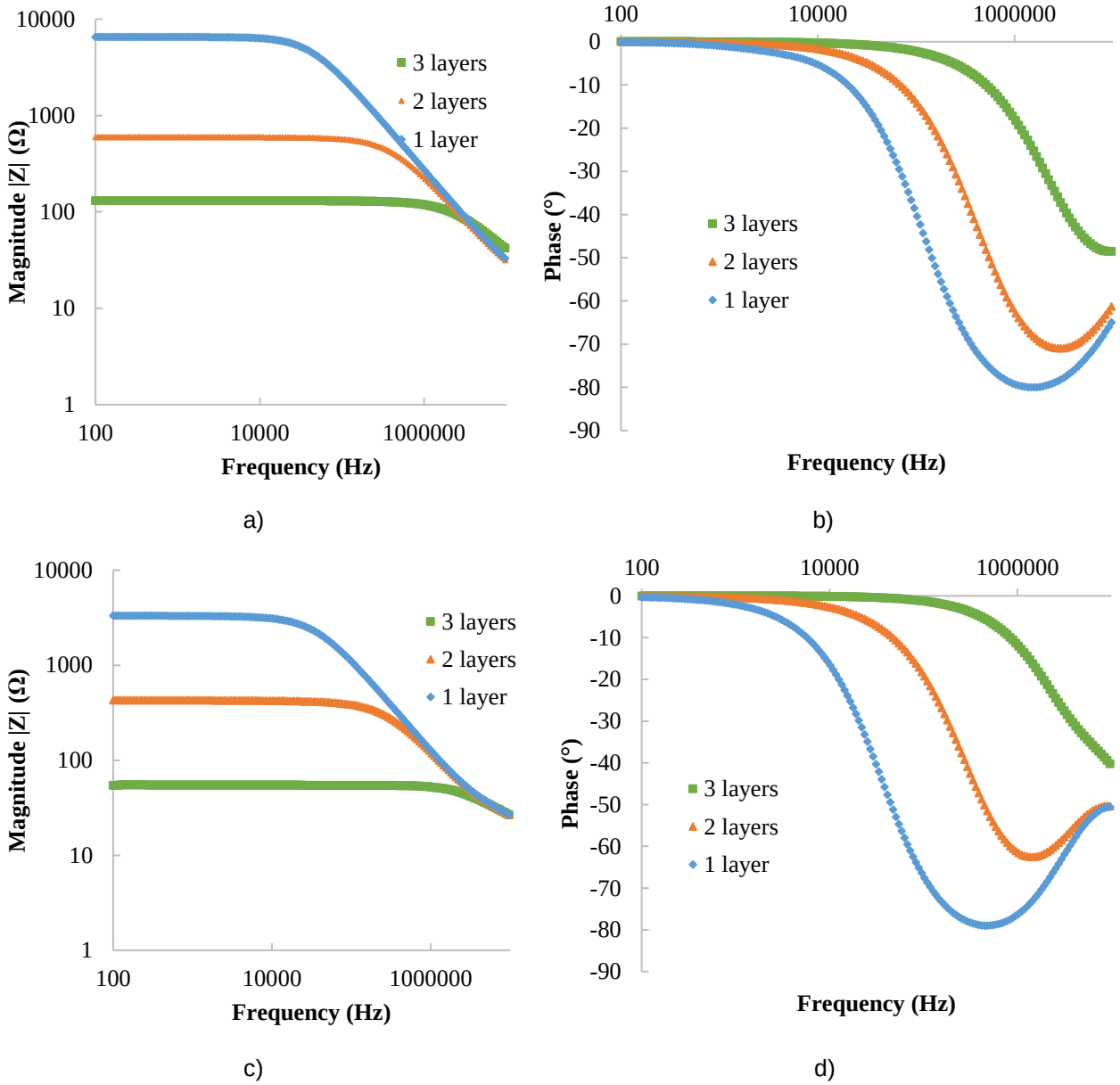

Fig. 1. Magnitude and Phase for different number of layers with CMC as dispersant (a) and (b); with SDS as dispersant (c) and (d). The IDEs spacing is 200µm.

Table I
Cut-Off Frequency and Dc Resistance of the Study Cases

Number of sprayed layers	CNT-type	Cut-off Frequency (kHz)	DC Resistance (Ω)
1	CMC	72.8 ± 0.8	6539 ± 53
2	CMC	653 ± 27	600 ± 43
3	CMC	4430 ± 89	131 ± 20
1	SDS	59.5 ± 1.2	3330 ± 47
2	SDS	461 ± 23	428 ± 42
3	SDS	1230 ± 45	54.2 ± 24

From these results, we deduce as well, how the cut-off frequency moves to higher values as the number of layers increase. **Error! Reference source not found.** introduces our measurements for the six cases under study. On its side, the dc resistance takes higher values for the least number of layers, as there is less material for the current to flow.

Regarding the different dispersants used, the explained trend is not modified. However, there are small differences in the absolute values, due to the differences of the final process when alternative dispersants are used. The choice on which one to employ will be defined by the exact values needed in

each application, as well as by the well-known inherent advantages of each one.

It is important to point out how the impedance phase starts rising again from frequencies above 0.5 MHz. This is due to the metallic contacts used for connecting the CNT network to the experimental setup. From this frequency, the inductance of the cables soldered for realizing the measurements is no longer negligible.

3.2 Spacing

After an analysis of the influence of the electrodes spacing on the impedance, we carried out a similar experiment with the spacing between electrodes, reaching similar results. In particular, as **Error! Reference source not found.** depicts, for the highest separation between the IDE fingers, the impedance magnitude has the highest values at low frequencies; converging again to the same line for high frequencies, with a similar behavior as a capacitor. The results go along with what we expected, since more separation means bigger path for the current to flow through, i.e., greater resistance. Similarly, as with the thickness variation as well, the phase presents more stable values for the narrower structure at low frequencies, although in this case, the lobes also have a bigger slope.

As regards the cut-off frequency, although the figures follow the same fashion as in the previous experiment, in this case we achieve lower values, around a decade below.

Resultantly, the three parameters we considered so far (dispersant, distance and thickness) can be used to vary the resistance and the overall frequency behavior of the RC networks we manufactured. It is then possible to employ them together in any of the possible combinations, fine tuning them for their special application. One possibility, could be to design multiple IDEs capacitors and combine them to be used as load circuit or as filtering network. These degrees of freedom allow to easily find the best trade-off in terms of employable space, processing constraints and cost (amount of material to be used).

3.3 Filters

A second order low pass filter can be easily designed by connecting two structures with different cut-off frequencies. As seen in **Error! Reference source not found.**, the impedance magnitude remains remarkably stable up to the new cut-off frequency, where a steep drop follows, coinciding with the model.

This opens a wide new variety of possibilities related to their use. A filter out of this technology can be completely personalized and fine tuned on each situation, without the necessity of sitting between commercial values of discrete components or integrated filters. Likewise, for applications where the thickness of the whole device matters (e.g., wearables, stickers, etc.), CNT filters stand up, since integrated filters such as multilayer, ceramic monoblocks or even discrete components get substantially bulkier in comparison. In addition to this, the well-known properties of transparency of CNTs might allow for the realization of semi-transparent filters integrated in glass or plastic surfaces.

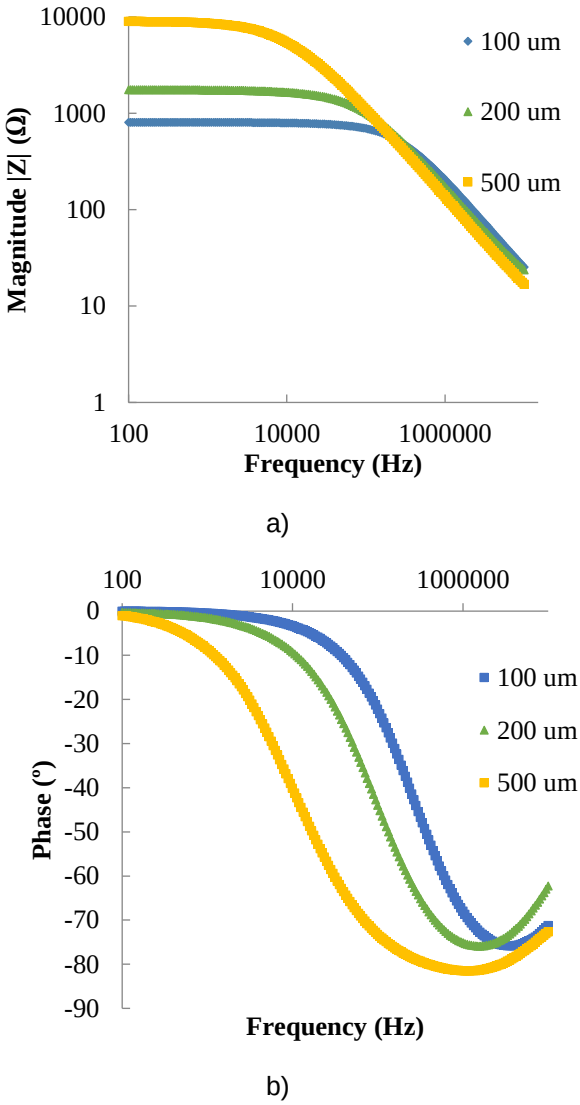

Fig. 2. Impedance magnitude (a) and phase (b) for different IDE finger spacing values with 1 CNT layer with CMC as dispersant.

4. Conclusions

In this letter, we have presented and summarized experimental results on how different parameters affect the impedance of IDEs realized with conducting fingers and mixed CNTs. The parameters we considered were the finger spacing, the CNT thickness and the dispersant employed. Understanding their effects for fine-tuning in cut-off frequency and impedance magnitude paves the way to the creation of customizable, flexible and cost-effective passive

components and filters. Particularly, given the observed behavior, the most immediate application is the development of second order low pass filters with the possibility of

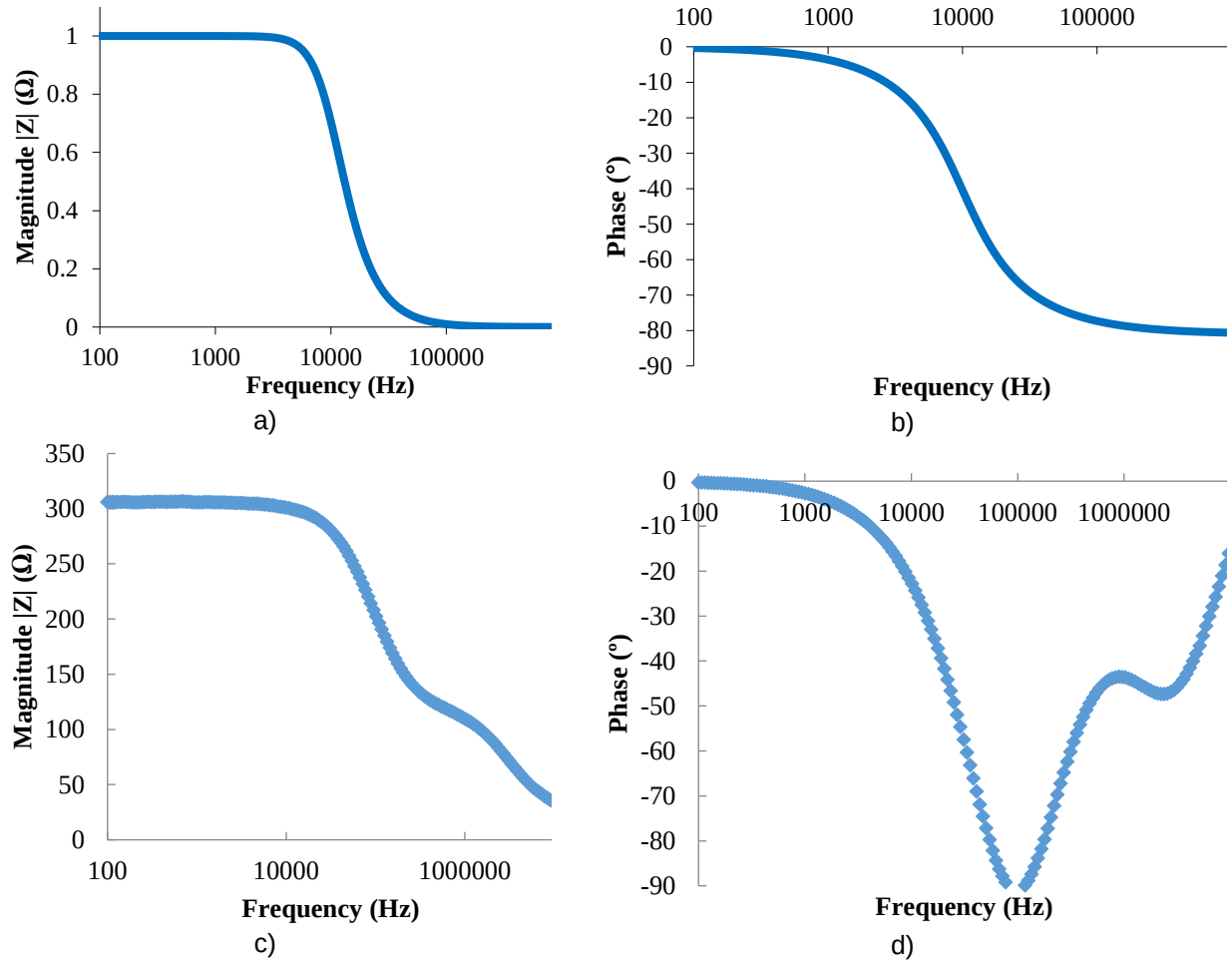

Fig. 3. Model (a) Magnitude and (b) Phase of a second order low pass filter. Magnitude (c) and Phase (d) of a CNT second order filter implemented with one IDE structure with 1 layer and another connected in series with 3 layers (both with CMC as dispersant and spacing of 200 µm).

customization on each application case for exact cut-off frequency. Such filters could be integrated in applications where the thickness is a critical constraint or in the domain of transparent electronics.

Acknowledgements

This work was partially funded by the fellowship H2020-MSCA-IF-2017-794885-SELFSENS and the TUM Graduate School..

References

[1] S. Iijima, "Helical microtubules of graphitic carbon," *nature*, vol. 354, pp. 56-58, 1991.

[2] Y. Wang and J. T. W. Yeow, "A review of carbon nanotubes-based gas sensors," *Journal of sensors*, vol. 2009, 2009.

[3] J. Chaste, A. Eichler, J. Moser, G. Ceballos, R. Rurali and A. Bachtold, "A nanomechanical mass sensor with yoctogram resolution," *Nature nanotechnology*, vol. 7, pp. 301-304, 2012.

[4] B. Arash and Q. Wang, "Detection of gas atoms with carbon nanotubes," *Scientific reports*, vol. 3, pp. 1-6, 2013.

[5] X.-M. Liu, Z. Huang, S. Oh, B. Zhang, P.-C. Ma, M. M. F. Yuen and J.-K. Kim, "Carbon nanotube (CNT)-based composites as electrode material for rechargeable Li-ion batteries: a review," *Composites Science and Technology*, vol. 72, pp. 121-144, 2012.

[6] J. Chen, A. I. Minett, Y. Liu, C. Lynam, P. Sherrell, C. Wang and G. G. Wallace, "Direct growth of flexible carbon nanotube electrodes," *Advanced Materials*, vol. 20, pp. 566-570, 2008.

[7] Q. Wang and B. Arash, "A review on applications of carbon nanotubes and graphenes as nano-resonator sensors," *Computational Materials Science*, vol. 82, pp. 350-360, 2014.

[8] M. Moniruzzaman and K. I. Winey, "Polymer nanocomposites containing carbon nanotubes," *Macromolecules*, vol. 39, pp. 5194-5205, 2006.

[9] D. S. Bethune, R. D. Johnson, J. R. Salem, M. S. De Vries and C. S. Yannoni, "Atoms in carbon cages: the structure and properties of endohedral fullerenes," *Nature*, vol. 366, pp. 123-128, 1993.

[10] M. S. Dresselhaus, G. Dresselhaus, P. C. Eklund and A. M. Rao, "Carbon nanotubes," in *The physics of fullerene-based and fullerene-related materials*, Springer, 2000, pp. 331-379.

[11] D. Qian, Wagner, G. J. W. K. Liu, M.-F. Yu and R. S. Ruoff, "Mechanics of carbon nanotubes," *Appl. Mech. Rev.*, vol. 55, pp. 495-533, 2002.

[12] H. Dai, "Nanotube growth and characterization," in *Carbon Nanotubes*, Springer, 2001, pp. 29-53.

[13] P. Nikolaev, M. J. Bronikowski, R. K. Bradley, F. Rohmund, D. T. Colbert, K. A. Smith and R. E. Smalley, "Gas-phase catalytic growth of single-walled carbon nanotubes from carbon monoxide," *Chemical physics letters*, vol. 313, pp. 91-97, 1999.

[14] E. T. Thostenson, Z. Ren and T.-W. Chou, "Advances in the science and technology of carbon nanotubes and their composites: a review," *Composites science and technology*, vol. 61, pp. 1899-1912, 2001.

[15] F. a. C. S. a. W. A. a. F. A. a. A. A. a. L. P. a. A. A. Loghin, "Scalable spray deposition process for highly uniform and reproducible CNT-TFTs," *Flexible and Printed Electronics*, vol. 1, no. 4, p. 045002, 2016.

[16] A. a. F. B. a. L. P. a. S. G. Abdellah, "Spray deposition of organic semiconducting thin-films: Towards the fabrication of arbitrary shaped organic electronic devices," *Organic Electronics*, vol. 11, no. 6, pp. 1031--1038, 2010.

[17] A. a. L. F. C. a. F. A. Rivadeneyra, "Technological integration in printed electronics," *Flexible Electronics*, 2018.

[18] K. Suganuma, Introduction to Printed Electronics, New York, NY, USA: Springer Science & Business Media, 2014.

[19] A. a. L.-V. J. A. Rivadeneyra, "Recent Advances in Printed Capacitive Sensors," *Micromachines*, vol. 11, no. 4, p. 367, 2020.

[20] A. Falco, A. Rivadeneyra, F. C. Loghin, J. F. Salmeron, P. Lugli and A. Abdelhalim, "Towards low-power electronics: Self-recovering and flexible gas sensors," *Journal of Materials Chemistry A*, vol. 6, pp. 7107-7113, 2018.

Chapter 3

Results

3.1 Methodology

In this section we describe the methodologies carried out in pursuance of the objectives described in Section 1.2.

3.1.1 Study on the Electromagnetic Spectrum

We realized an analysis of the European regulations related to the frequency allocations and associated applications, as well as the maximum permitted emitting power [19]. We measured the electromagnetic spectrum in our dependencies and characterized it, with the time presence of the signals equally important as their strength.

We identified the most profitable frequency bands and modeled the signal (energy) input of the system. We also considered the active emitting option (WET), although it was immediately discarded because of its inefficiency and not environmental-friendliness. Ultimately, we analyzed the solid viability of RFEH.

Results gathered in Moreno-Cruz *et al.* IEEE Internet of Things Journal [13].

3.1.2 Research on Antennas

Our investigations in diverse innovative techniques on the rest of the system stages required antennas beyond the ordinary. Therefore, with a broad examination of the commercial options and state-of-the-art, we analyzed the

convenience of multi-band and ultra-wide band designs, different directivity characteristics, different materials and the simultaneous transfer of information and power. The last, considering within a single antenna both alternatives of transferring in the same and in a different band.

As a result, we developed a custom tri-band microstrip stacked-patch antenna for our frequencies of interest. First, we designed it with the assistance of dedicated software tools such as Keysight Technologies' ADS 2020 software (ADS) [20], where we tested several configurations; and later, we measured it in the laboratory and the anechoic chamber.

Results gathered in Moreno-Cruz *et al.* "Custom Tri-Band Antenna within RF Energy Harvesting" [17].

3.1.3 Study on Rectification and Impedance Matching Stages

We explored the latest state-of-the-art circuits for energy-autonomous and low voltage rectification; as well as diverse technologies for diode topologies, finally focusing on Schottky diodes. We simulated with software tools like ADS and Spice [21] their behavior, for later manufacturing module boards with the ones that gave the best results, together with their matching networks. The last were likewise developed first with ADS based on regular designs.

In the end, we characterized the modules in the laboratory and selected the ones with the highest efficiencies, i. e., the modules with the highest dc voltage outputs in the expected power input range.

Results gathered in Moreno-Cruz *et al.* IEEE Internet of Things Journal [13] and Moreno-Cruz *et al.* "Custom Tri-Band Antenna within RF Energy Harvesting" [17].

3.1.4 Research on Power Management Stage

In order to maximize the energy input to the dc/dc converter and its efficiency, we evaluated diverse innovative ideas on the power management as a previous stage. Adaptions and improvements to the state-of-the-art, together with novel concepts and topologies were simulated and analyzed in Spice. The focus was given to techniques of multi-band dc mixing, isolation of the load with respect to the source, energy accumulation and simplicity, always assuming energy-autonomous circuits.

Lastly, we developed a novel concept (*MSwitch*) and manufactured several versions of it, that were characterized in the laboratory and integrated in a complete IoT node prototype. Other state-of-the-art concepts from the literature were also built, in order to compare them in the same conditions with the proposed ideas.

Results gathered in Moreno-Cruz *et al.* IEEE Internet of Things Journal [13], Moreno-Cruz *et al.* "Custom Tri-Band Antenna within RF Energy Harvesting" [17] and Moreno-Cruz *et al.* ALLSENSORS [16].

3.1.5 Study on Dc/Dc Converter and Energy Storage Stages

We performed a deep scrutiny among all commercially available dc/dc converters to date and filtered the most efficient ones for ultra-low power conditions according to their data-sheets. Next, we simulated their operation with software tools as Spice under the modeled circumstances, for later manufacturing modules of the next filtered batch. Finally, we measured them, taking them often out of the data-sheet characterization, and selected the most efficient ones for the diverse scenarios contemplated of low voltage and energy scarcity.

Regarding the storage, we examined the commercially available elements inside the groups of batteries, capacitors and super-capacitors, seeking for the lowest losses and leakage currents within our application voltage range. We also studied the possibility of the storage at a different voltage level than the application would use, on the lookout for better efficiencies.

Results gathered in Moreno-Cruz *et al.* IEEE Internet of Things Journal [13].

3.1.6 Research on Embedded OSs and WCPs

As important as the efficiency of the harvester module, is the efficient use of the energy in the application. Consequently, we investigated the possible improvements to the processes run in µCs and transceivers, meaning this in embedded devices the OS and WCP. After analyzing the current options in the market and its requirements, we tested several combinations of them. Ultimately, we designed a novel cross-layer WCP, focused on the power consumption of the nodes and tailored to the EH and IoT requirements.

For its characterization, we implemented it in a hardware evaluation board, together with a BLE application for its comparison purposes. The measurements in the laboratory were made for several realistic scenarios.

In addition, other techniques for saving energy were considered, such as the inclusion of extra hardware as a wake-up radio or flooding protocols.

Results gathered in Moreno-Cruz *et al.* MDPI Sensors [14] and Moreno-Cruz *et al.* IEEE CAMAD [8].

3.1.7 Study on Application Components

Given the advances on the semiconductors technologies, the power consumptions of the fundamental elements of the application stage have substantially decreased. Therefore, we analyzed the novel market options for µCs and radio transceivers, along with the sensors ones. The search was aimed to demonstrating purposes and we finally picked a combination of them for setting up an application unit. Its development included also its programming, selecting the best fitting and low power operation modes.

Besides, we examined the advances on flexible printed electronics, that could lead to new use-cases in areas such as wearables, electronic skin (e-skin) or implantable devices.

Results gathered in Moreno-Cruz *et al.* IEEE Internet of Things Journal [13], Moreno-Cruz *et al.* ALLSENSORS [16], Moreno-Cruz *et al.* MDPI Sensors [14] and Loghin *et al.* "Facile Manufacturing of Sub-mm Thick CNT-Based RC Filters" [18].

3.1.8 Research on Security

The inclusion of security levels on IoT applications is directly related to more power consumption, going against the EH usage. Our focus was to explore novel approaches that do not have large impact on the energy utilization but still achieve proper security levels. For that, we analyzed hardware concepts in the RFID area and manufactured a prototype realizing it with printable electronics. Besides, we proposed new schemes in the implementation of security standards, which decrease the overhead of the protocol frame without decreasing the security level.

Results gathered in Rivadeneyra *et al.* IEEE Access [15] and Moreno-Cruz *et al.* MDPI Sensors [14].

3.2 Achievements

Following, we describe the conclusive results accomplished, that served for the publication of the previously appended articles.

3.2.1 Moreno-Cruz *et al.* IEEE Internet of Things Journal, 2020

In this work, we introduced the novel power management stage *MSwitch*, implementing dual-band dc mixing in both of its two final versions, through a genuine procedure based on the store-and-use and switched capacitor principles.

By isolating the load (i. e., the dc/dc converter), managing the scarce energy input and efficiently mixing both dc lines, it achieved a substantial improvement over the single band case. The minimum RF power input decreased by a 34% and 31% for the cold-start and hot operations, respectively; and the efficiency increased by a 9.5% at -15 dBm (value taken as reference). Additionally, *MSwitch Version 2* improved the "in-series design" (the best performing circuit up to the date to the eyes of the authors [22]) by a 21% and 2% in its minimum RF power input for the cold-start and hot operations, respectively, and by a 3.1% in its efficiency.

Taking into account also the common behavior studied of the RF spectrum, where the energy levels might not be stable over time, *MSwitch* performed as well better when the inputs had different power magnitudes, even increasing its efficiency.

Moreover, we presented a valuable analysis of the off-the-shelf dc/dc converters and Schottky diodes and of the state-of-the-art rectifier circuits under ultra-low power and low voltage conditions.

Besides, with the measurements of the electromagnetic spectrum, in addition to selecting the more energetic bands, we concluded that RFEH was a feasible option for harvesting in our dependencies.

3.2.2 Moreno-Cruz *et al.* MDPI Sensors, 2020

In this article, we presented an innovative WCP for embedded systems, intended for the harshest EH environments of IoT. *treNch* operates with a light cross-layer architecture by means of asynchronous transmissions, synchronous (subsequent) and optional receptions, short frame sizes and a

dynamic operation that self-adapts depending on the energy status. This cross-layer principle is manifested in the proposed energy-management algorithm that uses two different operation modes for the sleep phase depending on the power input.

For evaluating our design, we carried out an exhaustive experimental examination of it under several realistic ultra-low power scenarios, comparing the results at the same conditions with different BLE profiles. *treNch* demonstrated better performance in each of them, achieving power consumptions from 1 to 2 orders of magnitude lower than BLE.

We spotlighted the power consumption at the nodes, but the discussion included other features as well, such as, the security, latency or reliability, among others. Regarding the security, we proposed a scheme straightforward to integrate that uses standard and well-established mechanisms. It implements low-overhead secure mechanisms that reduced the packet size without decreasing the security level, such as shorter over-the-air counters.

3.2.3 Rivadeneyra *et al.* IEEE Access, 2020

In this work, we introduced an extra security level for RFID tags operating at the high frequency (HF) band (13.56 MHz), consisting on a printed hardware mechanism that deactivates the system while it is not used. The structure implements a force sensor with a switch between the chip and the antenna, so that the tag is unreadable until it touches the reader with enough pressure normal to its surface.

The imperceptible printed button results in the inhibition of unwanted readings, avoiding undesirable tracking, relay attack or eavesdropping, but without renouncing to the comfort of a wireless tag in uses-cases such as, credit cards or access batches. The fact that it is a low-cost hardware modification (due to the use of printed materials) and that its employment does not require any software adjustment, neither an increase of the power consumption, makes its deployment straightforward.

3.2.4 Moreno-Cruz *et al.* IEEE CAMAD, 2018

In this contribution, we introduced how RFEH can be included in the new paradigm of smart grid, through its utilization in remote nodes, which are part of the monitoring network. We proposed several use-cases where

RFEH has clear advantages over other harvesting technologies and detailed its benefits, that open new application opportunities.

Besides, we outlined a generic hardware architecture for the nodes and a WCP, seeking in both cases for the best adaption to the smart grid scenarios and proposing diverse configuration options for them.

3.2.5 Moreno-Cruz *et al.* ALLSENSORS, 2020

In this paper, we provided the fundamentals for the conjunction use of RFEH with flexible printed sensors, in a search of costs reduction and novel applications and pinpointing the extraordinary properties of printed electronics in sensor employment. In particular, their low power consumption and flexibility that match entirely with the requirements and use-cases associated to RFEH.

For demonstrating our inferences, we proposed a solution scheme for a node, formed by a sprayed humidity sensor based on graphene oxide (GO) and a RFEH block using the store-and-use principle.

3.2.6 Moreno-Cruz *et al.* "Custom Tri-Band Antenna within RF Energy Harvesting", 2020. ***Under Review***

In this work, we presented a novel microstrip asymmetric stacked-patch antenna, customized for our frequency bands of interest (868, 949 and 2159 MHz) and for being used in RFEH devices. In the measurements, the antenna demonstrated efficient resonant and radiating behaviors at the target frequencies, as well as favorable polarization and directivity characteristics.

In addition, we proposed three different concepts for its utilization in RFEH systems, where a dual-band power management stage such as *MSwitch* can operate with a single antenna instead of three, i. e., using two bands for harvesting and a third for communications, or even using the three bands for harvesting, where the last would power the comparator of *MSwitch Version 1*. The third use-case entails a new version for *MSwitch* with three power inputs. These scenarios clearly imply cost and space savings.

3.2.7 Loghin *et al.* "Facile Manufacturing of Sub-mm Thick CNT-Based RC Filters", 2020. *Under Review*

In this letter, we presented the experimental results about an analysis on how different parameters affect the impedance of RC networks based on carbon nanotubes (CNTs). The studied parameters were the interdigitated electrodes (IDEs) spacing, the dispersant compound and the number of CNT deposited layers. Our conclusions led us to propose use-cases for these variables adjustments where the cut-off frequency of second order filters can be easily fine-tuned, having additionally these devices the inherent properties of CNTs and printed electronics.

3.3 Conclusions

As main conclusion of the carried out labor, it has been deduced that the utilization of RFEH in WSNs is at present a feasible alternative for feeding ultra-low power nodes. While it is indeed true that, for a major deployment, the efficiencies of circuits and components still need to be increased in order to reach lower minimum spectral energy densities from where the applications can start their operation; the prospects let us expect its immediate growth within ultra-low power applications.

Along the doctorate duration, we have contributed to the state-of-the-art in a broad ensemble of fields, all relevant to WET and RFEH, achieving remarkable advances to it that allowed us to publish our results in journals of high academic impact (Q1) and conferences of international relevance. In particular, in IEEE Internet of Things Journal, which has an impact factor of 9.936 and ranks of 3/156 in category *Computer Science, Information Systems*, 9/266 in *Engineering, Electrical & Electronic* and 5/90 in *Telecommunications*. MDPI Sensors, with impact factor of 3.275 and ranks of 5/64 in category *Instruments & Instrumentation* and 77/266 in *Engineering, Electrical & Electronic*. IEEE Access, with 3.745 of impact factor and ranks of 35/156 in category *Computer Science, Information Systems* and 61/266 in *Engineering, Electrical & Electronic*. Aside of the publications that are still in review process.

Summarizing, we obtained notable improvements in the efficiency of power management circuits that regulate the energy input previous to a commercial dc/dc converter (objective 2-b). With *MSwitch*, we decreased, with respect to the best options from the literature, the minimum power input per line from where an IoT system can start its operation, as well as its general efficiency in more favorable energy conditions and in more realistic scenarios.

With *treNch*, we diminished up to 2 decades the power consumption needed by a WCP in comparison with several BLE profiles, without losing features or QoS (objective 3-a). Our concepts included the customization of the protocol for EH nodes, but also revolutionary strategies of cross-layer design and for the security (objective 3-c).

We contributed to more secure RFID systems with a hardware design that disables their connectivity by integrating a printed pressure button, preventing undesirable tracking, relay attack or eavesdropping. Again, without incrementing neither its power requirements nor its costs (objective 3-c).

We proposed novel use-cases within RFEH for multi-band antennas that bring more energy into the harvesting systems, in parallel to lower costs and space needs. Moreover, we presented a custom design of a tri-band microstrip asymmetric stacked-patch antenna (objective 1-b).

Besides, we contributed with extensive analyses on the frequency allocations of the electromagnetic spectrum and its applications (objective 1-a); on state-of-the-art circuits and components for autonomous rectification of signals for RFEH (objective 2-a); on commercial dc/dc converters under extremely scarce energy conditions and energy storage options (objective 2-c); and on novel components, materials and fabrication techniques for the application stage (objective 3-b).

To conclude, based on our studies we foresee a clear spreading of RFEH for ultra-low power scenarios in the upcoming years, as a result of the ebullient deployment of the IoT and 5G in our lives, and due to the improvements in its techniques.

Bibliography

[1] P. Kamalinejad, C. Mahapatra, Z. Sheng, S. Mirabbasi, V. C. Leung, and Y. L. Guan, "Wireless energy harvesting for the internet of things", *IEEE Communications Magazine*, vol. 53, no. 6, pp. 102–108, 2015.

[2] G. Zhou, L. Huang, W. Li, and Z. Zhu, "Harvesting ambient environmental energy for wireless sensor networks: a survey", *Journal of Sensors*, vol. 2014, pp. 1–20, 2014.

[3] X. Lu, P. Wang, D. Niyato, D. I. Kim, and Z. Han, "Wireless networks with RF energy harvesting: A contemporary survey", *IEEE Communications Surveys & Tutorials*, vol. 17, no. 2, pp. 757–789, 2015.

[4] M. Russo, P. Šolić, and M. Stella, "Probabilistic modeling of harvested GSM energy and its application in extending UHF RFID tags reading range", *Journal of Electromagnetic Waves and Applications*, vol. 27, no. 4, pp. 473–484, 2013.

[5] A. Palaios, V. Miteva, J. Riihijärvi, and P. Mähönen, "When the whispers become noise: A contemporary look at radio noise levels", in *Wireless Communications and Networking Conference (WCNC), 2016 IEEE*, IEEE, 2016, pp. 1–7.

[6] M. Yılmaz, D. G. Kuntalp, and A. Fidan, "Determination of spectrum utilization profiles for 30 MHz–3 GHz frequency band", in *Communications (COMM), 2016 International Conference on*, IEEE, 2016, pp. 499–502.

[7] H. Yan, J. M. Montero, A. Akhnoukh, L. C. De Vreede, and J. Burghartz, "An integration scheme for RF power harvesting", in *Proc. STW Annual Workshop on Semiconductor Advances for Future Electronics and Sensors*, 2005, pp. 64–66.

[8] F. Moreno-Cruz, A. Escobar-Molero, E. Castillo, M. Becherer, A. Rivadeneyra, and D. P. Morales, "Why Use RF Energy Harvesting in Smart Grids", in *2018 IEEE 23rd International Workshop on Computer Aided Modeling and Design of Communication Links and Networks (CAMAD)*, IEEE, 2018, pp. 1–6. DOI: 10.1109/CAMAD.2018.8514966.

[9] F. Moreno-Cruz, V. Toral López, F. J. Romero, C. Hambeck, D. P. Morales, and A. Rivadeneyra, "Use of Low-Cost Printed Sensors with RF Energy Harvesting for IoT", in *2019 Smart Systems Integration (SSI)*, 2019.

[10] S. S. Chouhan, M. Nurmi, and K. Halonen, "Efficiency enhanced voltage multiplier circuit for RF energy harvesting", *Microelectronics Journal*, vol. 48, pp. 95–102, 2016.

[11] P. Nintanavongsa, "A survey on RF energy harvesting: circuits and protocols", *Energy Procedia*, vol. 56, pp. 414–422, 2014.

[12] J. Park, Y. Kim, Y. J. Yoon, J. So, and J. Shin, "Rectifier design using distributed Greinacher voltage multiplier for high frequency wireless power transmission", *Journal of electromagnetic engineering and science*, vol. 14, no. 1, pp. 25–30, 2014.

[13] F. Moreno-Cruz, V. Toral-López, M. Ramos Cuevas, J. F. Salmerón, A. Rivadeneyra, and D. P. Morales, "Dual-Band Store-and-Use System for RF Energy Harvesting with Off-the-Shelf DC/DC Converters", *IEEE Internet of Things Journal*, pp. 1–1, 2020. DOI: 10.1109/JIOT.2020.3024017.

[14] F. Moreno-Cruz, V. Toral-López, A. Escobar-Molero, V. U. Ruíz, A. Rivadeneyra, and D. P. Morales, "treNch: Ultra-Low Power Wireless Communication Protocol for IoT and Energy Harvesting", *Sensors*, vol. 20, no. 21, p. 6156, 2020, ISSN: 1424-8220. DOI: 10.3390/s20216156. [Online]. Available: http://dx.doi.org/10.3390/s20216156.

[15] A. Rivadeneyra, A. Albrecht, F. Moreno-Cruz, D. P. Morales, M. Becherer, and J. F. Salmerón, "Screen Printed Security-Button for Radio Frequency Identification Tags", *IEEE Access*, vol. 8, pp. 49 224–49 228, 2020. DOI: 10.1109/ACCESS.2020.2979548.

[16] F. Moreno-Cruz, F. J. Romero Maldonado, N. Rodríguez Santiago, D. P. Morales, and A. Rivadeneyra, "Low-cost energy-autonomous sensor nodes through RF energy harvesting and printed technology", in *ALLSENSORS 2020: The Fifth International Conference on Advances in Sensors, Actuators, Metering and Sensing*, ser. 5, ISBN: 978-1-61208-766-5, Jaime Lloret Mauri et al., 2020.

[17] F. Moreno-Cruz, M. Ramos-Cuevas, P. Padilla de la Torre, D. P. Morales, and A. Rivadeneyra, "Custom Tri-Band Antenna within RF Energy Harvesting", *UNDER REVIEW*, 2020.

[18] F. C. Loghin, A. Falco, F. Moreno-Cruz, P. Lugli, D. P. Morales, J. F. Salmerón, and A. Rivadeneyra, "Facile Manufacturing of Sub-mm Thick CNT-Based RC Filters", *UNDER REVIEW*, 2020.

[19] Electronic Communications Committee (ECC) within the European Conference of Postal and T. A. (CEPT), *The European table of frequency allocations and applications in the frequency range 8.3 kHz to 3000 GHz (ECA table)*, 2016.

[20] Keysight Technologies, *Advanced Design System (ADS) 2020*, 2019.

[21] Linear Technologies, *LTspice XVII*, 2020.

[22] M. Piñuela, P. D. Mitcheson, and S. Lucyszyn, "Ambient RF energy harvesting in urban and semi-urban environments", *IEEE Transactions on microwave theory and techniques*, vol. 61, no. 7, pp. 2715–2726, 2013.

[23] X. Liu and E. Sanchez-Sinencio, "20.7 a 0.45-to-3v reconfigurable charge-pump energy harvester with two-dimensional mppt for internet of things", in *Solid-State Circuits Conference-(ISSCC), 2015 IEEE International*, IEEE, 2015, pp. 1–3.

[24] D. Pavone, A. Buonanno, M. D'Urso, and F. Della Corte, "Design considerations for radio frequency energy harvesting devices", *Progress In Electromagnetics Research B*, vol. 45, pp. 19–35, 2012.

[25] X. Liu and E. Sánchez-Sinencio, "A highly efficient ultralow photovoltaic power harvesting system with MPPT for internet of things smart nodes", *IEEE transactions on very large scale integration (vlsi) systems*, vol. 23, no. 12, pp. 3065–3075, 2015.

[26] H. Jayakumar, K. Lee, W. S. Lee, A. Raha, Y. Kim, and V. Raghunathan, "Powering the internet of things", in *Proceedings of the 2014 international symposium on Low power electronics and design*, ACM, 2014, pp. 375–380.

[27] V. C. Gungor, D. Sahin, T. Kocak, S. Ergut, C. Buccella, C. Cecati, and G. P. Hancke, "Smart grid technologies: Communication technologies and standards", *IEEE transactions on Industrial informatics*, vol. 7, no. 4, pp. 529–539, 2011.

[28] V. C. Gungor, B. Lu, and G. P. Hancke, "Opportunities and challenges of wireless sensor networks in smart grid", *IEEE transactions on industrial electronics*, vol. 57, no. 10, pp. 3557–3564, 2010.

[29] V. C. Gungor, D. Sahin, T. Kocak, S. Ergut, C. Buccella, C. Cecati, and G. P. Hancke, "A survey on smart grid potential applications and communication requirements", *IEEE Transactions on industrial informatics*, vol. 9, no. 1, pp. 28–42, 2013.

[30] S. M. Amin and B. F. Wollenberg, "Toward a smart grid: power delivery for the 21st century", *IEEE power and energy magazine*, vol. 3, no. 5, pp. 34–41, 2005.

[31] K. Moslehi and R. Kumar, "A reliability perspective of the smart grid", *IEEE Transactions on Smart Grid*, vol. 1, no. 1, pp. 57–64, 2010.

[32] Y. Yan, Y. Qian, H. Sharif, and D. Tipper, "A survey on smart grid communication infrastructures: Motivations, requirements and challenges", *IEEE communications surveys & tutorials*, vol. 15, no. 1, pp. 5–20, 2013.

[33] J. Lippelt and M. Sindram, *Global energy consumption*, 1. Spring, 2011, vol. 12.

[34] K. Rennings, B. Brohmann, J. Nentwich, J. Schleich, T. Traber, and R. Wüstenhagen, *Sustainable energy consumption in residential buildings*. Springer Science & Business Media, 2012, vol. 44.

[35] G. C. Wilshuse and D. C. Trimble, "CYBERSECURITY Challenges in Securing the Modernized Electricity Grid", United States Government Accountability Office, Tech. Rep., 2012.

[36] W. Lutz, W. P. Butz, and K. e. Samir, *World Population & Human Capital in the Twenty-First Century: An Overview*. Oxford University Press, 2017.

[37] X. Fang, S. Misra, G. Xue, and D. Yang, "Smart grid—The new and improved power grid: A survey", *IEEE communications surveys & tutorials*, vol. 14, no. 4, pp. 944–980, 2012.

[38] T. Tsoutsos, N. Frantzeskaki, and V. Gekas, "Environmental impacts from the solar energy technologies", *Energy Policy*, vol. 33, no. 3, pp. 289–296, 2005.

[39] A. Palaios, J. Riihijarvi, and P. Mahonen, "From Paris to London: Comparative analysis of licensed spectrum use in two European metropolises", in *Dynamic Spectrum Access Networks (DYSPAN), 2014 IEEE International Symposium on*, IEEE, 2014, pp. 48–59.

[40] A. Escobar, J. Garcia-Jimenez, F. J. Cruz, J. Klaue, A. Corona, and D. Tati, "Competition: Redfixhop with channel hopping", in *Proceedings of the 2017 International Conference on Embedded Wireless Systems and Networks*, Junction Publishing, 2017, pp. 264–265.

[41] S. Kim, R. Vyas, J. Bito, K. Niotaki, A. Collado, A. Georgiadis, and M. M. Tentzeris, "Ambient RF energy-harvesting technologies for self-sustainable standalone wireless sensor platforms", *Proceedings of the IEEE*, vol. 102, no. 11, pp. 1649–1666, 2014.

[42] A. Nathan, A. Ahnood, M. T. Cole, S. Lee, Y. Suzuki, P. Hiralal, F. Bonaccorso, T. Hasan, L. Garcia-Gancedo, A. Dyadyusha, *et al.*, "Flexible electronics: the next ubiquitous platform", *Proceedings of the IEEE*, vol. 100, no. Special Centennial Issue, pp. 1486–1517, 2012.

[43] S. Khan, L. Lorenzelli, and R. S. Dahiya, "Technologies for printing sensors and electronics over large flexible substrates: a review", *IEEE Sensors Journal*, vol. 15, no. 6, pp. 3164–3185, 2015.

[44] U. Muncuk, K. Alemdar, J. D. Sarode, and K. R. Chowdhury, "Multi-band ambient RF energy harvesting circuit design for enabling batteryless sensors and IoT", *IEEE Internet of Things Journal*, vol. 5, no. 4, pp. 2700–2714, 2018.

[45] G. Singh, R. Ponnaganti, T. Prabhakar, and K. Vinoy, "A tuned rectifier for RF energy harvesting from ambient radiations", *AEU-International Journal of Electronics and Communications*, vol. 67, no. 7, pp. 564–569, 2013.

[46] E. Khansalee, K. Nuanyai, and Y. Zhao, "A Dual-Band Rectifier for RF Energy Harvesting", *Engineering Journal*, vol. 19, no. 5, pp. 189–197, 2015. DOI: 10.4186/ej.2015.19.5.189.

[47] D. D. Donno, L. Catarinucci, and L. Tarricone, "An UHF RFID Energy-Harvesting System Enhanced by a DC-DC Charge Pump in Silicon-on-Insulator Technology", *IEEE Microwave and Wireless Components Letters*, vol. 23, no. 6, pp. 315–317, 2013. DOI: 10.1109/lmwc.2013.2258002.

[48] M. B. Asl and M. H. Zarifi, "RF to DC micro-converter in standard CMOS process for on-chip power harvesting applications", *AEU - International Journal of Electronics and Communications*, vol. 68, no. 12, pp. 1180–1184, 2014. DOI: 10.1016/j.aeue.2014.06.008.

[49] J. O. McSpadden, L. Fan, and K. Chang, "Design and experiments of a high-conversion-efficiency 5.8-GHz rectenna", *IEEE Transactions on Microwave Theory and Techniques*, vol. 46, no. 12, pp. 2053–2060, 1998.

[50] J.-Y. Park, S.-M. Han, *et al.*, "A rectenna design with harmonic-rejecting circular-sector antenna", *IEEE Antennas and Wireless Propagation Letters*, vol. 3, pp. 52–54, 2004.

[51] Powercast Co., *Power harvester development kit*, Accessed: 26-04-2019. [Online]. Available: http://www.powercastco.com/products/development-kits/#P2110-EVB.

[52] T. Le, K. Mayaram, and T. Fiez, "Efficient far-field radio frequency energy harvesting for passively powered sensor networks", *IEEE Journal of solid-state circuits*, vol. 43, no. 5, pp. 1287–1302, 2008.

[53] S. Agrawal, S. K. Pandey, J. Singh, and M. S. Parihar, "Realization of efficient RF energy harvesting circuits employing different matching technique", in *Fifteenth International Symposium on Quality Electronic Design*, IEEE, 2014, pp. 754–761.

[54] M. Stoopman, S. Keyrouz, H. J. Visser, K. Philips, and W. A. Serdijn, "Co-design of a CMOS rectifier and small loop antenna for highly sensitive RF energy harvesters", *IEEE Journal of Solid-State Circuits*, vol. 49, no. 3, pp. 622–634, 2014.

[55] S. Oh and D. D. Wentzloff, "A- 32dBm sensitivity RF power harvester in 130nm CMOS", in *2012 IEEE radio frequency integrated circuits symposium*, IEEE, 2012, pp. 483–486.

[56] H. Sun, Y.-x. Guo, M. He, and Z. Zhong, "Design of a high-efficiency 2.45-GHz rectenna for low-input-power energy harvesting", *IEEE Antennas and Wireless Propagation Letters*, vol. 11, pp. 929–932, 2012.

[57] B. R. Franciscatto, V. Freitas, J.-M. Duchamp, C. Defay, and T. P. Vuong, "High-efficiency rectifier circuit at 2.45 GHz for low-input-power RF energy harvesting", in *2013 European Microwave Conference*, IEEE, 2013, pp. 507–510.

[58] C. Pang, C. Lee, and K.-Y. Suh, "Recent advances in flexible sensors for wearable and implantable devices", *Journal of Applied Polymer Science*, vol. 130, no. 3, pp. 1429–1441, 2013.

[59] A. Nag, S. C. Mukhopadhyay, and J. Kosel, "Wearable flexible sensors: A review", *IEEE Sensors Journal*, vol. 17, no. 13, pp. 3949–3960, 2017.

[60] I.-C. Cheng and S. Wagner, "Overview of flexible electronics technology", in *Flexible Electronics*, Springer, 2009, pp. 1–28.

[61] V. Scardaci, R. Coull, P. E. Lyons, D. Rickard, and J. N. Coleman, "Spray deposition of highly transparent, low-resistance networks of silver nanowires over large areas", *Small*, vol. 7, no. 18, pp. 2621–2628, 2011.

[62] F. Wang, K. Wang, B. Zheng, X. Dong, X. Mei, J. Lv, W. Duan, and W. Wang, "Laser-induced graphene: preparation, functionalization and applications", *Materials technology*, vol. 33, no. 5, pp. 340–356, 2018.

[63] J. Bito, J. G. Hester, and M. M. Tentzeris, "Ambient RF energy harvesting from a two-way talk radio for flexible wearable wireless sensor devices utilizing inkjet printing technologies", *IEEE Transactions on Microwave Theory and Techniques*, vol. 63, no. 12, pp. 4533–4543, 2015.

[64] S.-E. Adami, P. Proynov, G. S. Hilton, G. Yang, C. Zhang, D. Zhu, Y. Li, S. P. Beeby, I. J. Craddock, and B. H. Stark, "A flexible 2.45-GHz power harvesting wristband with net system output from- 24.3 dBm of RF power", *IEEE Transactions on Microwave Theory and Techniques*, vol. 66, no. 1, pp. 380–395, 2017.

[65] J. Fernández-Salmerón, A. Rivadeneyra, F. Martínez-Martí, L. Capitán-Vallvey, A. Palma, and M. Carvajal, "Passive UHF RFID tag with multiple sensing capabilities", *Sensors*, vol. 15, no. 10, pp. 26 769–26 782, 2015.

[66] S. Lehtimaki, M. Li, J. Salomaa, J. Porhonen, A. Kalanti, S. Tuukkanen, P. Heljo, K. Halonen, and D. Lupo, "Performance of printable supercapacitors in an RF energy harvesting circuit", *International Journal of Electrical Power & Energy Systems*, vol. 58, pp. 42–46, 2014.

[67] J. Maeng, C. Meng, and P. P. Irazoqui, "Wafer-scale integrated micro-supercapacitors on an ultrathin and highly flexible biomedical platform", *Biomedical microdevices*, vol. 17, no. 1, p. 7, 2015.

[68] S. Borini, R. White, D. Wei, M. Astley, S. Haque, E. Spigone, N. Harris, J. Kivioja, and T. Ryhanen, "Ultrafast graphene oxide humidity sensors", *ACS nano*, vol. 7, no. 12, pp. 11 166–11 173, 2013.

[69] F. J. Romero, A. Rivadeneyra, A. Salinas-Castillo, A. Ohata, D. P. Morales, M. Becherer, and N. Rodriguez, "Design, fabrication and characterization of capacitive humidity sensors based on emerging flexible technologies", *Sensors and Actuators B: Chemical*, vol. 287, pp. 459–467, 2019.

[70] F. J. Romero, A. Rivadeneyra, V. Toral, E. Castillo, F. García-Ruiz, D. P. Morales, and N. Rodriguez, "Design guidelines of laser reduced graphene oxide conformal thermistor for IoT applications", *Sensors and Actuators A: Physical*, vol. 274, pp. 148–154, 2018.

[71] Y. Zheng, R. Wu, W. Shi, Z. Guan, and J. Yu, "Effect of in situ annealing on the performance of spray coated polymer solar cells", *Solar energy materials and solar cells*, vol. 111, pp. 200–205, 2013.

[72] H.-W. Hsu and C.-L. Liu, "Spray-coating semiconducting conjugated polymers for organic thin film transistor applications", *RSC advances*, vol. 4, no. 57, pp. 30 145–30 149, 2014.

[73] Texas Instruments, *Ultra Low-Power Boost Converter With Battery Management For Energy Harvester Applications. BQ25504 datasheet*, Revised Nov. 2019, Oct. 2011.

[74] Nordic Semiconductor, *nRF52 DK for Bluetooth LE, Bluetooth mesh, ANT and 2.4 GHz applications. nRF52 product brief*, 2019.

[75] Infineon Technologies, *Series silicon RF Schottky diode pair. BAT15-04W datasheet*, 2018.

[76] S. Iijima, "Helical microtubules of graphitic carbon", *nature*, vol. 354, no. 6348, pp. 56–58, 1991.

[77] M. S. Dresselhaus and P. Avouris, "Introduction to carbon materials research", in *Carbon nanotubes*, Springer, 2001, pp. 1–9.

[78] H. Dai, "Nanotube growth and characterization", in *Carbon Nanotubes*, Springer, 2001, pp. 29–53.

[79] M. S. Whittingham, "Lithium batteries and cathode materials", *Chemical reviews*, vol. 104, no. 10, pp. 4271–4302, 2004.

[80] C. Jiang, E. Hosono, and H. Zhou, "Nanomaterials for lithium ion batteries", *Nano today*, vol. 1, no. 4, pp. 28–33, 2006.

[81] M. S. Whittingham, "Materials challenges facing electrical energy storage", *Mrs Bulletin*, vol. 33, no. 4, pp. 411–419, 2008.

[82] E Frackowiak, S Gautier, H Gaucher, S Bonnamy, and F Beguin, "Electrochemical storage of lithium in multiwalled carbon nanotubes", *Carbon*, vol. 37, no. 1, pp. 61–69, 1999.

[83] J. Chen, A. I. Minett, Y. Liu, C. Lynam, P. Sherrell, C. Wang, and G. G. Wallace, "Direct growth of flexible carbon nanotube electrodes", *Advanced Materials*, vol. 20, no. 3, pp. 566–570, 2008.

[84] A. S. Claye, J. E. Fischer, C. B. Huffman, A. G. Rinzler, and R. E. Smalley, "Solid-state electrochemistry of the Li single wall carbon nanotube system", *Journal of the Electrochemical Society*, vol. 147, no. 8, p. 2845, 2000.

[85] H. Hsoeh, N. Tai, C. Lee, J. Chen, and F. Wang, "Electrochemical properties of the multi-walled carbon nanotube electrode for secondary lithium-ion battery", *Rev. Adv. Mater. Sci*, vol. 5, pp. 67–71, 2003.

[86] S. Iijima, "Helical microtubules of graphitic carbon", *Nature*, vol. 354, pp. 56–58, Nov. 1991. DOI: 10.1038/354056a0.

[87] M. Moniruzzaman and K. I. Winey, "Polymer nanocomposites containing carbon nanotubes", *Macromolecules*, vol. 39, no. 16, pp. 5194–5205, 2006.

[88] D. Bethune, R. Johnson, J. Salem, M. De Vries, and C. Yannoni, "Atoms in carbon cages: the structure and properties of endohedral fullerenes", *Nature*, vol. 366, no. 6451, pp. 123–128, 1993.

[89] A. Rinzler, J. Liu, H Dai, P Nikolaev, C. Huffman, F. Rodriguez-Macias, P. Boul, A. H. Lu, D. Heymann, D. Colbert, *et al.*, "Large-scale purification of single-wall carbon nanotubes: process, product, and characterization.", *Applied Physics A: Materials Science & Processing*, vol. 67, no. 1, 1998.

[90] P. Nikolaev, M. J. Bronikowski, R. K. Bradley, F. Rohmund, D. T. Colbert, K. Smith, and R. E. Smalley, "Gas-phase catalytic growth of single-walled carbon nanotubes from carbon monoxide", *Chemical physics letters*, vol. 313, no. 1-2, pp. 91–97, 1999.

[91] Z. Ren, Z. Huang, J. Xu, J. Wang, P Bush, M. Siegal, and P. Provencio, "Synthesis of large arrays of well-aligned carbon nanotubes on glass", *Science*, vol. 282, no. 5391, pp. 1105–1107, 1998.

[92] E. T. Thostenson, Z. Ren, and T.-W. Chou, "Advances in the science and technology of carbon nanotubes and their composites: a review", *Composites science and technology*, vol. 61, no. 13, pp. 1899–1912, 2001.

[93] D. Qian, G. J. Wagner and, W. K. Liu, M.-F. Yu, and R. S. Ruoff, "Mechanics of carbon nanotubes", *Appl. Mech. Rev.*, vol. 55, no. 6, pp. 495–533, 2002.

[94] R. Mateiu, A. Kühle, R. Marie, and A. Boisen, "Building a multi-walled carbon nanotube-based mass sensor with the atomic force microscope", *Ultramicroscopy*, vol. 105, no. 1-4, pp. 233–237, 2005.

[95] B Lassagne, D Garcia-Sanchez, A Aguasca, and A Bachtold, "Ultrasensitive mass sensing with a nanotube electromechanical resonator", *Nano letters*, vol. 8, no. 11, pp. 3735–3738, 2008.

[96] J. Chaste, A Eichler, J Moser, G Ceballos, R Rurali, and A Bachtold, "A nanomechanical mass sensor with yoctogram resolution", *Nature nanotechnology*, vol. 7, no. 5, pp. 301–304, 2012.

[97] H.-Y. Chiu, P. Hung, H. W. C. Postma, and M. Bockrath, "Atomic-scale mass sensing using carbon nanotube resonators", *Nano letters*, vol. 8, no. 12, pp. 4342–4346, 2008.

[98] Q. Wang and B. Arash, "A review on applications of carbon nanotubes and graphenes as nano-resonator sensors", *Computational Materials Science*, vol. 82, pp. 350–360, 2014.

[99] B Arash and Q Wang, "Detection of gas atoms with carbon nanotubes", *Scientific reports*, vol. 3, no. 1, pp. 1–6, 2013.

[100] S. J. Tans, A. R. Verschueren, and C. Dekker, "Room-temperature transistor based on a single carbon nanotube", *Nature*, vol. 393, no. 6680, pp. 49–52, 1998.

[101] R. Martel, T Schmidt, H. Shea, T Hertel, and P. Avouris, "Single-and multi-wall carbon nanotube field-effect transistors", *Applied physics letters*, vol. 73, no. 17, pp. 2447–2449, 1998.

[102] A Falco, A Rivadeneyra, F. Loghin, J. Salmeron, P Lugli, and A Abdelhalim, "Towards low-power electronics: Self-recovering and flexible gas sensors", *Journal of Materials Chemistry A*, vol. 6, no. 16, pp. 7107–7113, 2018.

[103] X.-M. Liu, Z. dong Huang, S. woon Oh, B. Zhang, P.-C. Ma, M. M. Yuen, and J.-K. Kim, "Carbon nanotube (CNT)-based composites as electrode material for rechargeable Li-ion batteries: a review", *Composites Science and Technology*, vol. 72, no. 2, pp. 121–144, 2012.

[104] Q. Wang and B. Arash, "A review on applications of carbon nanotubes and graphenes as nano-resonator sensors", *Computational Materials Science*, vol. 82, pp. 350–360, 2014.

[105] Y. Wang and J. T. Yeow, "A review of carbon nanotubes-based gas sensors", *Journal of sensors*, vol. 2009, 2009.

[106] M. S. Dresselhaus, G. Dresselhaus, P. Eklund, and A. Rao, "Carbon nanotubes", in *The physics of fullerene-based and fullerene-related materials*, Springer, 2000, pp. 331–379.

[107] T.-L. Nguyen, Y. Sato, and K. Ishibashi, "A 2.77 μW Ambient RF Energy Harvesting Using DTMOS Cross-Coupled Rectifier on 65 nm SOTB and Wide Bandwidth System Design", *Electronics*, vol. 8, no. 10, p. 1173, 2019.

[108] P. Xu, D. Flandre, and D. Bol, "Analysis, Modeling, and Design of a 2.45-GHz RF Energy Harvester for SWIPT IoT Smart Sensors", *IEEE Journal of Solid-State Circuits*, vol. 54, no. 10, pp. 2717–2729, 2019.

[109] S. Al-Sarawi, M. Anbar, K. Alieyan, and M. Alzubaidi, "Internet of Things (IoT) communication protocols", in *2017 8th International conference on information technology (ICIT)*, IEEE, 2017, pp. 685–690.

[110] F. Al-Turjman and M. Abujubbeh, "IoT-enabled smart grid via SM: An overview", *Future Generation Computer Systems*, vol. 96, pp. 579–590, 2019.

[111] X. Feng, F. Yan, and X. Liu, "Study of wireless communication technologies on Internet of Things for precision agriculture", *Wireless Personal Communications*, vol. 108, no. 3, pp. 1785–1802, 2019.

[112] I. Unwala and J. Lu, "IoT protocols: Z-Wave and Thread", in *International Journal on Future Revolution in Computer Science & Communication Engineering (IJFRSCE)*, 11, vol. 3, ijfrcsce.org, 2017, pp. 355–359.

[113] S. M. Mahmoud and A. A. H. Mohamad, "A study of efficient power consumption wireless communication techniques/modules for internet of things (IoT) applications", *Advances in Internet of Things*, 2016.

[114] A. Dementyev, S. Hodges, S. Taylor, and J. Smith, "Power consumption analysis of Bluetooth Low Energy, ZigBee and ANT sensor nodes in a cyclic sleep scenario", in *2013 IEEE International Wireless Symposium (IWS)*, IEEE, 2013, pp. 1–4.

[115] H. Sharma and S. Sharma, "A review of sensor networks: Technologies and applications", in *2014 Recent Advances in Engineering and Computational Sciences (RAECS)*, IEEE, 2014, pp. 1–4.

[116] C. Withanage, R. Ashok, C. Yuen, and K. Otto, "A comparison of the popular home automation technologies", in *2014 IEEE Innovative Smart Grid Technologies-Asia (ISGT ASIA)*, IEEE, 2014, pp. 600–605.

[117] *enOcean alliance web site*, 2020. [Online]. Available: `https://www.enocean-alliance.org`.

[118] *thread group web site*, 2020. [Online]. Available: `https://www.threadgroup.org`.

[119] *ANT web site*, 2020. [Online]. Available: `https://www.thisisant.com`.

[120] F. Deng, X. Yue, X. Fan, S. Guan, Y. Xu, and J. Chen, "Multisource energy harvesting system for a wireless sensor network node in the field environment", *IEEE Internet of Things Journal*, vol. 6, no. 1, pp. 918–927, 2018.

[121] M. M. Sandhu, K. Geissdoerfer, S. Khalifa, R. Jurdak, M. Portmann, and B. Kusy, "Towards Optimal Kinetic Energy Harvesting for the Batteryless IoT", *arXiv preprint arXiv:2002.08887*, 2020.

[122] S. Figueroa Lorenzo, J. Añorga Benito, P. García Cardarelli, J. Alberdi Garaia, and S. Arrizabalaga Juaristi, "A comprehensive review of RFID and bluetooth security: Practical analysis", *Technologies*, vol. 7, no. 1, p. 15, 2019.

[123] M. R. Ghori, T.-C. Wan, M. Anbar, G. C. Sodhy, and A. Rizwan, "Review on Security in Bluetooth Low Energy Mesh Network in Correlation with Wireless Mesh Network Security", in *2019 IEEE Student Conference on Research and Development (SCOReD)*, IEEE, 2019, pp. 219–224.

[124] F. Álvarez, L. Almon, A.-S. Hahn, and M. Hollick, "Toxic Friends in Your Network: Breaking the Bluetooth Mesh Friendship Concept", in *Proceedings of the 5th ACM Workshop on Security Standardisation Research Workshop*, 2019, pp. 1–12.

[125] J. Tosi, F. Taffoni, M. Santacatterina, R. Sannino, and D. Formica, "Performance evaluation of bluetooth low energy: A systematic review", *Sensors*, vol. 17, no. 12, p. 2898, 2017.

[126] X. Liu and A. Goldsmith, "Wireless medium access control in networked control systems", in *Proceedings of the 2004 American Control Conference*, IEEE, vol. 4, 2004, pp. 3605–3610.

[127] D. Whiting, R. Housley, and N. Ferguson, "Counter with cbc-mac (ccm)", *Internet Engineering Task Force Report*, 2003.

[128] P. FIPS, "113 Computer Data Authentication", *National Institute of Standards and Technology, Federal Information Processing Standards*, p. 29, 1985.

[129] A. Nikoukar, S. Raza, A. Poole, M. Güneş, and B. Dezfouli, "Low-power wireless for the Internet of Things: Standards and applications", *IEEE Access*, vol. 6, pp. 67 893–67 926, 2018.

[130] Y. B. Zikria, S. W. Kim, O. Hahm, M. K. Afzal, and M. Y. Aalsalem, "Internet of Things (IoT) operating systems management: opportunities, challenges, and solution", *Sensors*, vol. 19, no. 8, 2019.

[131] Y. B. Zikria, H. Yu, M. K. Afzal, M. H. Rehmani, and O. Hahm, "Internet of things (iot): Operating system, applications and protocols design, and validation techniques", *Future Generation Computer Systems*, vol. 88, pp. 699–706, 2018.

[132] M. Amirinasab, S. Shamshirband, A. T. Chronopoulos, A. Mosavi, and N. Nabipour, "Energy-efficient method for wireless sensor networks low-power radio operation in internet of things", *Electronics*, vol. 9, no. 2, p. 320, 2020.

[133] N. Sornin, M. Luis, T. Eirich, T. Kramp, and O. Hersent, "Lorawan specification", *LoRa alliance*, 2015.

[134] P. San Cheong, J. Bergs, C. Hawinkel, and J. Famaey, "Comparison of LoRaWAN classes and their power consumption", in *2017 IEEE symposium on communications and vehicular technology (SCVT)*, IEEE, 2017, pp. 1–6.

[135] E Bäumker, A. M. Garcia, and P Woias, "Minimizing power consumption of LoRa® and LoRaWAN for low-power wireless sensor nodes", in *Journal of Physics: Conference Series*, IOP Publishing, vol. 1407, 2019, p. 012 092.

[136] V. Freschi and E. Lattanzi, "A Study on the Impact of Packet Length on Communication in Low Power Wireless Sensor Networks Under Interference", *IEEE Internet of Things Journal*, vol. 6, no. 2, pp. 3820–3830, 2019.

[137] A Aripriharta, A Firmansah, M Yazid, I. Wahyono, G. Horng, *et al.*, "Modelling of adaptive power management circuit with feedback for self-powered IoT", in *Journal of Physics: Conference Series*, IOP Publishing, vol. 1595, 2020, p. 012 023.

[138] M. Collotta, R. Ferrero, and M. Rebaudengo, "A Fuzzy Approach for Reducing Power Consumption in Wireless Sensor Networks: A Testbed with IEEE 802.15. 4 and WirelessHART", *IEEE Access*, vol. 7, pp. 64 866–64 877, 2019.

[139] P. Detterer, C. Erdin, J. Huisken, H. Jiao, M. Nabi, T. Basten, and J. P. De Gyvez, "Trading sensitivity for power in an IEEE 802.15. 4 conformant adequate demodulator", in *2020 Design, Automation & Test in Europe Conference & Exhibition (DATE)*, IEEE, 2020, pp. 1674–1679.

[140] Y. Zhang, J. Weng, R. Dey, Y. Jin, Z. Lin, and X. Fu, "On the (In) security of Bluetooth Low Energy One-Way Secure Connections Only Mode", *arXiv preprint arXiv:1908.10497*, 2019.

[141] B. Mao, Y. Kawamoto, J. Liu, and N. Kato, "Harvesting and threat aware security configuration strategy for IEEE 802.15. 4 based IoT networks", *IEEE Communications Letters*, vol. 23, no. 11, pp. 2130–2134, 2019.

[142] S. Meka and B. Fonseca, "Improving route selections in ZigBee wireless sensor networks", *Sensors*, vol. 20, no. 1, p. 164, 2020.

[143] F. L. Coman, K. M. Malarski, M. N. Petersen, and S. Ruepp, "Security issues in internet of things: Vulnerability analysis of LoRaWAN, sigfox and NB-IoT", in *2019 Global IoT Summit (GIoTS)*, IEEE, 2019, pp. 1–6.

[144] R. Bomfin, M. Chafii, and G. Fettweis, "A Novel Modulation for IoT: PSK-LoRa", in *2019 IEEE 89th Vehicular Technology Conference (VTC2019-Spring)*, 2019, pp. 1–5.

[145] V. Palazzi, J. Hester, J. Bito, F. Alimenti, C. Kalialakis, A. Collado, P. Mezzanotte, A. Georgiadis, L. Roselli, and M. M. Tentzeris, "A novel ultra-lightweight multiband rectenna on paper for RF energy harvesting in the next generation LTE bands", *IEEE Transactions on Microwave Theory and Techniques*, vol. 66, no. 1, pp. 366–379, 2017.

[146] X. Li, L. Yang, and L. Huang, "Novel design of 2.45-GHz rectenna element and array for wireless power transmission", *IEEE Access*, vol. 7, pp. 28 356–28 362, 2019.

[147] A. M. Jie, M. F. Karim, K. T. Chandrasekaran, *et al.*, "A wide-angle circularly polarized tapered-slit-patch antenna with a compact rectifier for energy-harvesting systems [Antenna Applications Corner]", *IEEE Antennas and Propagation Magazine*, vol. 61, no. 2, pp. 94–111, 2019.

[148] S. Shen, Y. Zhang, C.-Y. Chiu, and R. Murch, "An ambient RF energy harvesting system where the number of antenna ports is dependent on frequency", *IEEE Transactions on Microwave Theory and Techniques*, vol. 67, no. 9, pp. 3821–3832, 2019.

[149] Y. Tawk, J. Costantine, F. Ayoub, and C. G. Christodoulou, "A communicating antenna array with a dual-energy harvesting functionality [wireless corner]", *IEEE Antennas and Propagation Magazine*, vol. 60, no. 2, pp. 132–144, 2018.

[150] J.-w. Zhang, X. Bai, W.-y. Han, B.-h. Zhao, L.-j. Xu, and J.-j. Wei, "The design of radio frequency energy harvesting and radio frequency-based wireless power transfer system for battery-less self-sustaining applications", *International Journal of RF and Microwave Computer-Aided Engineering*, vol. 29, no. 1, e21658, 2019.

[151] Y. Shi, Y. Fan, Y. Li, L. Yang, and M. Wang, "An efficient broadband slotted rectenna for wireless power transfer at LTE band", *IEEE transactions on Antennas and Propagation*, vol. 67, no. 2, pp. 814–822, 2018.

[152] V. Palazzi, M. Del Prete, and M. Fantuzzi, "Scavenging for energy: A rectenna design for wireless energy harvesting in UHF mobile telephony bands", *IEEE Microwave Magazine*, vol. 18, no. 1, pp. 91–99, 2016.

[153] M. Mattsson, C. I. Kolitsidas, and B. L. G. Jonsson, "Dual-band dual-polarized full-wave rectenna based on differential field sampling", *IEEE Antennas and Wireless Propagation Letters*, vol. 17, no. 6, pp. 956–959, 2018.

[154] A. Alex-Amor, Á. Palomares-Caballero, J. M. Fernández-González, P. Padilla, D. Marcos, M. Sierra-Castañer, and J. Esteban, "RF Energy Harvesting System Based on an Archimedean Spiral Antenna for Low-Power Sensor Applications", *Sensors*, vol. 19, no. 6, p. 1318, 2019.

[155] A Eid, J Costantine, Y Tawk, A. Ramadan, M Abdallah, R ElHajj, R Awad, and I. Kasbah, "An efficient RF energy harvesting system", in *2017 11th European Conference on Antennas and Propagation (EUCAP)*, IEEE, 2017, pp. 896–899.

[156] G. A. Vera, A. Georgiadis, A. Collado, and S. Via, "Design of a 2.45 GHz rectenna for electromagnetic (EM) energy scavenging", in *2010 IEEE Radio and Wireless Symposium (RWS)*, IEEE, 2010, pp. 61–64.

[157] B. L. Pham and A.-V. Pham, "Triple bands antenna and high efficiency rectifier design for RF energy harvesting at 900, 1900 and 2400 MHz", in *2013 IEEE MTT-S International Microwave Symposium Digest (MTT)*, IEEE, 2013, pp. 1–3.

[158] A. Georgiadis, G. V. Andia, and A. Collado, "Rectenna design and optimization using reciprocity theory and harmonic balance analysis for electromagnetic (EM) energy harvesting", *IEEE Antennas and Wireless Propagation Letters*, vol. 9, pp. 444–446, 2010.

[159] M. Wagih, A. S. Weddell, and S. B. Beeby, "Rectennas for RF energy harvesting and wireless power transfer: a review of antenna design", *IEEE Antennas and Propagation Magazine*, 2019.

[160] H. Sun, Y. Guo, M. He, and Z. Zhong, "A Dual-Band Rectenna Using Broadband Yagi Antenna Array for Ambient RF Power Harvesting", *IEEE Antennas and Wireless Propagation Letters*, vol. 12, pp. 918–921, 2013, ISSN: 1536-1225. DOI: 10.1109/LAWP.2013.2272873.

[161] Z. Zhou, W. Liao, Q. Zhang, F. Han, and Y. Chen, "A multi-band fractal antenna for RF energy harvesting", in *2016 IEEE International Symposium on Antennas and Propagation (APSURSI)*, Jun. 2016, pp. 617–618. DOI: 10.1109/APS.2016.7696017.

[162] M. Mrnka, P. Vasina, M. Kufa, V. Hebelka, and Z. Raida, *The RF Energy Harvesting Antennas Operating in Commercially Deployed Frequency Bands: A Comparative Study*, en, Research article, 2016. DOI: 10.1155/2016/7379624. [Online]. Available: https://www.hindawi.com/journals/ijap/2016/7379624/ (visited on 05/19/2019).

[163] Minhong Mi, M. H. Mickle, C. Capelli, and H. Swift, "RF energy harvesting with multiple antennas in the same space", *IEEE Antennas and Propagation Magazine*, vol. 47, no. 5, pp. 100–106, Oct. 2005, ISSN: 1045-9243. DOI: 10.1109/MAP.2005.1599171.

[164] T. Peter, T. A. Rahman, S. W. Cheung, R. Nilavalan, H. F. Abutarboush, and A. Vilches, "A Novel Transparent UWB Antenna for Photovoltaic Solar Panel Integration and RF Energy Harvesting", *IEEE Transactions on Antennas and Propagation*, vol. 62, no. 4, pp. 1844–1853, Apr. 2014, ISSN: 0018-926X. DOI: 10.1109/TAP.2014.2298044.

[165] C. A. Balanis, *Antenna theory: analysis and design*. Wiley-Interscience, 2005.

[166] Z. W. Sim, R. Shuttleworth, M. J. Alexander, and B. Grieve, "compact patch antenna design for outdoor rf energy harvesting in wireless sensor networks", 2010.

[167] *AD600A™, AD1000™*, Accessed: 2019-05-29. [Online]. Available: `https://www.rogerscorp.com/acs/products/80/AD600A-AD1000.aspx`.